



ANTARCTIC CLIMATE
& ECOSYSTEMS
COOPERATIVE RESEARCH CENTRE

climate futures for tasmania

TECHNICAL REPORT

General Climate Impacts

Grose MR, Barnes-Keoghan I,
Corney SP, White CJ, Holz GK, Bennett JB, Gaynor SM and Bindoff NL

October 2010



**Climate Futures for Tasmania
General Climate Impacts Technical Report**

ISBN 978-1-921197-05-5

© Copyright The Antarctic Climate & Ecosystems Cooperative Research Centre 2010.

This work is copyright. It may be reproduced in whole or in part for study or training purposes subject to the inclusion of an acknowledgement of the source, but not for commercial sale or use. Reproduction for purposes other than those listed above requires the written permission of the Antarctic Climate & Ecosystems Cooperative Research Centre.

Requests and enquiries concerning reproduction rights should be addressed to:

The Manager
Communications
Antarctic Climate & Ecosystems Cooperative Research Centre

Private Bag 80
Hobart Tasmania 7001
Tel: +61 3 6226 7888
Fax: +61 3 6226 2440
Email: climatefutures@acecrc.org.au

Disclaimer

The material in this report is derived from climate change scenarios and projections by the Antarctic Climate & Ecosystems Cooperative Research Centre that are based on computer modelling. Modelling involves simplification of real physical processes that are not fully understood and which must be anticipated.

The Antarctic Climate & Ecosystems Cooperative Research Centre undertakes no duty to or accepts any responsibility to any party who may rely upon this document.

While every effort has been made to ensure that data is accurate, the information is provided without warranty of any kind whatsoever including any warranties as to the accuracy of the data or its performance or fitness for a particular use or purpose whatsoever.

The user of this information accepts any and all risks of such use, whether direct or indirect, and in no event shall the Antarctic Climate & Ecosystems Cooperative Research Centre be liable for any damages and/or costs, including but not limited to incidental or consequential damages of any kind, including economic damage or loss or injury to person or property, regardless of whether the Antarctic Climate & Ecosystems Cooperative Research Centre shall be advised, have reason to know, or in fact shall know of the possibility.

Science Reviewers: Neil Adams, Jozef Syktus, Blair Trewin, Andrew Watkins.

Photo Credits: Suzie Gaynor (front cover and pages 24,68), Ian Barnes-Keoghan (pp 2,5,34-35, 38-39, 44-45), Melanie Webb (pp 8, 54), Mike Anderson (pp 21, 32-33), Tony Coates (p 23), Jennifer Sheridan (p60).

Graphic Design and Layout: Suzie Gaynor

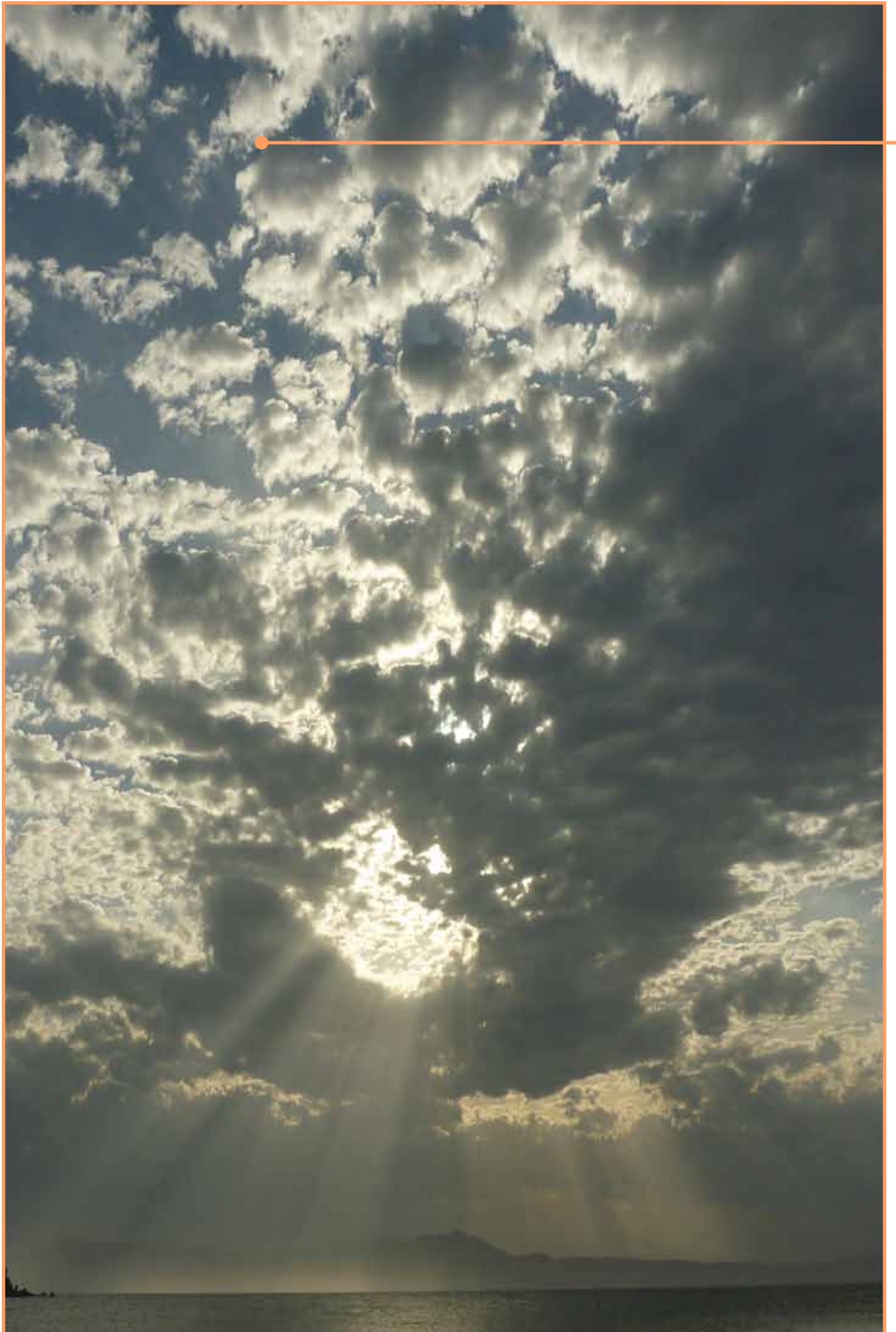
Citation

Grose MR, Barnes-Keoghan I, Corney SP, White CJ, Holz GK, Bennett JB, Gaynor SM and Bindoff NL 2010, *Climate Futures for Tasmania: general climate impacts technical report*, Antarctic Climate & Ecosystems Cooperative Research Centre, Hobart, Tasmania.

Climate Futures for Tasmania:
general climate impacts

Grose MR, Barnes-Keoghan I,
Corney SP, White CJ, Holz GK, Bennett JB, Gaynor SM and Bindoff NL

October 2010



Foreword

The Climate Futures for Tasmania research project is Tasmania's most important source of climate change information at the local level. This first report provides significant insight into the past and present climate, and projected changes to the general climate in Tasmania for the 21st century.

Climate Futures for Tasmania has generated local climate information at a scale and level of detail not previously available in Australia. This work will become the envy of other states. The project forms an essential part of the Tasmanian Government's climate change response and will be invaluable in informing evidence-based decision making for government, industry, business and communities in Tasmania.

The Tasmanian Government recently created the Adaptation Unit within the Tasmanian Climate Change Office to coordinate adaptation actions by government agencies and to work closely with local government, industry sectors and community groups. The climate projections developed by Climate Futures for Tasmania will provide an essential foundation for our work in this area.

This is the first of seven reports from Climate Futures for Tasmania to be released over the coming months. Data from these reports will be made available to our councils, emergency services, farmers, infrastructure managers and planners, energy and water authorities, community groups and researchers, and will assist them in planning for the future and ensuring that Tasmania is climate change-ready.

Climate Futures for Tasmania, led by Professor Nathan Bindoff, is a fine example of innovative leadership and is a further demonstration of Tasmania's great research capacity.

On behalf of the Tasmanian Government, I thank all those who have contributed to the project.



Nick McKim MP

Minister for Climate Change

Executive Summary

Tasmanian temperatures have risen since the 1950s, but at a slower rate than mainland Australia.

Tasmania has experienced a stable mean temperature for the first half of the 20th century, followed by a rising mean temperature since the 1950s. During this period, the rise in mean annual temperature was less for Tasmania than for Australia or the globe. The Tasmanian average rise is 0.10 °C per decade since the middle of the 20th century, compared to the 0.16 °C per decade rise for the Australian national average. Daily minimum temperatures in Tasmania have risen more than daily maximum temperatures, consistent with other regions of the globe.

Tasmanian rainfall has declined since the 1970s, especially in autumn, similar to other areas of southern Australia.

Tasmania has experienced a reduction in total annual rainfall and a change in inter-annual variability of rainfall since 1975. This reduction in rainfall has been greatest in autumn, and is similar to other regions of southern Australia. There have also been shifts in the large-scale climate drivers over this region in the last fifty years. There have been observed changes in the Hadley Circulation, with the subtropical ridge moving slightly southward and intensifying. An increase in the frequency of El Niño events and a strengthening of the Southern Annular Mode (SAM) have been observed. Finally, there has been an increase in atmospheric blocking in summer. Tasmanian rainfall changes appear to be at least partly linked to these climate drivers, although the contribution from each driver and the combination of drivers is still not fully understood.

Tasmanian temperature is projected to rise by about 2.9 °C under high greenhouse gas emissions and is 0.5 °C less than the projected global temperature increase.

The Climate Futures for Tasmania project presents a set of six global climate model (GCM) simulations dynamically downscaled for Tasmania under two IPCC SRES emissions scenarios (one high, A2, and one low, B1). Under the high emissions scenario, the average of the six downscaled GCM simulations shows Tasmania will experience a change in mean temperature of 2.9 °C over the 21st century. The temperature increase for Tasmania under this emissions scenario is less than the projected global warming of 3.4 °C. The six models show a range of temperature rise from 2.6 °C to 3.3 °C. The projections suggest temperature increases are smaller in the early part of the century, but the rate of change increases towards the end of the century.

Tasmanian temperature is projected to rise by about 1.6 °C under low greenhouse gas emissions. This increase is 0.2 °C less than the projected global temperature increase.

Under the lower emissions scenario, the average of the six modelling projections shows a rise in mean temperature of 1.6 °C over the 21st century. The six models used for the B1 emissions scenario show a range of temperature increase from 1.3 °C to 2.0 °C. Under the low emissions scenario, the projected temperature change for Tasmania is less than the projected global change of 1.8 °C. Compared to the high emissions scenario simulations, the rate of temperature rise under the lower emissions scenario in the later part of the century increases at a slower rate.

Temperature change under the two emissions scenarios is similar until they separate mid-21st century.

The high and low emissions scenarios show a similar climate response for the first half of the 21st century. The temperature response in the emissions scenarios separates beyond the range of uncertainty of the modelling after 2070. The last decades of the century show a rapidly rising temperature under the high emissions scenario, but a levelling off under the low emissions scenario. The pattern of the projected mean temperature change is reasonably uniform over Tasmania. Daily minimum temperature is projected to increase more than daily maximum temperature, in agreement with the observed changes from the recent past and projections from other regions of Australia and the globe.

The Southern Ocean moderates the increase of Tasmanian temperature to climate change.

The projected temperature changes for both emissions scenarios are less than the Australian and the global average changes for the same period, and are much less than some regions of the globe. For example, the Arctic is projected to experience an increase of 5.9 °C under the A2 emissions scenario. The smaller projected changes for Tasmania are due in part to the Southern Ocean storing the excess heat during the 21st century and moderating the temperature increase over Tasmania. The Southern Ocean is projected in the 21st century to have the slowest rate of warming of any region on the globe.

The projected range of responses from the simulations is smaller than global projections produced for the IPCC Fourth Assessment Report. This reduction in the range is due to the explicit matching of the simulated ocean climate with the observed ocean climate for the reference period prior to simulating the atmospheric response.

Spatial and seasonal patterns of rainfall show significant changes with climate change.

There is no significant change to projected total annual rainfall over Tasmania under either emissions scenario. Total annual rainfall over the state is expected to remain within the range of 1390 ± 200 mm seen in historical observations. However, there are significant changes in the spatial pattern of rainfall. Annual rainfall shows a steadily emerging pattern of increased rainfall over the coastal regions, and reduced rainfall over central Tasmania and in some areas of north-west Tasmania. The changes in seasonal rainfall are more prominent than annual total rainfall. The west coast of Tasmania experiences a significant increase in rainfall in winter and a significant decrease in summer rainfall after 2050. The central plateau district shows a steady decrease in rainfall in every season throughout the 21st century. A narrow strip along the northern east coast shows a steady increase in autumn and summer rainfall throughout the 21st century.

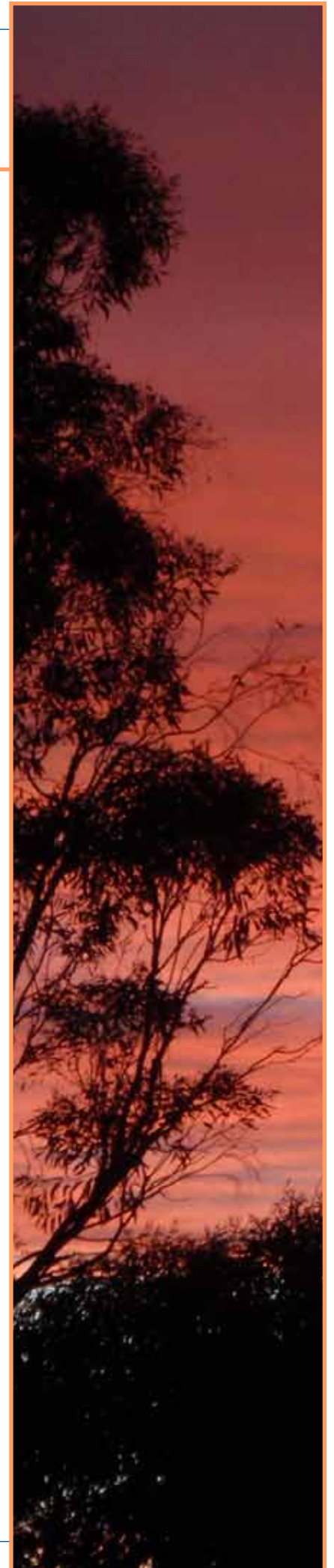
Projected rainfall changes are in line with our knowledge of climate drivers.

The projected rainfall trends are consistent with changes to the large-scale climate in the modelling simulations. These changes in the climate include a change to the dominant pressure patterns over the region and a change to the sea surface temperature in the surrounding seas. There is a projected increase in pressure in the mid-latitudes on either side of Tasmania, and a decrease in mean pressure at high latitudes with a different gradient in the different seasons. These pressure changes are associated with the subtropical ridge of high pressure moving southward and intensifying, especially in summer, and an increasing prevalence of the high phase of the Southern Annular Mode. These pressure changes are likely to drive the changes to west coast rainfall.

There is an increase in sea surface temperature off the east coast of up to $3.5\text{ }^{\circ}\text{C}$ by 2100 in the GCM inputs used in our downscaling models. This enhanced warming is caused by a southward extension of the East Australia Current over the 21st century. The sea surface temperature rise, along with changes to the dominant pressure patterns, is projected to lead to an increase in moisture flux, atmospheric instability and convective processes. These changes, combined with a continuing increase in atmospheric blocking in summer and autumn, are consistent with the increase in rainfall on the east coast margin during these seasons.

A warming of the climate leads to changes to many climate variables.

The projected changes to the general climate in the Climate Futures for Tasmania simulations also impact upon a range of other environmental variables. The projections suggest spatially complex changes to the average wind speed. Average cloud cover is projected to decrease slightly and radiation is projected to remain relatively constant. Relative humidity is projected to increase on average, but with a spatially varied pattern over Tasmania. The increasing temperature over the 21st century is the dominant driver of a significant increase in pan evaporation of up to 19%, which is likely to impact water availability.



FREQUENTLY USED ACRONYMS

Australian Water Availability Project	AWAP
Bureau of Meteorology	BoM
Convective Available Potential Energy	CAPE
Conformal Cubic Atmospheric Model	CCAM
Dipole Mode Index	DMI
El Niño Southern Oscillation	ENSO
Fourth Assessment Report	AR4
Global Climate Model	GCM
Indian Ocean Dipole	IOD
Intergovernmental Panel on Climate Change	IPCC
Mean Sea Level Pressure	MSLP
National Centres for Environmental Prediction	NCEP
Special Report on Emissions Scenarios	SRES
Sea Surface Temperature	SST
Southern Annual Mode	SAM
Southern Oscillation Index	SOI
Subtropical Ridge	STR

Table of Contents

Foreword	3
Executive Summary	4
1. Introduction	8
2. The climate of Tasmania	10
3. Large-scale drivers of Tasmanian climate	12
3.1 <i>Hadley Circulation and mid-latitude westerlies</i>	12
3.2 <i>El Niño Southern Oscillation (ENSO)</i>	13
3.3 <i>Indian Ocean Dipole (IOD)</i>	13
3.4 <i>Southern Annular Mode (SAM)</i>	14
3.5 <i>Blocking highs</i>	14
3.6 <i>Relative influence of each climate driver</i>	15
4. Trends in Tasmanian climate over the last century	16
4.1 <i>Temperature trends</i>	16
4.2 <i>Rainfall trends</i>	18
4.3 <i>Other variables</i>	20
5. Modelling Tasmanian climate	22
6. Changes to future climate	24
6.1 <i>Temperature</i>	24
6.2 <i>Rainfall</i>	29
6.3 <i>Historic context of rainfall changes</i>	36
6.4 <i>National and global context of temperature and rainfall changes</i>	40
6.5 <i>Mean wind speed</i>	42
6.6 <i>Cloud, radiation and relative humidity</i>	43
6.7 <i>Evaporation</i>	46
7. Projections of climate drivers of rainfall variability	48
7.1 <i>Patterns of mean sea level pressure (MSLP), Hadley Circulation</i>	48
7.2 <i>Regional wind</i>	52
7.3 <i>Atmospheric blocking</i>	54
7.4 <i>Changes to sea surface temperature</i>	56
7.5 <i>Convection and atmospheric stability</i>	57
7.6 <i>Ocean-atmosphere phenomena</i>	57
8. Synthesis	60
References	62
Appendices	66

1 Introduction

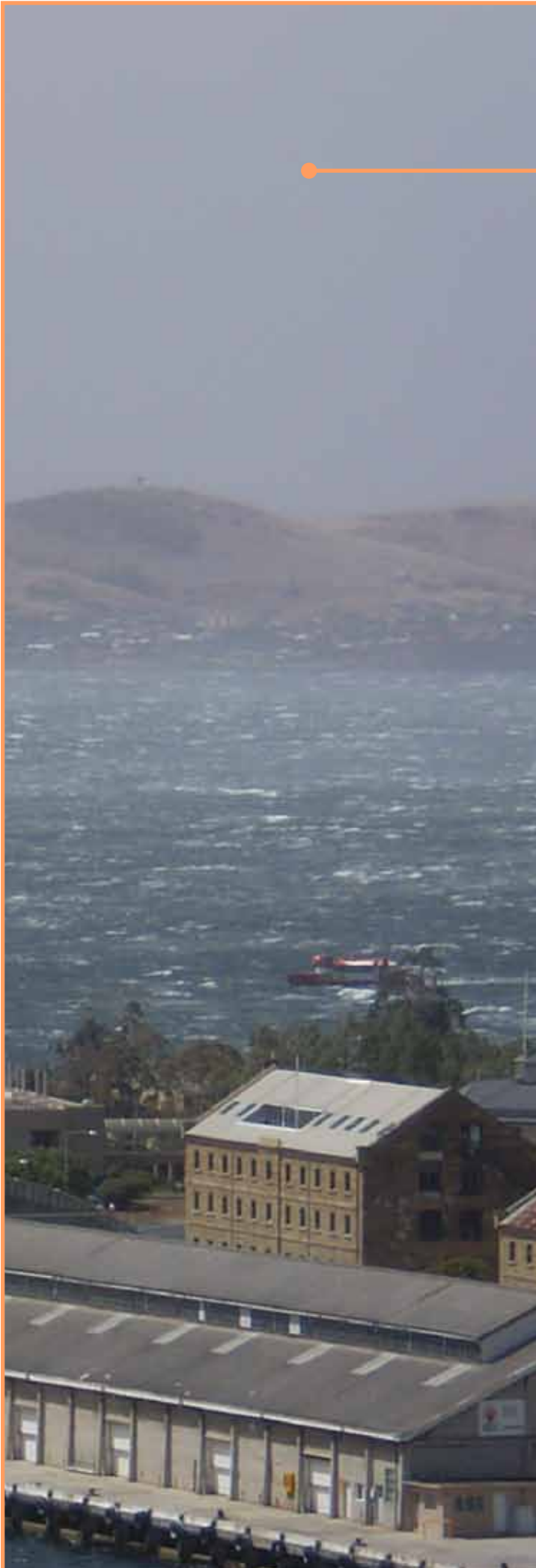
1. Introduction

Scientific evidence that the earth is warming is unequivocal and there is overwhelming evidence that increased concentrations of greenhouse gases caused by human activity are contributing to this warming (IPCC 2007). The observed warming over the 20th century of approximately 0.7 °C is consistent with our knowledge of the physical climate system (the atmosphere, oceans, land and sea ice) and its response to increasing greenhouse gases in the atmosphere.

Anthropogenic greenhouse warming is caused by a change to the radiative balance of the earth's atmosphere that influences the entire climate system. A change in global mean temperature is just one aspect of this influence. Global warming also causes changes to rainfall, wind, evaporation, cloudiness and other climate variables. Climate change is not restricted to changes in the mean state of the atmosphere.

Some of the most notable impacts of climate change result from a shift in the frequency of events and the strength of climate extremes. For example, climate change may lead to a change in the frequency of heatwaves, flooding rains or severe frosts. The projected effects of global climate change are unevenly distributed over the globe. Climate change is a global phenomenon whose specific impacts at any location will be felt as a change to local weather conditions. It is because of this regional variation that local or regional studies are required to understand the effects of climate change to specific areas. Tasmania has a temperate maritime climate with a complex set of influences from nearby oceans. It is situated in a transition zone with regard to climate change. It lies on the border between a region where most global climate models project a drying trend and a region that will undergo a wetting trend (Meehl et al 2007).

Climate and climate changes are critical to the planning of future water management. Hydro Tasmania commissioned a study in 2004 to examine the impact of climate change to 2040 for Tasmania. The pilot study was undertaken by the Tasmanian Partnership for Advanced Computing (TPAC) and CSIRO (McIntosh et al 2005). That project served as the initial exploration of the impact of climate change over Tasmania and was fundamental to the creation of the Climate Futures for Tasmania project. A major recommendation of the first climate change study in Tasmania was to use multiple models and multiple emissions scenarios. These recommendations were adopted in the Climate Futures for Tasmania project. In addition, there was a widening of the scope to include the assessment of impacts of climate change on agriculture, water catchments, and extreme events.



The Climate Futures for Tasmania project generated climate projections specific to Tasmania through fine-scale climate modelling using dynamical downscaling. The project used CSIRO's Conformal Cubic Atmospheric Model (CCAM) to dynamically downscale outputs from global climate models. The technical details of the modelling strategy are described in the project's modelling report (Corney et al 2010). In summary, we used two emissions scenarios (one high, A2 and one low, B1) from the IPCC Special Report on Emissions Scenarios (SRES), we increased the number of global climate models (GCMs) to six, extended the time period of simulations to 2100, and produced a separate suite of ensemble simulations. By using multiple models, two emissions scenarios and running a suite of ensemble simulations it was possible to better quantify the uncertainty in the projections. The aim of the project was to produce projections of climate change for the Tasmanian region of sufficient spatial resolution to allow the analysis of climate impacts at different locations within Tasmania. In addition, the project aimed to produce projections at sufficient temporal resolution to allow the analysis of changes to seasonality and extreme events.

From the pilot study, the project significantly expanded the involvement of end-users. Climate Futures for Tasmania was driven by the information requirements of end-users including local and state governments in Tasmania, local and state businesses, and industry and agriculture. This collaborative research project is unique in its involvement of state and federal governments, universities, research organisations and Tasmanian stakeholders.

The Climate Futures for Tasmania project complements climate analysis and projections done at the continental scale for the IPCC Fourth Assessment Report (Christensen et al 2007), at the national scale in the *Climate Change in Australia* report and data tool (CSIRO & Bureau of Meteorology 2007), as well as work done in the south-east Australia region in the South Eastern Australia Climate Initiative (SEACI). The work also complements projections done specifically on water availability and irrigation in Tasmania by the Tasmania Sustainable Yields Project (CSIRO 2009).

This general climate report represents the major reporting in one of five components of research undertaken in the project. The other four research components are presented in a series of reports as follows: modelling (Corney et al 2010), extreme events (White et al 2010), water and catchments (Bennett et al 2010) and agriculture (Holz et al 2010).

About the project

Climate change is a feature of the 21st century global climate. The need to understand the consequences and impacts of climate change on Tasmania and to enable planning for adaptation and mitigation of climate change at a regional level has been recognised by both the state and federal governments.

The Climate Futures for Tasmania project is the Tasmanian Government's most important source of climate change data at a local scale. It is a key part of Tasmania's climate change strategy as stated in the *Tasmanian Framework for Action on Climate Change* and is supported by the Commonwealth Environment Research Facilities as a significant project.

This project has used an ensemble of global climate models to simulate the Tasmanian climate. The project is unique in Australia: it was designed from conception to understand and integrate the impacts of climate change on Tasmania's weather, water catchments, agriculture and climate extremes, including aspects of sea level, floods and wind damage. In addition, through complementary research projects supported by the project, new assessments were made of the impacts of climate change on coastal erosion, biosecurity and energy production, and the development of tools to deliver climate change information to infrastructure asset managers and local government.

As a consequence of this wide scope, Climate Futures for Tasmania is an interdisciplinary and multi-institutional collaboration of twelve core participating partners (both state and national organisations). The project was driven by the information requirements of end users and local communities. This is one of seven technical reports from the project.

This report covers the past and present climate of Tasmania, and the projected changes to the general climate for the 21st century. There is a focus on changes in the mean state and changes in the spatial pattern of the Tasmanian climate. In Section 2, a general description of the Tasmanian climate is given, followed by an account of the large-scale climate mechanisms in Section 3. Section 4 outlines changes in the climate of Tasmania over the past century. Section 5 presents some detail of the modelling used to examine projected changes in the climate to 2100. Section 6 gives a description of changes to the average state of general climate variables (primarily temperature and rainfall) in the downscaled modelling projections to 2100. Finally, in Section 7, we examine the projected changes to the climate mechanisms and large-scale climate drivers that affect Tasmania.

2 The climate of Tasmania

2. The climate of Tasmania

Tasmania is an island that lies to the south-east of mainland Australia between 40 degrees south and 43.5 degrees south. No point in Tasmania is more than 115 km from the ocean and as such, Tasmania has a temperate maritime climate where temperature is moderated by the surrounding seas. There is an average daily temperature range of approximately 7 °C at the coast increasing to around 14 °C inland. The seasonal temperature range is also small compared to areas further from the ocean, with mean maximum temperatures of 18 °C to 23 °C in summer and 9 °C to 14 °C in winter (Bureau of Meteorology 1993). Tasmania is mountainous in the west, central and north-east regions, affecting the flow of air over land and therefore the rainfall distribution. The Bureau of Meteorology divides Tasmania into seven forecast districts representing distinct climate zones (Figure 2.1).

Tasmania lies in the 'Roaring 40s' belt of westerly airflow. The principle characteristic of the Tasmanian climate is the interaction between prevailing westerly wind and the mountain ranges near the west coast and the central plateau. This interaction

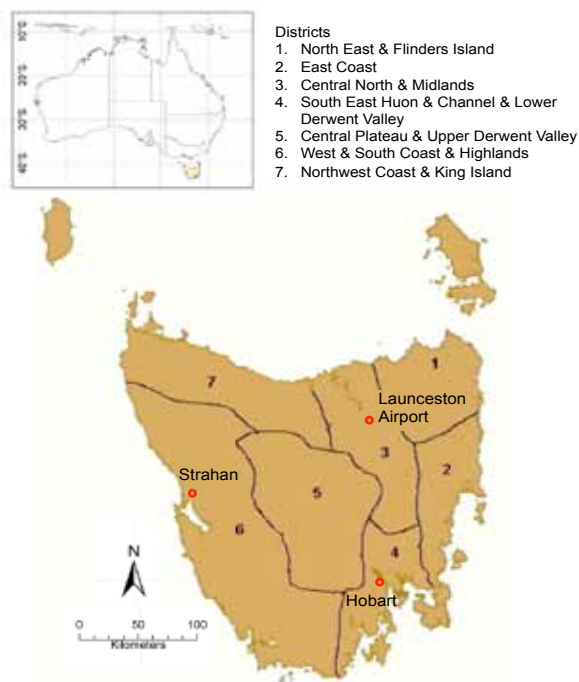


Figure 2.1 The map of Tasmania showing the boundaries of the seven forecast districts and the location of three key weather station sites referred to in later sections (marked with red dots), Hobart, Strahan and Launceston Airport, Source: www.bom.gov.au.

strongly influences the spatial variation of cloudiness and rainfall across Tasmania (Langford 1965). The seasonal cycle in the strength and persistence of the westerly wind is a key driver of the seasonal rainfall pattern, especially in the western and central regions of Tasmania. These persistent westerly systems are related to features of the general circulation of the atmosphere in the southern hemisphere. Specifically, the interaction between the Antarctic circumpolar trough of low pressure over the Southern Ocean and the Subtropical Ridge (STR), causes increases and decreases in the meridional pressure gradient, as well as changes in the strength and latitudinal extent of the westerly winds that reach Tasmania (Langford 1965). The westerlies over Tasmania are strongest in winter and spring. In summer, these westerlies are weaker and there are more frequent intervals of north-easterly to south-easterly wind. However, cold fronts regularly cross Tasmania in summer between high-pressure cells. In general, these fronts are preceded by a warm north to north-west wind and are followed by a cooler south to south-west wind.

The westerly flow at Tasmanian latitudes is dominant year-round and generally strongest in winter and spring. However, slow-moving high-pressure systems (anticyclones) can interrupt these westerly systems. These 'blocking highs' develop in numerous regions of the globe and persist for several days or even weeks. The blocking highs that affect Tasmanian rainfall are those that develop to the south of mainland Australia or in the Tasman Sea. These systems can block the approach of rain-bearing cold fronts to Tasmania and steer them to the south-east (Sturman & Tapper 1996). Blocking events in the Tasman Sea strongly affect rainfall distribution over Tasmania. They can occur year-round, but reach a maximum in the transition from summer to winter as the westerlies weaken.

The paths of individual low pressure systems from where they form to where they decay are called 'storm tracks'. In winter, a persistent set of storm tracks passes from the Great Australian Bight over Bass Strait and into the Tasman Sea (Leighton & Deslandes 1991; Jones & Simmonds 1994; Keable et al 2002). The strength of these systems and their proximity to Tasmania strongly affect rainfall over Tasmania (Godfred-Spenning & Gibson 1995). On occasions, these low pressure systems become cut off from the westerly flow and become slow moving. Such 'cutoff' lows occur infrequently but can strongly affect the rainfall of northern, central and eastern regions. Cutoff lows in this region are correlated with blocking highs (Pook et al 2006).

The combination of mountainous topography, prevailing westerly wind, the annual pressure cycle, winter storm tracks, blocking highs and cutoff lows results in a large spatial variation in rainfall across Tasmania. Mean annual rainfall varies from less than 600 mm in the central midlands to more than 3000 mm near the west coast (Figure 2.2a). There is a steep gradient in total annual rainfall from the western region across the eastern central plateau, resulting in a rain shadow region over the central midlands, east coast and south east regions. The midlands receives the lowest rainfall of any region in Tasmania.

The annual cycle of pressure, storm tracks, blocking highs and cutoff lows also leads to different seasonal cycles of rainfall across Tasmania. When Tasmania is split into three, roughly equal zones of east, west and north (after Shepperd 1995), the annual cycles of rainfall in these three zones are different (Figure 2.2b). The west coast has a distinct seasonal cycle with the highest rainfalls in winter and early spring. There is a smaller but still distinct annual cycle in rainfall in the north, with the peak of the rainfall cycle occurring through autumn to winter. There is no distinct annual cycle in the eastern zone, with approximately 50 mm to 70 mm falling each month of the year. The different seasonal cycle in rainfall in the different zones can also be seen as a distinct zonation as the size of the seasonal cycle normalised for the mean monthly rainfall (Figure 2.2c).

Despite the similarity of seasonal cycle in the west and the north, there are marked differences in characteristics of the rainfall between these two regions (Langford 1965). The west receives prolonged heavy rainfall events associated with a westerly airstream, whereas the north receives shorter duration rainfall events in mid to late autumn in moist north-easterly airstreams, commonly associated with the cutoff low pressure systems described above. These cutoff lows can occasionally produce extreme rainfall events in east and south-east Tasmania and into the midlands, however these events are less frequent in the north.

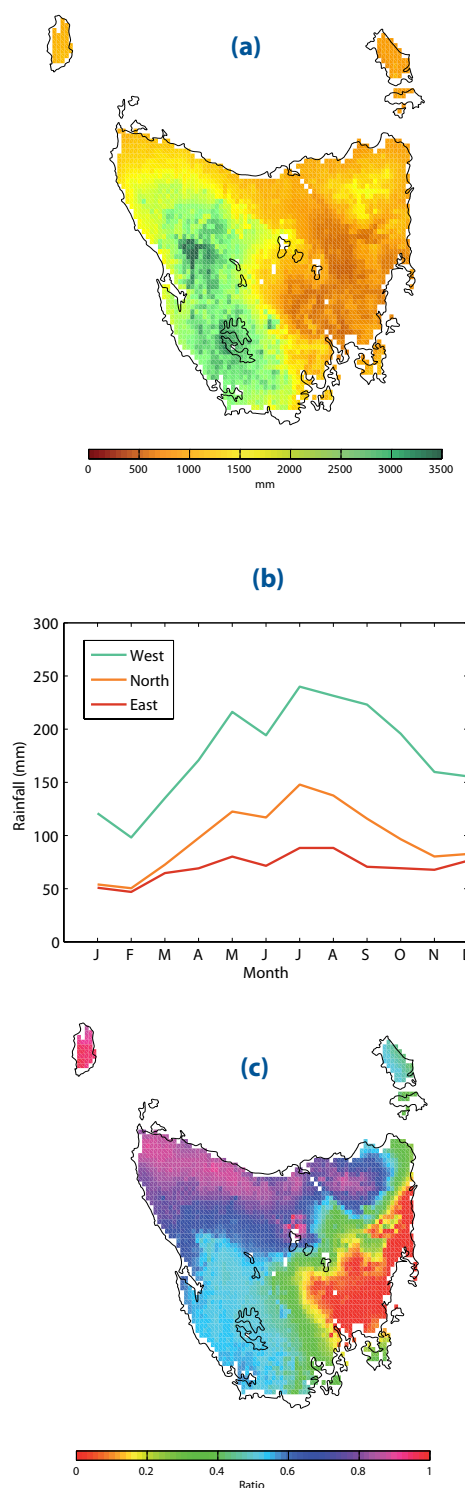


Figure 2.2 Rainfall for Tasmania for 1961-1990. (a) The mean annual rainfall, (b) annual cycle of rainfall by month divided spatially into West, East, North and all-of-state, (c) ratio of the seasonal cycle normalised for mean monthly rainfall (produced from 0.05-degree gridded AWAP data, accessed March 2010).

3 Large-scale drivers of Tasmanian climate

3. Large-scale drivers of Tasmanian climate

Just as total annual rainfall and the seasonal cycle of rainfall vary across Tasmania, the relationships between rainfall and various large-scale climate drivers vary greatly as well. The strength of these relationships also varies by season, with the different climate drivers having a greater effect on rainfall in different seasons. Variations in the dominant westerly flow occur seasonally and inter-annually. Tasmania is also close enough to the Southern Ocean, Pacific Ocean, Indian Ocean and the Tasman Sea to be influenced by ocean-atmosphere climate drivers present in these areas. These large-scale climate drivers include, but are not restricted to, the El Niño Southern Oscillation (ENSO), the Indian Ocean Dipole (IOD), the Southern Annular Mode (SAM) and atmospheric blocks in the Australian region. A schematic diagram of the major climate drivers affecting Australian rainfall variability is found in Figure 3.1.

3.1 Hadley Circulation and mid-latitude westerlies

The Hadley Circulation is the dominant large-scale atmospheric circulation of the Earth driven by solar heating. The Subtropical Ridge (STR) of high pressure forms the descending arm of the Hadley Circulation. The STR normally lies to the north of Tasmania and consequently the wind is predominantly westerly at Tasmanian latitudes. This mid-latitude region is known as the Ferrel Cell. The position and intensity of the STR in relation to Tasmania has an influence on the number and impact of mid-latitude pressure systems reaching Tasmania. There is evidence that in the last 50 years the STR in autumn has moved further south (Murphy & Timbal 2008) and has become more intense (Larsen & Nicholls 2009). These changes have the effect of inhibiting mid-latitude weather systems bringing rain in autumn and are associated with changes to the southern annular mode associated with this (discussed below).

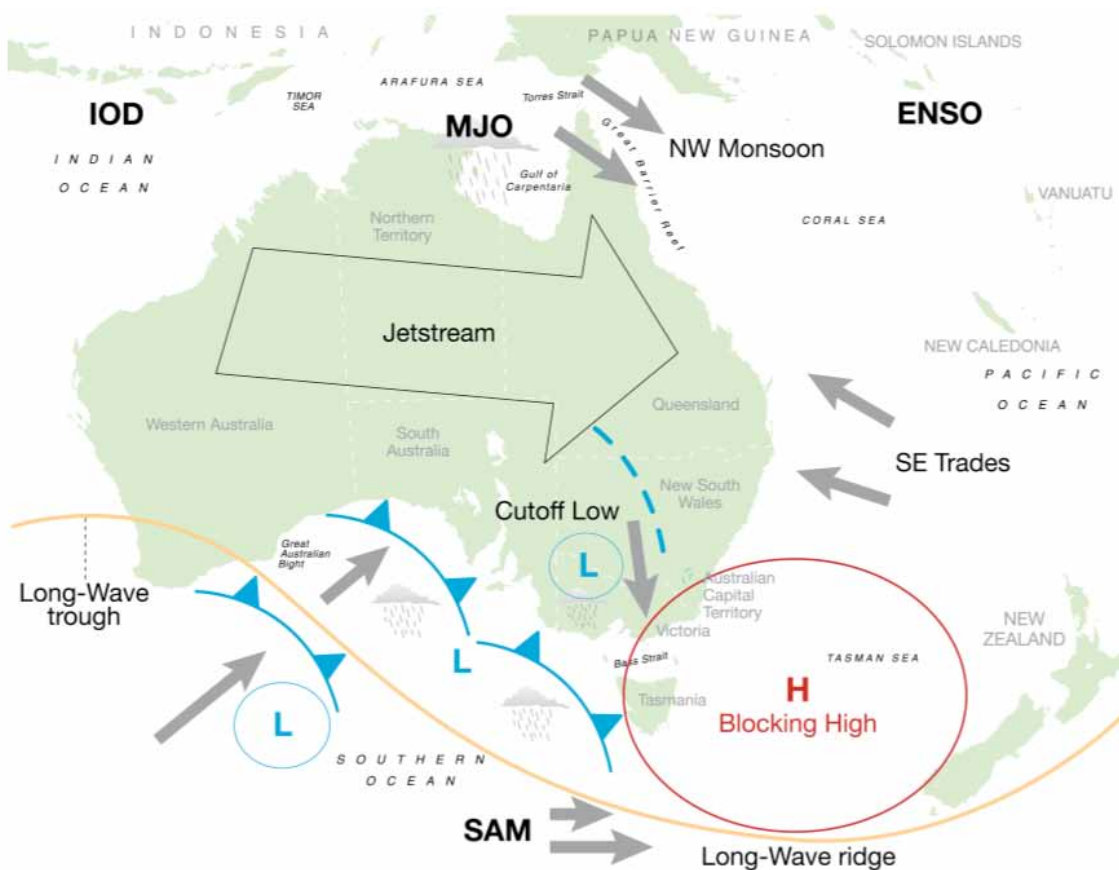


Figure 3.1 A schematic representation of the main climate drivers of rainfall variability in the Australian region (Source: Risbey et al 2009). The climate drivers most relevant to Tasmania are the Southern Annular Mode (SAM), El Niño Southern Oscillation (ENSO), Indian Ocean Dipole (IOD), cutoff lows and blocking highs.

The strength and latitudinal boundary of the westerlies changes on long time scales, including glacial cycles (Shulmeister et al 2004). Proxy records indicate that during the Little Ice Age (1400-1850 AD) the circumpolar trough was further south, causing strengthened westerly circulation over Tasmania, while during the preceding period (800-1400 AD) the westerly flow was probably reduced (Shulmeister et al 2004). The westerly flow in the mid-latitudes is as strong now as it has been at any time during the last glacial cycle (Shulmeister et al 2004), and would be expected to decline were the globe to move into a glacial period. The mean annual position of westerlies also varies over decadal and inter-annual time scales through shifts of the Pacific Decadal Oscillation, Southern Annular Mode (SAM) and the El Niño Southern Oscillation (ENSO). The strengths of these phenomena have changed over time. The observed inter-annual zonal shifts of the mean latitudinal boundary of the westerlies (two degrees maximum) may be nearly as large as the shifts during glacial-interglacial cycles (three to four degrees) (Shulmeister et al 2004).

3.2 El Niño Southern Oscillation (ENSO)

The El Niño Southern Oscillation (ENSO) has been shown to modulate rainfall over much of Australia (Nicholls 1989), with rainfall across Australia as a whole showing an in-phase linear relationship with the Southern Oscillation Index (SOI). At most locations across Australia annual mean rainfall is higher when SOI is positive (La Niña) and generally lower than average when SOI is negative (El Niño). The impact of ENSO measured as a correlation with SOI over the entire cycle is greater in the eastern states of Australia than the west. However, correlations are lower in Victoria and Tasmania than in some other regions of eastern Australia (Nicholls 1989). The effect of ENSO is felt most strongly in winter and spring in Australia (McBride & Nicholls 1983), but the effects of La Niña conditions can extend into summer.

While Australian rainfall is correlated with SOI, the correlation in some phases of the cycle can be weaker than others. Murphy and Timbal (2008) note the influence of ENSO on rainfall may be shown by the rainfall anomaly in winter and spring during twelve strong El Niño years (mean SOI less than -8.0 in June to November), and twelve strong La Niña events (mean SOI more than 12 in winter to spring). Regions where the rainfall is above or below the median show some influence of SOI. The north-east region of Tasmania shows a strong response in these years, with rainfall well below the median during strong El Niño years and well above the median in strong La Niña years.

A strongly negative SOI may not always be a reliable indicator of potential rainfall deficiency. This is likely to be because sea surface temperature anomalies in the Pacific Ocean appear to determine the impact of El Niño on Australian rainfall rather than the strength of the pressure difference indicated by the SOI (Wang & Hendon 2007). An index of sea surface temperature (SST) of the Pacific Ocean near Australia known as Niño4 has a negative correlation with rainfall in south-east Australia in winter and spring (Murphy & Timbal 2008). There is a difference in the impact of 'classic' El Niño events, where the peak in SST is in the eastern Pacific Ocean, and 'Modoki' El Niño events, where the peak in SST is in the central Pacific Ocean. The maximum rainfall response for Modoki events occurs in autumn, compared to a peak response in spring for classic events (Taschetto & England 2009).

There has been some indication that the ENSO-rainfall link varies substantially on inter-decadal time scales (Power et al 2006). The link may have changed considerably after the early 1970s, with the greatest change in south-east Australia (Nicholls et al 1996). The change in the nature of this relationship may be coincident with changes in rainfall trend discussed above, but this remains an area of active research.

3.3 Indian Ocean Dipole (IOD)

The Indian Ocean Dipole (IOD) is a coupled ocean-atmosphere oscillation in the northern Indian Ocean, most obviously seen as an oscillation in sea surface temperature (SST) between the north-east and north-west Indian Ocean. As such, it can be measured as the difference in SST between these two regions of the Indian Ocean. This difference in temperature is known as the Dipole Mode Index (DMI) (Saji et al 1999), and is positive when the western Indian Ocean is warm relative to the eastern Indian Ocean.

The IOD affects rainfall over Australia from May to November, with the influence peaking in the southern spring (Saji et al 1999). The influence of the IOD varies across the continent and is seen mainly in the central and southern regions of Australia, including some effect over Tasmania. Correlations of Indian Ocean SST with minimum temperature and with rainfall in south-east Australia are small but statistically significant in winter (Timbal & Murphy 2007). The IOD shows some correlation of June to October rainfall in northern Tasmania (Risbey et al 2009). However, this correlation is reduced when the effect of El Niño Southern Oscillation (ENSO) is removed.

The interaction of the IOD with ENSO is important, and there is some uncertainty as to how independent the two cycles are (Saji et al 1999; Ashok et al 2007; Meyers et al 2007). The combination of ENSO and IOD is important for Tasmania, where the link between Indo-Pacific SST and winter rainfall is more prominent than for south-west Western Australia or any other southern region (Ansell et al 2000). The combination of a positive phase in the IOD with a strong El Niño can create low rainfall years in some regions of Australia, including Tasmania. An example is 2006, which was the driest year on record in much of northern and eastern Tasmania. Conversely, a negative phase of the IOD combined with a strong La Niña year may result in higher than average June to October rainfall.

3.4 Southern Annular Mode (SAM)

The Southern Annular Mode (SAM) is a low-frequency mode of atmospheric variability over the southern hemisphere with a circumpolar influence. It is also known as the Antarctic Oscillation (AAO) (as opposed to the Arctic Oscillation - AO), or the Southern Hemisphere Annular Mode. Over the last half of the 20th century, SAM has intensified, driven primarily by changes to stratospheric ozone, but also greenhouse warming and natural variability (Arblaster & Meehl 2006). Photochemical ozone loss affects the stratospheric polar vortex, which in turn affects the tropospheric circulation (Thompson & Solomon 2002).

A simple index of SAM is the difference between normalised monthly zonal mean sea level pressure at 40 degrees south and 65 degrees south (Gong & Wang 1999; Marshall 2003). There is also a regional index for the local expression of SAM in the Australian zone of 90 degrees east to 180 degrees east (Meneghini et al 2007). There is a statistically significant relationship between the SAM indices and annual total rainfall in southern Australia (Meneghini et al 2007). Variations in SAM can explain up to 15% of the weekly rainfall variance in western Tasmania in winter and spring, and this is comparable to the influence of El Niño Southern Oscillation (ENSO) in other regions of Australia (Hendon et al 2007). The sign of the influence of SAM varies with season and district. For western Tasmania, there is a negative relationship in winter, spring and into summer, and for the north-east coast of Tasmania, there is a slight positive effect in summer only (Timbal & Murphy 2007; Hendon et al 2007). Changes to SAM are likely to have contributed to the observed increases in rainfall over eastern Tasmania and the decreases in rainfall over western Tasmania during summer between 1979 and 2005 (Hendon et al 2007).

3.5 Blocking highs

Blocking highs are slow moving high pressure systems that can alter the broad scale of air flow and weather. They occur frequently in the Tasman Sea and tend to disrupt the dominant westerly airstreams. Blocking highs can cause rain-bearing cold fronts to steer to the south-east of Tasmania, and are also correlated with the incidence of cutoff lows that affect rainfall over some areas of Tasmania, such as the north-east (Sturman & Tapper 1996; Pook et al 2006). Prolonged periods of atmospheric blocking can alter the rainfall over Tasmania, with the west coast receiving well below the mean seasonal rainfall in some years, while above average rainfall occurs in the east and north of Tasmania (Pook & Gibson 1999). The strength of atmospheric blocking over the Tasmanian region can be measured with an index at 140 degrees east (Pook & Gibson 1999). The Blocking Index is calculated at a given meridian from a formula based on the zonal component of wind on the 500 hPa pressure level at selected latitudes.

Southern hemisphere blocking events, including those in the Tasman Sea, may interact with larger hemispheric phenomena such as El Niño Southern Oscillation (ENSO). For example, southern hemisphere atmospheric blocking occurs more frequently in the warm phase of ENSO cycles, however the mean intensity of that event does not appear to change during ENSO cycles (Dong et al 2008). The Blocking Index at 140 degrees east has a moderate positive correlation with ENSO indices (Risbey et al 2009).

There has been a reduction in the annual number of days with blocking events in the southern hemisphere as a whole over the period 1948 to 1999 (Dong et al 2008). The Blocking Index calculated over eastern Australia has shown an increase in summer, and a decrease in winter and spring since 1950 (M Pook 2009, pers comm 09 July). The frequency of high pressure systems (not necessarily blocking highs) in the Tasman Sea steadily increased between 1950 and 2007, although the central pressure of those highs has not changed markedly (Simmonds & Key 2000).

3.6 Relative influence of each climate driver

There are multiple drivers of rainfall variability acting on each district of Tasmania in each season. One method of gauging the relative influence of each climate driver is the strength of the correlation of an index of the driver with rainfall variability for that season. There are other methods of measuring the influence of each driver, but the amplitude of the correlation gives a broad suggestion of the influence of each driver. The driver with the highest correlation to rainfall variability in each calendar season is shown in Figure 3.2 (adapted from Risbey et al 2009). Each of these drivers explains between 10% to 50% of the rainfall variance, and these levels are noteworthy for this type of comparison.

This analysis indicates that the index of El Niño Southern Oscillation (ENSO) has the strongest correlation to rainfall in the north and east during autumn and winter. This is consistent with the rainfall deficits experienced during strong El Niño and La Niña events described above. The correlation to the index of the Indian Ocean Dipole is greater than for other drivers in spring for the north and midlands, and the correlation with an index of the Southern Annular Mode (SAM) is greater than others in the west throughout winter, spring and summer.

the east in spring, summer and autumn, and in the west throughout autumn and winter. Atmospheric blocking may interact with other phenomena such as ENSO, however some significant correlations persist even after the effect of ENSO is removed (Risbey et al 2009).

The influence from these various climate drivers contribute to the different modes of inter-annual rainfall variability in the different districts of Tasmania. There is also always a component of random variability. Empirical orthogonal functions (EOFs) of Tasmania-wide rainfall indicate a leading mode of variance at two and five years (Hill et al 2009). The eastern and northern regions have a significant mode of variability centred around five years (range 3.6 years to 10.7 years), whereas the west has a mode at 2.7 years (Shepherd 1995). The five-year mode in the north and east is associated with ENSO, among other influences (Hill et al 2009). The periodicity of 2.7 years in the west represents a quasi-biennial oscillation linked to processes of the SAM among other drivers (Shepherd 1995; Hill et al 2009). These results are based on data from the last few decades and represent the recent relationships between rainfall variability and the various drivers. There have been changes to these relationships over long time scales (for example, Nicholls et al 1996; Risbey et al 2009) and thus they may not remain constant through this century.

Correlation to Climate Drivers

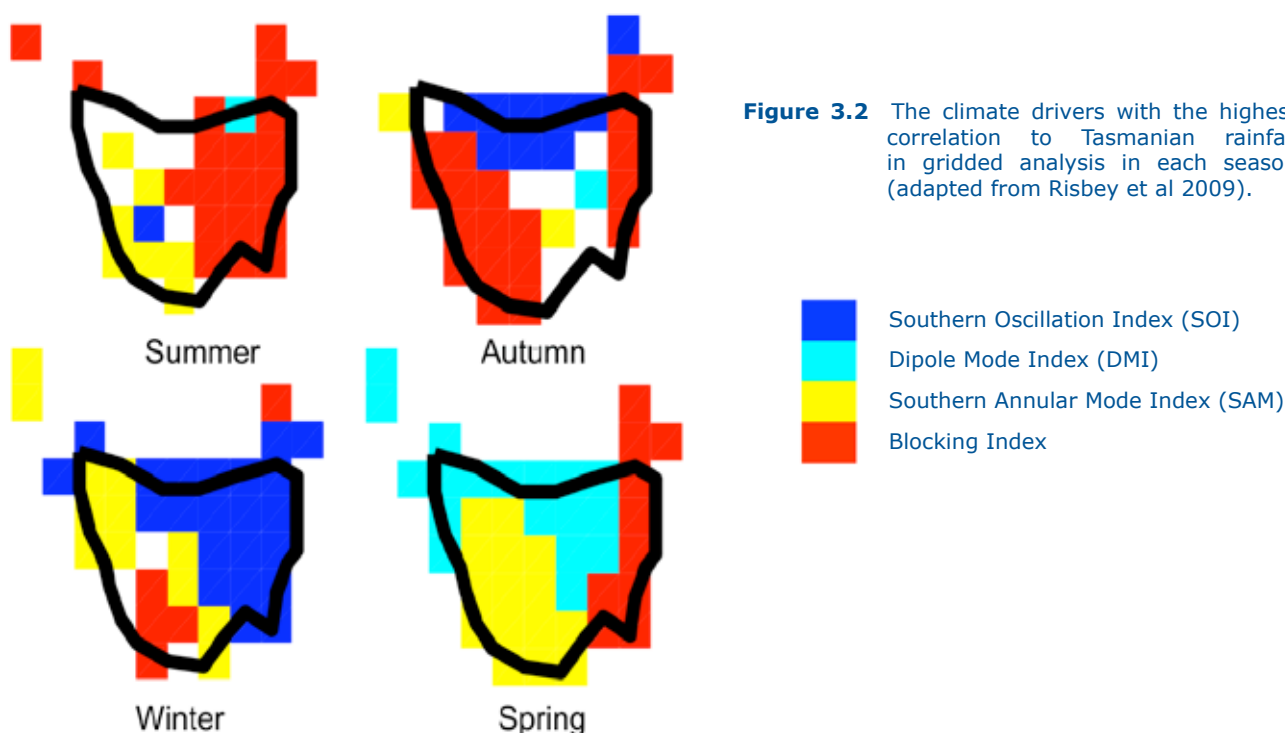


Figure 3.2 The climate drivers with the highest correlation to Tasmanian rainfall in gridded analysis in each season (adapted from Risbey et al 2009).

4 Trends in Tasmanian climate over the last century

4. Trends in Tasmanian climate over the last century

While indigenous Tasmanians have been observing the weather for millennia, a reliable observational dataset of Tasmanian temperature and rainfall did not start until the 1880s, and then in only limited locations. For the 20th century, the observational record is not perfect in spatial coverage, continuity or accuracy. To generate high-quality climate site data for Tasmania, the Bureau of Meteorology uses a measurement dataset from a site or group of sites that conform to strict standards of accuracy and homogeneity. The raw data is then subjected to a variety of quality control and correction techniques, including adjustments for discontinuities caused by changes in location, exposure, instruments or observation practice (Lavery et al 1992; Torok & Nicholls 1996; Della-Martin et al 2004). There are relatively few Tasmanian high-quality climate sites for long-term analyses, with only six stations for temperature and eleven for rainfall. However, it should be noted that there has been a marked increase in the number of reliable measurements in more recent decades.

To get a spatially complete picture of climate variables over Tasmania, interpolation or modelling is required to fill in the spaces between observations. Each interpolation scheme and modelling system brings with it a set of assumptions and potential. A particularly problematic area is rainfall over west and south-west Tasmania, where there are very sparse and discontinuous climate records, as well as potential inhomogeneities in those records that do exist. The introduction of new stations, including Strathgordon

in the late 1960s and Mount Read in 1996 have a large impact upon the estimation of spatial average of rainfall for the West Coast, South Coast and Highlands District. This in turn has a large influence on the estimation of Tasmanian total rainfall, since this district experiences the highest rainfall of any of the seven Bureau of Meteorology forecast districts.

For this project, we examined the high-quality climate site data, and a set of observations interpolated onto a 0.05 degree latitude/longitude grid from the Australian Water Availability Project (AWAP), accessed in March 2010. This gridded dataset is in two parts, with the first a set of meteorological variables interpolated from all available station observations as well as satellite data (Jones et al 2009), and the second a set of water-balance variables modelled from the meteorological variables (Raupach et al 2008). These datasets are referred to generically as 'AWAP' hereafter in this report.

4.1 Temperature trends

Mean surface air temperature has increased in Australia by 0.9 °C since 1910 (CSIRO & Bureau of Meteorology 2007). The largest fraction of this increase occurred after 1950 at a rate of 0.16 °C per decade (CSIRO & Bureau of Meteorology 2007). Australia's hottest year on record was 2005, and the ten hottest years on record in Australia have all occurred since 1980. The warming trend is not uniform across Australia, with the largest changes in central Australia. Tasmania experienced 0.1 °C per decade of warming since the 1950s and this is significantly less than for Australia or the globe (CSIRO & Bureau of Meteorology 2007).

Table 4.1 Mean decadal temperature trend (°C/decade) between 1940 and 2007 in 11-year smoothed high-quality climate site data from Hobart, Launceston Airport and Strahan. Seasonal means not available for Strahan.

Temperature	Hobart	Launceston	Strahan
Annual mean	0.10	0.18	0.07
Annual maximum	0.08	0.13	0.03
Annual minimum	0.11	0.23	0.12
Summer mean	0.15	0.24	-
Autumn mean	0.11	0.13	-
Winter mean	0.11	0.11	-
Spring mean	0.11	0.11	-

Records from three Tasmanian high-quality climate sites from different areas of Tasmania were examined: Hobart in the south-east, Launceston Airport in the north and Strahan in the west (see Figure 2.1). All of these sites recorded a rise in mean, maximum and minimum temperature since the 1940s (Table 4.1). The increase in maximum temperature was less pronounced than the increase in mean and minimum temperatures at all stations. Summer temperatures increased at a greater rate than other seasons, especially in Launceston. There was a steady increase in temperature in all other seasons, except in autumn in Hobart and Launceston, where temperature increased by 0.26 °C per decade from 1940 to 1980 but then remained steady or decreased after 1980.

These patterns are reflected in the time series of spatial average of all high-quality climate sites for Tasmania and the spatial patterns of trends indicated

in gridded AWAP data (Figure 4.1 and Figure 4.2). Using this gridded data, mean temperature in Tasmania has increased by >0.5 °C since 1950, with a higher trend in the north-east than the rest of the state (Figure 4.1). The increase has been greater for minimum temperatures than for maximum temperatures (Figure 4.2). The lower rate of warming of the daily maximum temperature compared with minimum daily temperature is consistent with greenhouse warming and analyses of observations globally (Trenberth et al 2007). The spatial pattern of the trend in daily maximum temperature since 1961 is for greater change in the north-east and the interior, whereas daily minimum temperature has generally increased more on the north coast and less in the interior.

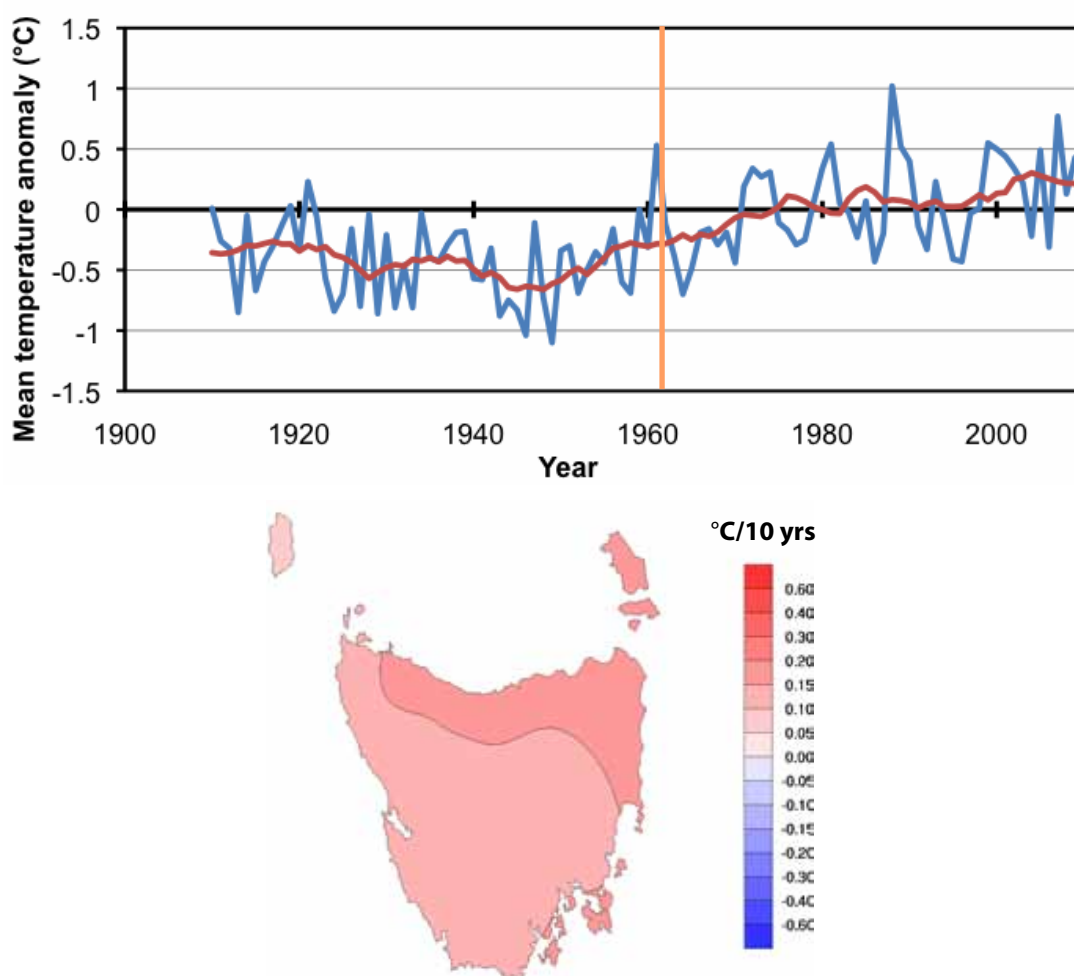


Figure 4.1 Annual mean temperature anomaly from the 1961-1990 baseline period mean for Tasmania (blue line) and 11-year moving average (red line) from Australian high-quality temperature data. The map below the plot shows the linear trend in mean temperature between 1961 and 2007, (the period after the orange line on the plot), using 0.05-degree gridded data (AWAP, accessed March 2010).

4.2 Rainfall trends

The largest decrease in rainfall in the observed record for south-east Australia has occurred since 1975 (Manton et al 2001). This decrease has been at a rate of about 20 mm per decade (Gallant et al 2007). This large change in recent decades shows that any estimate of rainfall trend is heavily dependent on the time period considered. For example, most regions in south-east Australia show an increase in rainfall between 1910 and 1990 (Hennessy et al 1999; Suppiah & Hennessy 1998; Haylock & Nicholls 2000; Nicholls & Lavery 1992). However, when recent data is considered, rainfall decreased in south-east Australia between 1910 and 2005 (Gallant et al 2007).

Tasmania has experienced similar rainfall trends to the south-east Australian region. There were two wet periods in the 1950s and in the 1970s, and a dry decade in the 1940s. There was no statistically significant trend in the mean annual rainfall of

Tasmania in the period 1910 to 1990 (Srikanthan & Stewart 1991). However, there was a downward trend in rainfall over the period 1970 to 1990 (Shepperd 1995), and this has continued from 1990 to 2007.

The patterns described above are reflected in the time series of spatial average of all high-quality climate sites for Tasmania and the spatial patterns of trends indicated in gridded AWAP data (Figure 4.3). There was a decrease in total rainfall since approximately 1975, accompanied by a marked reduction in variability. The spatial pattern of this decrease is seen to be relatively even over Tasmania. There are some localised pockets of greater decrease, centred on individual stations. This pattern is likely to be partly an artefact of the interpolated gridded dataset. Similarly, the increase seen in the small region near the west coast is probably an artefact of the Mount Read Station coming online in 1996.

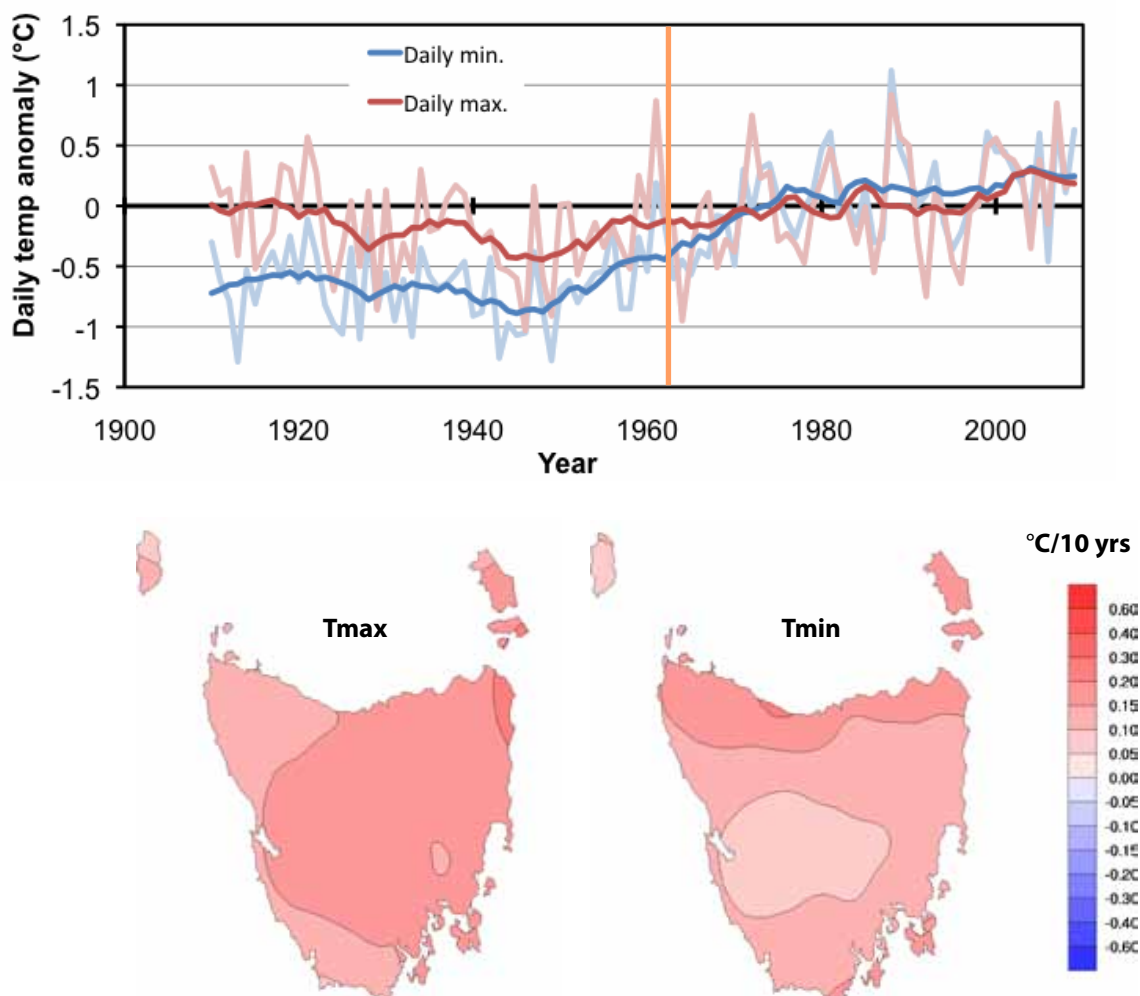


Figure 4.2 Annual mean daily minimum and daily maximum temperature anomalies from the 1961-1990 baseline period mean for Tasmania (faint lines) and the 11-year moving averages (bold lines) from Australian high-quality temperature data. The maps below the plot show the linear trend in daily maximum and minimum temperatures between 1961 and 2007, (the period after the orange line on the plot), using 0.05-degree gridded data (AWAP, accessed March 2010).

Changes in rainfall have not been uniform across seasons. The trend in annual total rainfall represents the sum of changes in all four seasons, which may be all different. The largest proportion of the change in rainfall in south-east Australia has been seen in autumn. Of the 20 mm per decade rainfall decrease in south-east Australia since 1975, 11 mm per decade has been in autumn (Alexander et al 2007). The largest changes in Tasmanian rainfall have also been observed in autumn. There was a slight increase in autumn rainfall in the west between 1913 to 1945 and 1946 to 1978 (Pittock 1983), and a statistically significant decrease of more than 10% in the south and south-east of Tasmania between 1951 and 2005 (Alexander et al 2007). Considering the whole period from 1910 to 2005, there was no significant trend in any season in Tasmanian rainfall, except a slight decrease in autumn rainfall in the far south-east (Alexander et al 2007).

The decrease in autumn rainfall since 1975 is reflected in the time series of spatial average rainfall for Tasmania using all high-quality climate sites and in the trend map made using AWAP gridded data (Figure 4.4). The dry decade in the 1940s was followed by the wet period in the 1950s to the 1970s. Since 1975, there was a sustained decrease in the mean autumn rainfall and also a change in the character of the inter-annual variability of autumn rainfall. The inter-annual variability of autumn rainfall about the mean rainfall has decreased markedly (Figure 4.4). The pattern of trend in autumn rainfall is of a greater decrease in the western district, however it should be noted that the total rainfall is also higher for this district. For both annual and autumn rainfall, there appears to be a lower inter-annual variability and a reduction in the number of exceptionally wet years since approximately 1975. This sustained reduction in wet years appears to be unique to the later part of the record.

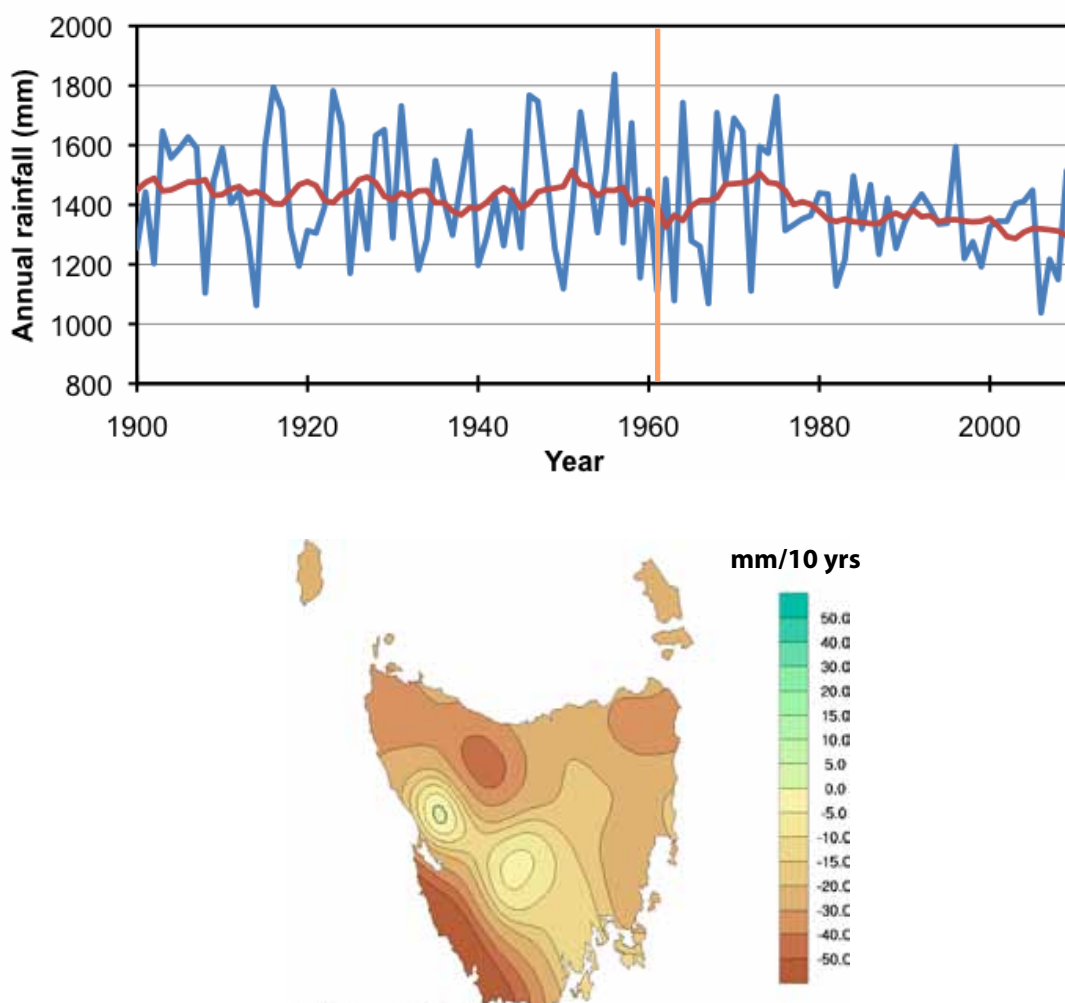


Figure 4.3 Statewide mean annual total rainfall for Tasmania (blue line) and the 11-year moving average (red line) from Australian high-quality rainfall data. The map below the plot shows the linear trend in annual total rainfall between 1961 and 2007, (the period after the orange line on the plot), using 0.05-degree gridded data (AWAP, accessed March 2010).

Taschetto and England (2008) reported a distinct east-west pattern in the rainfall trends in Tasmania since 1975, arising from an increase in winter and spring rainfall in the west and a decrease in rainfall in the east, especially during autumn. This east-west pattern in rainfall trend is not supported here, and this may be a function of the different observed datasets examined.

4.3 Other variables

Records for climate variables other than temperature and rainfall are even sparser, and there are similar or greater issues with interpolation of these variables to obtain a spatial average. Pan evaporation is the direct measurement of evaporation of water from a Class A evaporation pan. Pan evaporation is included

in the high-quality climate data, including three sites for Tasmania: Launceston Airport, Grove and Strathgordon (Jovanovic et al 2006). The longest record extends back to only 1968, and no record is entirely complete. Based on this limited dataset, average Tasmanian pan evaporation was 1004 mm per year for the 1975-2004 climatology period. Trends in pan evaporation since 1970 vary spatially and between seasons. In summer, there was a decrease in pan evaporation across Tasmania, and in winter, there was an increase. Annually, there was a slight increase over most of Tasmania, but a slight decrease in the far north-east. There are no complete and quality-controlled datasets of relative humidity, cloud, radiation and wind speed commonly available for trend analysis.

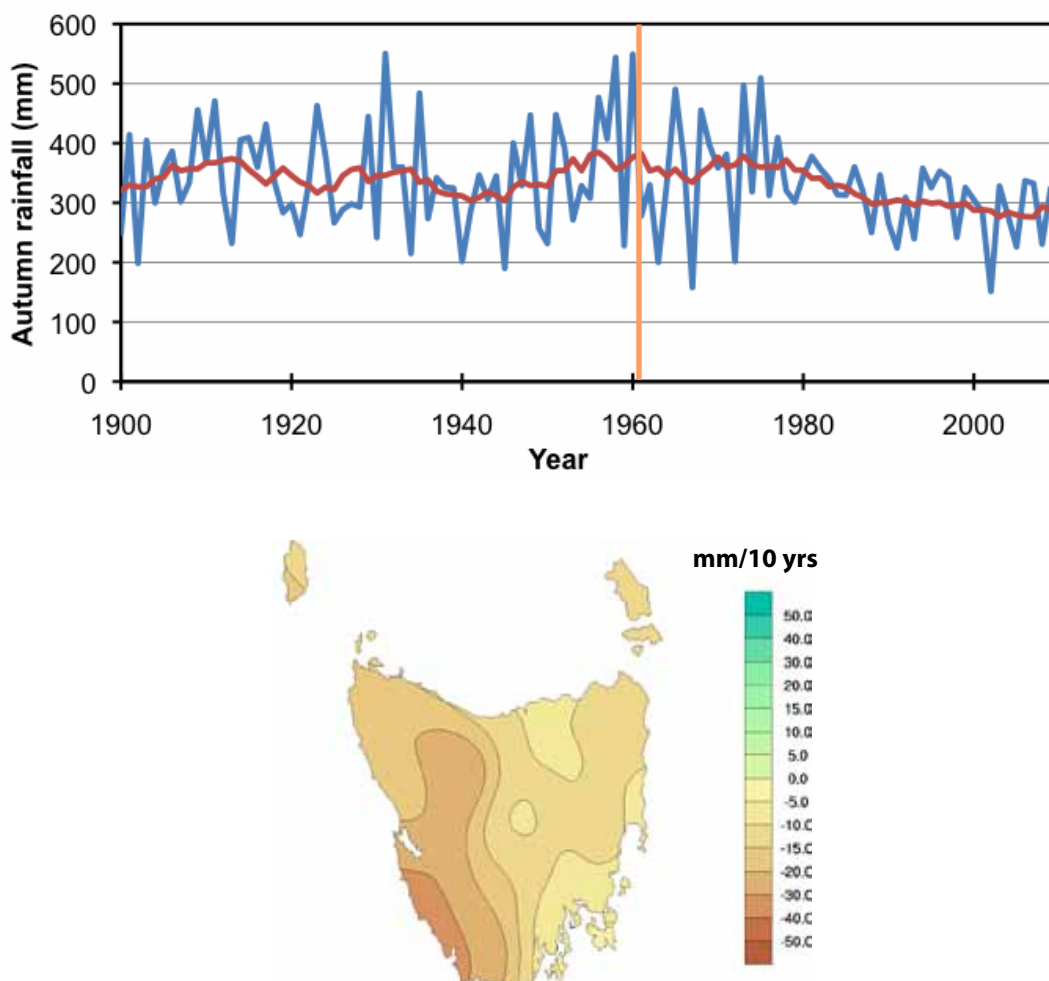


Figure 4.4 Statewide mean autumn total rainfall for Tasmania (blue line) and the 11-year moving average (red line) from Australian high-quality rainfall data. The map below the plot shows the linear trend in autumn total rainfall between 1961 and 2007, (the period after the orange line), using 0.05-degree gridded data (AWAP, accessed March 2010).



5 Modelling Tasmanian climate

5. Modelling Tasmanian climate

The Climate Futures for Tasmania project has examined projected changes to the Tasmanian climate under greenhouse gas emissions scenarios to the year 2100 using the most recent climate modelling techniques available. Coupled ocean-atmosphere modelling simulations from global climate models (GCMs) reported upon in the IPCC Fourth Assessment Report (Meehl et al 2007) were used as boundary conditions for a downscaling process to regional scales. A full account of the modelling strategy and methods used, and an evaluation of the modelling are in the modelling technical report (Corney et al 2010). This provides the context and framework for the interpretation of the modelling projections for the future period covered in this report. Only a basic account of the modelling is provided in this report as background.

Climate models are designed to simulate the main components of the earth's climate system in a simplified but robust manner. These components are the atmosphere, ocean, sea-ice and land surface. Climate models are a closed system and once initialised they operate independently from observations. Models can be used to indicate the response of the climate system to a given set of conditions, such as a particular composition of the atmosphere. The Climate Futures for Tasmania analysis considered the atmospheric composition under two scenarios of human emissions of greenhouse gases and aerosols through the next century. These emissions scenarios were A2 and B1 made for the Special Report of Emissions Scenarios (SRES) of the IPCC (Nakićenović & Swart 2000). The A2 emissions scenario results in higher emissions and a stronger climate response, the B1 emissions scenario results in lower emissions and a weaker climate response. These two emissions scenarios were chosen because they are the highest and lowest emissions scenarios where GCM simulations were available, thus gives a range of possible future climate responses. It is important to realise that the current human emissions over the last decade are tracking above the A2 emissions scenario (Le Quéré et al 2009).

The downscaling was performed using the CSIRO stretched-grid global atmospheric model; Conformal Cubic Atmospheric Model (CCAM). The only forcing data taken from GCMs was sea surface temperatures used as a bottom boundary condition. The sea surface temperature (SST) was used by CCAM to run an entirely dynamic atmospheric model. Persistent biases in the SST of each GCM in the current climate

were assessed against the Reynolds SST dataset (Reynolds 1988) for the current climate, and these biases were quantified and removed from the entire forcing dataset prior to the downscaling process. The SST fields were also interpolated onto the relevant grid scale to characterise the ocean-land interface at a higher resolution. The downscaling process was carried out in two stages: firstly from the original grid resolution (200 km to 300 km) down to a 0.5 degree latitude/longitude grid, and then down to a 0.1-degree grid.

A single modelling simulation gives a single projection of an emissions scenario, analogous to a single replicate of an experiment. More modelling simulations give further replicates of that experiment and help to give an estimate of the range of possible outcomes for a given emissions scenario. For this reason, the project has undertaken the maximum number of modelling simulations that computation time allowed, with the downscaling of six GCMs (CSIRO-Mk3.5, GFDL-CM2.0, GFDL-CM2.1, ECHAM5/MPI-OM, UKMO-HadCM3 and MIROC3.2(medres)) for both the A2 and B1 emissions scenarios. The six models were chosen for their performance over the Australian region. Multi-model ensemble simulations generally provide more robust information than simulations from any single model (Meehl et al 2007). Since the main focus in this report is the change to the mean state of the general climate, the focus will be on the results of the ensemble of all the models rather than any one particular simulation.

A limitation of any computational model is in the finite resolution of physical features, including a limit in the characterisation of topography. By necessity, a gridded model uses one value of surface height over the entire area of each grid cell. The finer scale resolution model (0.1-degree) uses the values from a 250 m digital elevation model (DEM) to assign a surface height to each grid cell. The 'envelope-topography' scheme of topography was chosen through a series of experiments to determine the scheme that gives the best characteristics of rainfall. This scheme assigns the height of each cell as the mean plus standard deviation of each point from the 250 m contour of the DEM.

For models to project future climate conditions reliably, they must simulate the current climate state with some degree of fidelity. Poor model skill in simulating the present climate could indicate that some physical or dynamical processes have been misrepresented (Meehl et al 2007). The Climate Futures for Tasmania modelling outputs displayed a

high level of skill in reproducing the recent climate of Tasmania across a range of climate variables. For example, the six-model-mean of Tasmanian average daily maximum temperature for the period 1961-90 is within 0.1 °C of the Bureau of Meteorology observed value of 10.4 °C, while the annual total rainfall of 1385 mm is very close to the observed value of 1390 mm. Furthermore, mean monthly temperature has a spatial correlation of 0.99 with gridded observations over the state, while for rainfall the spatial correlation for this period is 0.69. The level of skill in describing the climate of the recent past gives us confidence that the models are able to provide realistic projections of the Tasmanian climate out to 2100.

The simulated mean temperature and rainfall of Tasmania in the current climate compared well to observations, however some persistent biases at certain ranges in the frequency distribution were identified. Some analyses within the Climate Futures for Tasmania project such as agricultural research, water runoff modelling and extreme events analysis require daily data and that matches the absolute scale and range of observations with a high level of precision. For these purposes a series of bias-adjusted outputs were created. The method used to make the bias-adjusted outputs modifies the scale and frequency distribution of the modelled data to match an observed dataset, while retaining the time series and trends in the modelling projections. To demonstrate that these trends are retained, a comparison of the trends in the two datasets is included in the appendix. Changes in mean temperature (Appendix 1) and annual total rainfall (Appendix 2) are very similar in the two outputs. Since the focus of this report is the changes to the mean state of the climate, the modelling outputs were analysed for inclusion in this report.





6 Changes to future climate

6. Changes to future climate

In this section, we describe and discuss the trends of general climate variables over Tasmania in the simulations of future climate. Changes to mean values of daily maximum temperature, daily minimum temperature, cloud, radiation, humidity and evaporation show a relatively simple response to greenhouse forcing, and are described concisely in this section. Changes to rainfall are more complex and are influenced by a wider range of mechanisms. Therefore, changes to rainfall are described in more detail in this section, followed by a full discussion of changes to rainfall drivers that affect rainfall in Section 7.

6.1 Temperature

The Climate Futures for Tasmania modelling projections show an increase in annual mean screen temperature under both emissions scenarios (Figure 6.1). The rise in mean temperature is relatively uniform over Tasmania, despite the strong horizontal gradients in mean temperature associated with variations in elevation. There is a similar pattern of increase in daily maximum screen temperature (Figure 6.2) and in daily minimum temperature (Figure 6.3). There is more spatial diversity in the change in temperature in each season than in the annual change (Figure 6.4). It is likely that these seasonal patterns are related to changes in the dominant wind across Tasmania outlined in Section 7. For example, the gradient in temperature change in summer (greater increase near the west coast) may be related to the projected reduction in the dominant westerly wind, bringing cool air off the ocean.

The temperature trends are similar under both emissions scenarios until around 2025, where modelled temperatures in each emissions scenario begin to diverge (Figure 6.1 to Figure 6.3). However, the range of projected temperature from the six models for each emissions scenario overlap until about 2070. The range of temperature shown in these figures is defined by the warmest and coldest simulation for that emissions scenario in that year. The inter-model range in temperature is tighter than the global climate models (GCM) responses for the globe presented in the IPCC Fourth Assessment Report (Meehl et al 2007), both for the present climate and in to the future. This reduced inter-model range is due to the modelling strategy we used, which included a bias-adjustment of sea surface temperature prior to the downscaling process, causing the sea-surface temperature boundary condition from each parent GCM to correctly reflect observed climate during the 1961 to 1990 reference period.

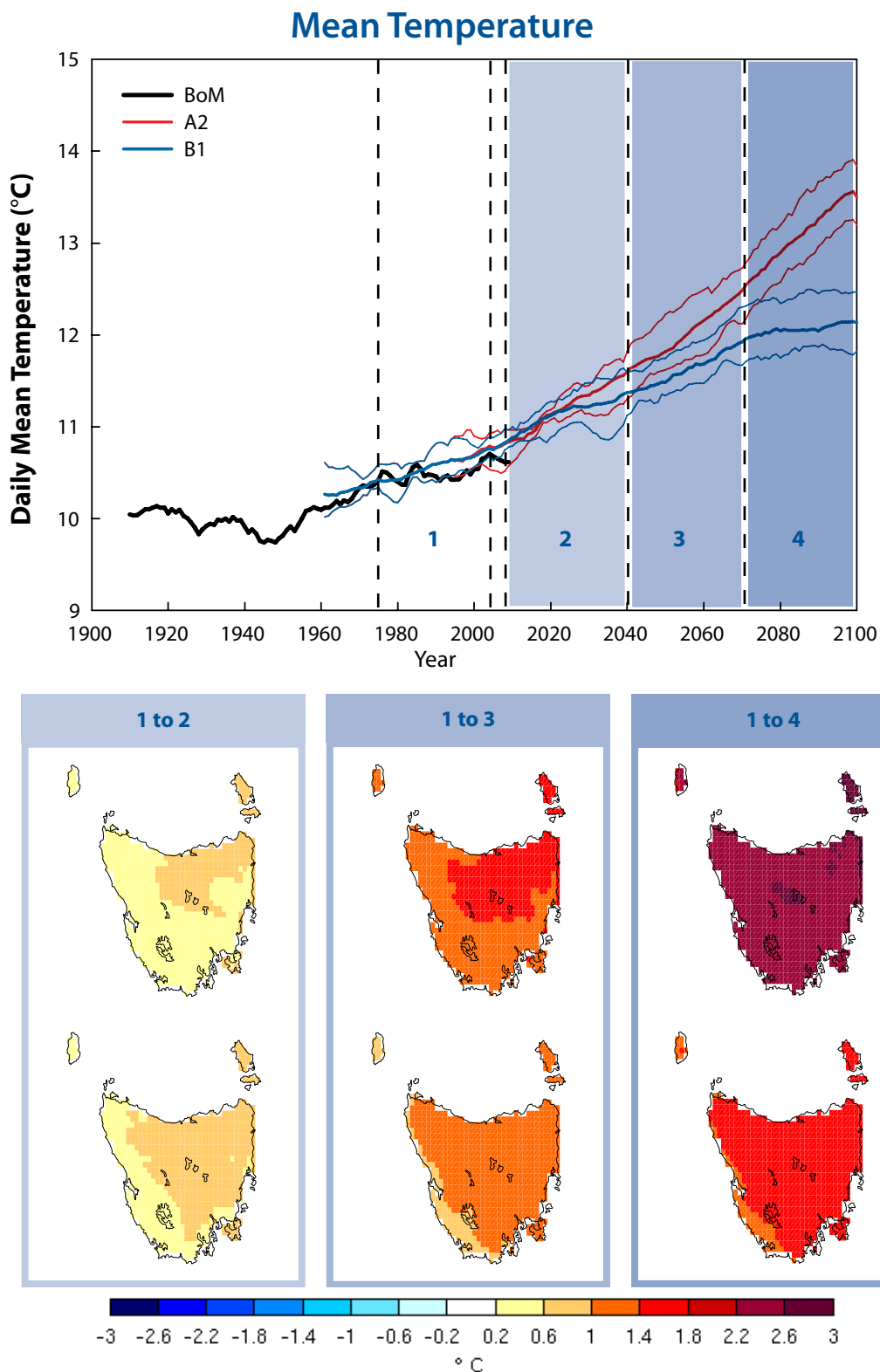


Figure 6.1 Mean screen temperature from the Bureau of Meteorology high-quality climate site data for Tasmania and from downscaled modelling simulations under the A2 and B1 emissions scenarios. The time series plot shows the 11-year moving average for the high-quality climate site data (black line), the six-model-mean (A2 = bold red line, B1 = bold blue line) and the range of the six models (respective faint lines). The maps show the spatial distribution of the six-model-mean of the temperature rise between periods marked by numerals (1 = 1978-2007, 2 = 2010-2039, 3 = 2040-2069, 4 = 2070-2099). The range of temperature shown in these figures is defined by the warmest and coldest simulation for that emissions scenario in that year.

Daily Maximum Temperature

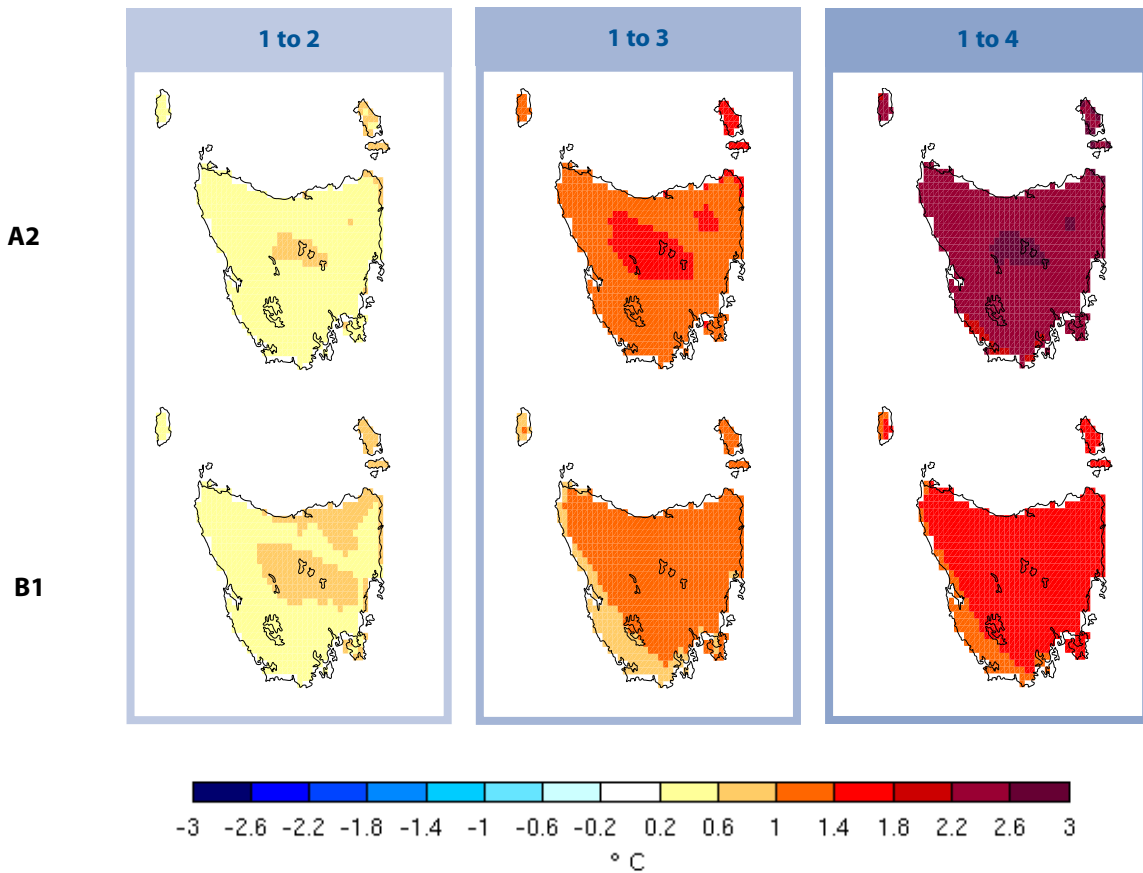
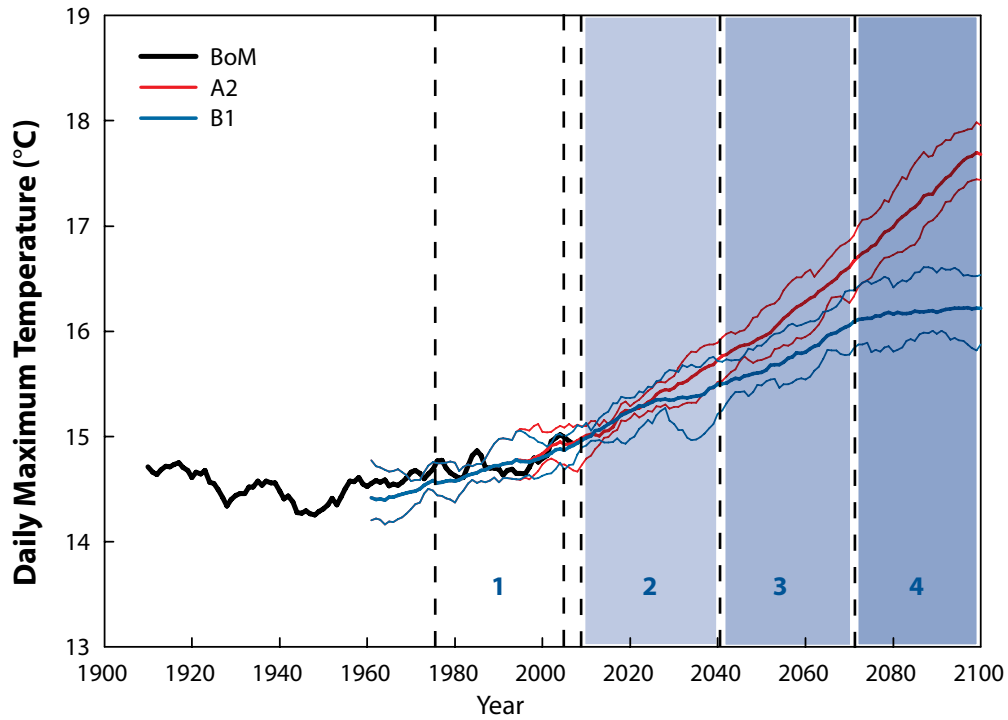


Figure 6.2 Mean daily maximum screen temperature from the Bureau of Meteorology high-quality climate site data for Tasmania and from downscaled modelling simulations under the A2 and B1 emissions scenarios. The time series plot shows the 11-year moving average the high-quality climate site data (black line), the six-model-mean (A2 = bold red line, B1 = bold blue line) and the range of the six models (respective faint lines). The maps show the spatial distribution of the six-model-mean of the temperature rise between periods marked by numerals (1 = 1978-2007, 2 = 2010-2039, 3 = 2040-2069, 4 = 2070-2099). The range of temperature shown in these figures is defined by the warmest and coldest simulation for that emissions scenario in that year.

Daily Minimum Temperature

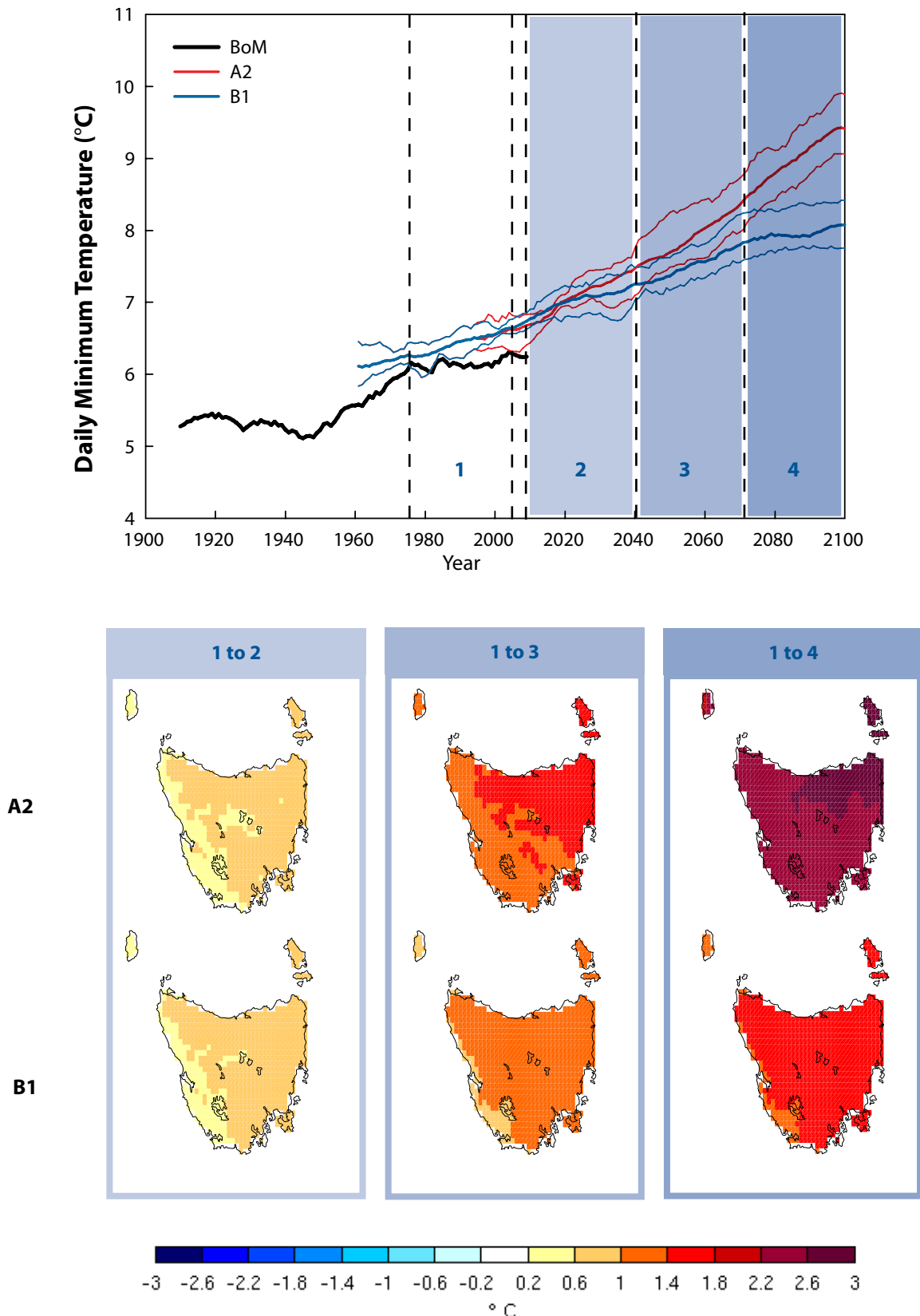


Figure 6.3 Mean daily minimum screen temperature from the Bureau of Meteorology high-quality climate site data for Tasmania and from downscaled modelling simulations under the A2 and B1 emissions scenarios. The time series plot shows the 11-year moving average the high-quality climate site data (black line), the six-model-mean (A2 = bold red line, B1 = bold blue line) and the range of the six models (respective faint lines). The maps show the spatial distribution of the six-model-mean of this temperature rise between periods marked by numerals (1 = 1978-2007, 2 = 2010-2039, 3 = 2040-2069, 4 = 2070-2099). The range of temperature shown in these figures is defined by the warmest and coldest simulation for that emissions scenario in that year.

Seasonal Temperature

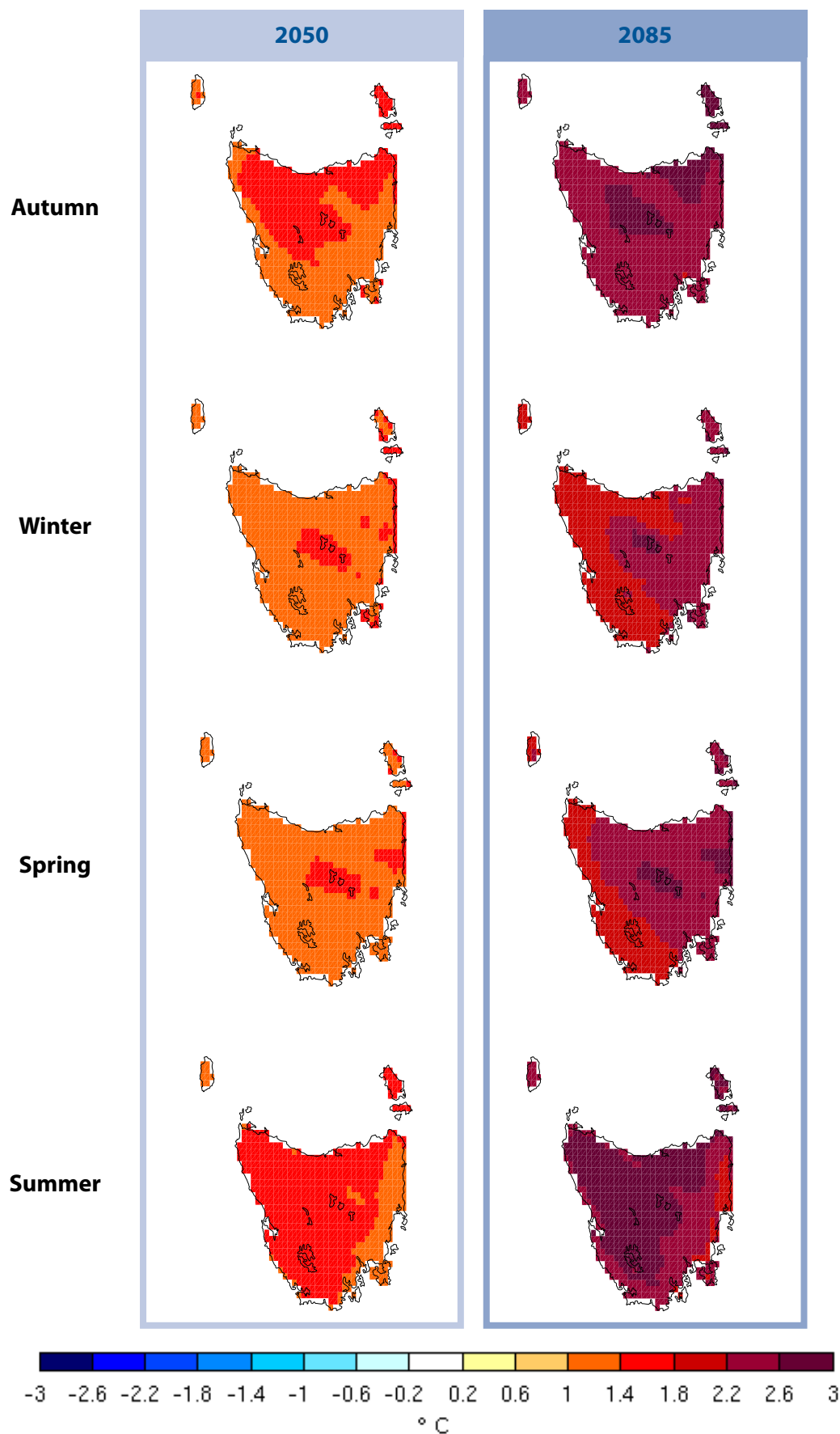


Figure 6.4 Daily maximum temperature differences between the six-model-mean in the baseline period 1978-2007 and two future periods centred on the years indicated (2050 = 2035-2064, 2085 = 2070-2099) under the A2 emissions scenario for each season.

Table 6.1 Projected changes under two emissions scenarios for Tasmanian mean, daily maximum and daily minimum temperatures between 1980 to 1999 and 2090 to 2099. Shown are the six-model-mean and the modelling range (highest and lowest).

Scenario and variable	Six-model-mean (°C)	Lowest model (°C)	Highest model (°C)
A2			
Mean Temp	2.88	2.59	3.30
Daily max. temp	2.84	2.66	3.23
Daily min. temp	2.89	2.51	3.36
B1			
Mean Temp	1.56	1.26	1.99
Daily max. temp	1.51	1.22	1.94
Daily min. temp	1.60	1.29	2.06

To quantify the temperature change over the 21st century, accounting for the steep upward trend toward the end of the century, it is common to report on the temperature change between the periods 1980 to 1999 and 2090 to 2099 (For example, IPCC 2007). All three temperature variables increase between these dates (Table 6.1). The six-model-mean changes in mean temperature are 2.9 °C (model range 2.6 °C to 3.3 °C) for A2 and 1.6 °C (model range 1.3 °C to 2.0 °C) for B1. The daily maximum temperature rise is slightly lower than for the minimum temperature in both emissions scenarios. The lower rate of warming of the daily maximum temperature compared with minimum daily temperature is consistent with greenhouse warming and analyses of observations globally (Trenberth et al 2007).

Projected changes to temperature are not only of an increase in the mean, but can also include a change in the shape of the frequency distribution. This means a change in the nature of the temperature distribution and a relative change in the incidence of days of different temperatures. This is particularly important for changes in the incidence of both hot and cold temperature extremes. An analysis of changes in the frequency distribution of temperature is included in the extreme events report (White et al 2010).

6.2 Rainfall

For the A2 emissions scenario (high), the six-model-mean total annual rainfall for Tasmania shows changes of less than 100 mm over the entire period of the modelling simulations (Figure 6.5a). The small change in the mean rainfall is due in part to the damping effect of averaging projections from six models. However, the smoothed time series for each individual model also show changes of

less than 250 mm or 20% (Figure 6.5b), with some showing a predominantly negative trend and others showing a predominantly positive trend, relative to the baseline period. The spatial pattern of rainfall change is indicated by the mean difference across the six models between baseline and future periods (Figure 6.5c). The mean of the six projections shows a steadily emerging pattern of drying in the central highlands and parts of the north-west, and an increase in rainfall on the east and west coasts.

The changes in rainfall under the B1 emissions scenario have a similar spatial pattern but are smaller in magnitude than the change under the A2 emissions scenario (Figure 6.6). The spatial correlation between the maps of rainfall change for the two emissions scenarios (Appendix 3) shows that the patterns of change by 2010-2039 for both emissions scenarios are very similar (correlation coefficient 0.97). For later periods, all of the spatial patterns of change between the A2 and B1 emissions scenarios still have a high correlation ($R^2 > 0.8$) for each period. This result means that the same general pattern of change can be expected for rainfall for the range of emissions scenarios examined in this work.

The range of rainfall change in the six different models is indicated by a measure of normalised standard deviation (Figure 6.6, small plots). These plots show that the normalised standard deviation between the six models is generally less than 5%, but is up to 9% in the north-east coast. The range of the six different models is also seen in maps of change in rainfall by the end of the century for each separate modelling simulation (Figure 6.7). There is a range of responses seen, however some of the most marked changes are present in virtually all modelling simulations, such as a reduction in rainfall in the central plateau region.

Annual Rainfall

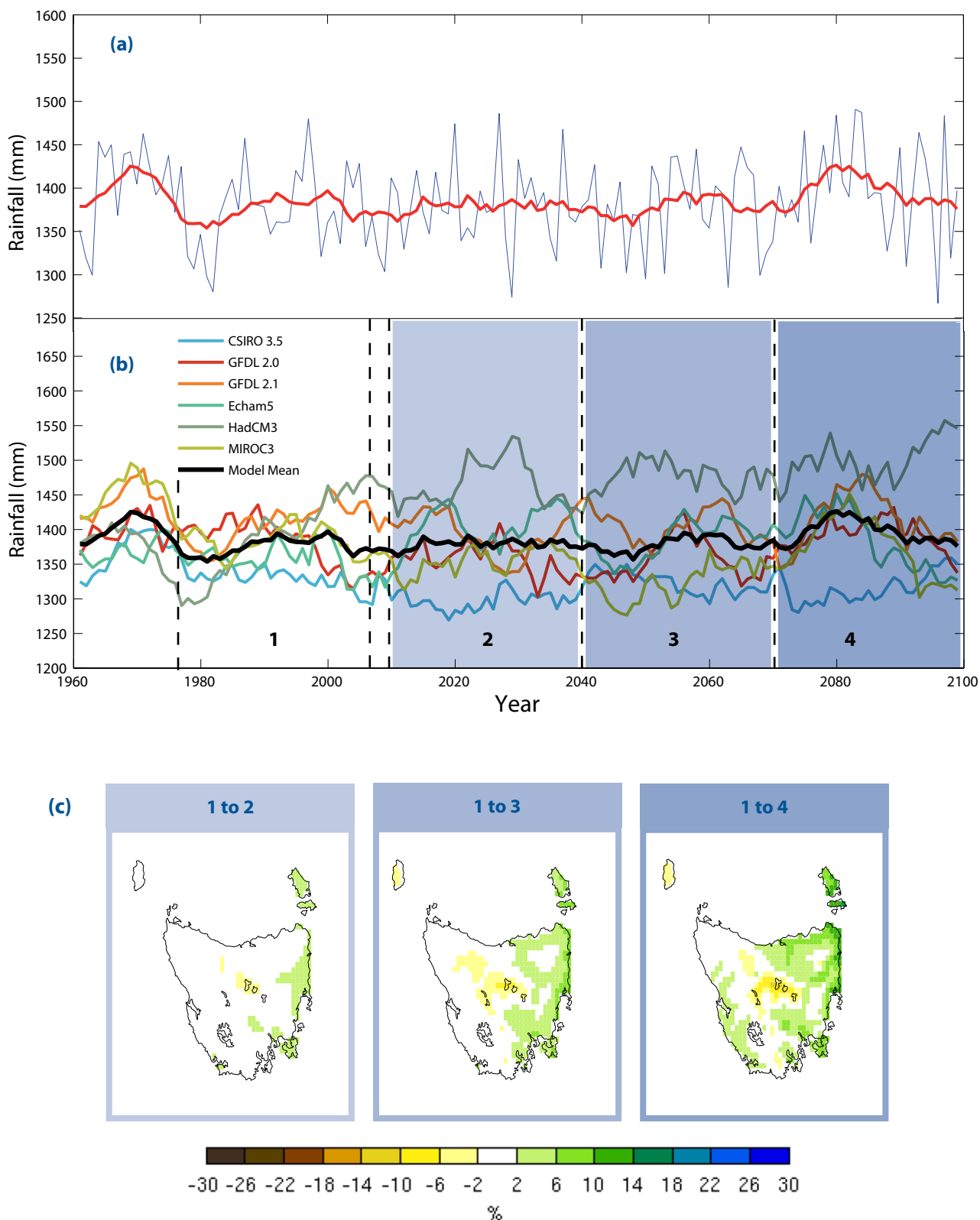


Figure 6.5 Total annual rainfall projections for Tasmania under the A2 emissions scenario. (a) Six-model-mean rainfall for the period 1961-2100 (blue line) and the 11-year moving average (red line). (b) 11-year moving average of total annual rainfall from six models (multiple coloured lines) and the six-model-mean (black line). (c) Maps of the six-model-mean proportional change in rainfall between 30-year periods indicated by numerals (1 = 1978-2007, 2 = 2010-2039, 3 = 2040-2069, 4 = 2070-2099).

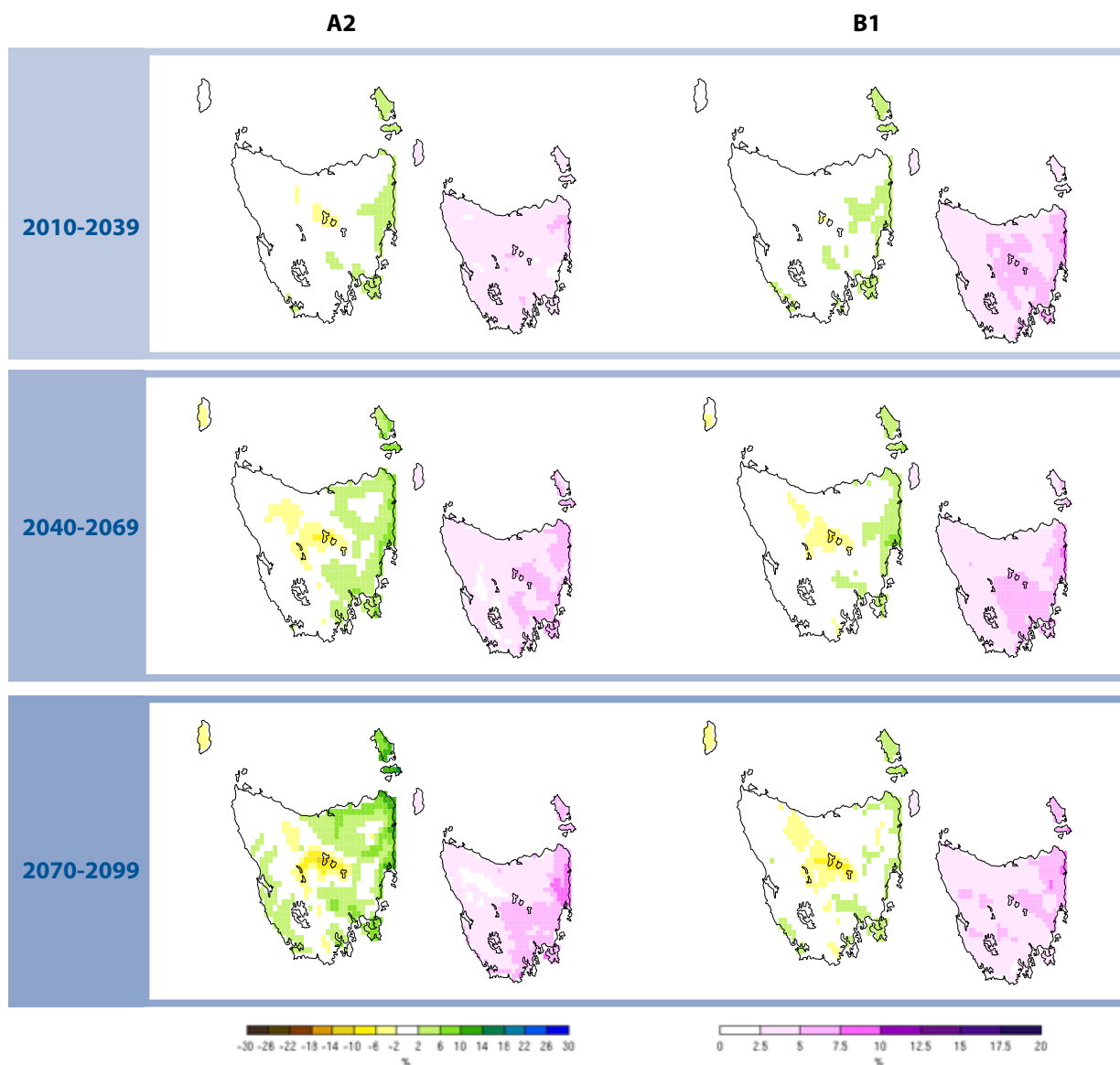


Figure 6.6 Maps of the six-model-mean proportional change in total annual rainfall between 1978-2007 and the periods indicated for the A2 emissions scenario and the B1 emissions scenario. The smaller maps next to each plot show the standard deviation of the proportional change of the six modelling simulations.

The pattern of change in annual total rainfall over Tasmania is the sum of four distinct and much larger amplitude changes in seasonal rainfall patterns. This effect is reflected in the change by the end of the century in all four seasons for the A2 emissions scenario (Figure 6.8). In summer and autumn, there is a strong rainfall reduction in the west and an increase along a strip down the east coast. Whereas in winter and spring, there is an increase in rainfall in the west and a slight reduction in most of the east coast. The reduction in rainfall in the central plateau appears consistent through all seasons. The standard deviation of the six models (Figure 6.8, small map plots) is generally less than 10%, but is up to 20% for the rainfall increase in the east and north-east in summer and autumn. This indicates that each the range between the six models is greatest for these regions in these seasons.

Just as with the changes to annual total rainfall, the changes in seasonal rainfall are similar in spatial pattern but with a smaller magnitude under the B1 emissions scenario compared to the A2 emissions scenario (Figure 6.9). The rainfall changes in summer and winter are larger in the A2 emissions scenario, and appear mainly after 2050 (Figure 6.9).

Tasmanian total rainfall is strongly affected by the high rainfall region in the west (the West Coast, South Coast and Highlands District). Sites in this district receive up to five times the annual rainfall of sites in other districts. Figure 6.10 presents time series of annual rainfall anomalies averaged over a set of grid cells that approximate three individual forecast districts (see Figure 2.1 for definitions). The plot for the West Coast, South Coast and Highlands District reflects the overall mean Tasmanian changes, with an increase in winter and a decrease in summer after 2050.

Annual Rainfall

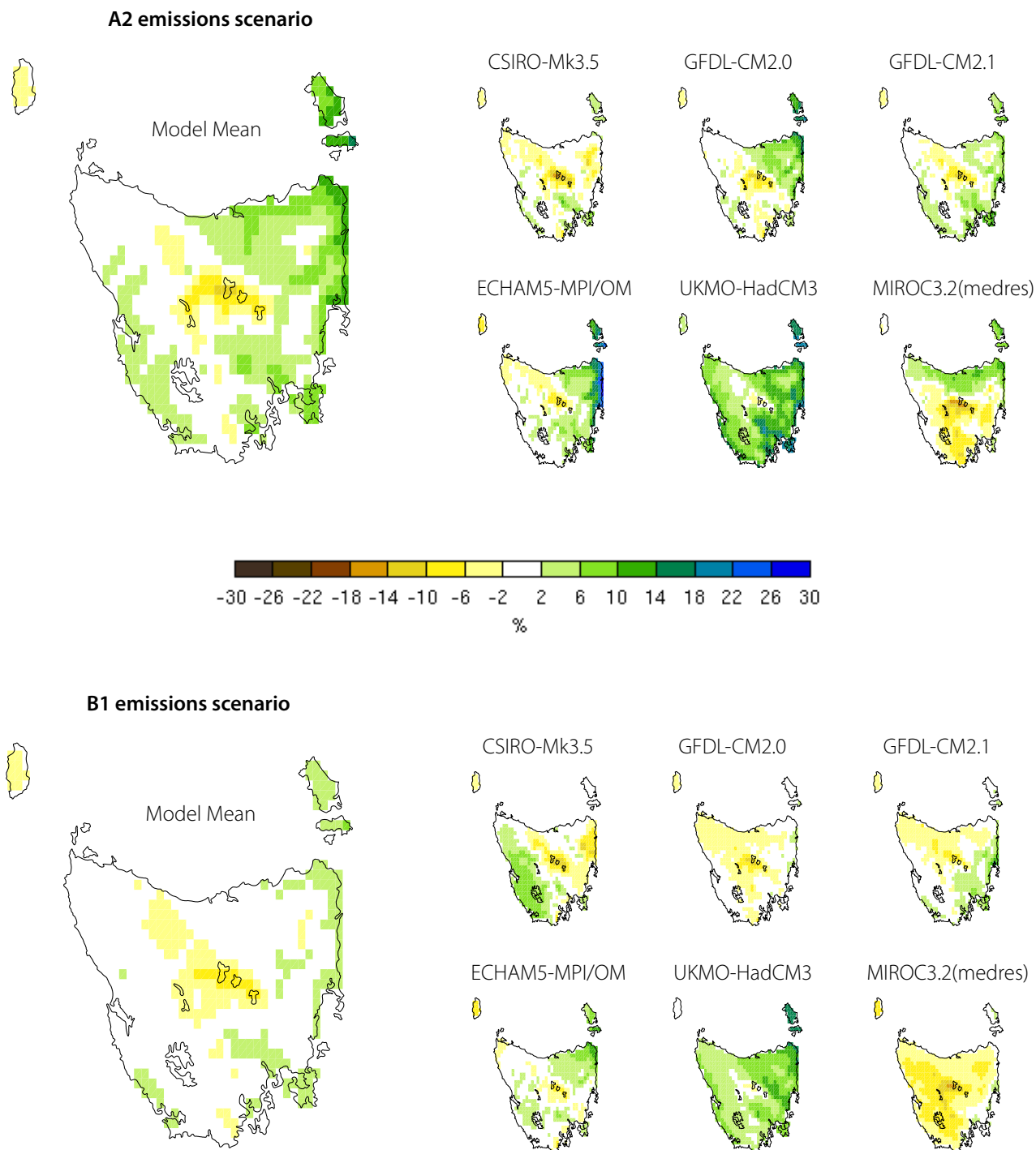


Figure 6.7 Maps of the proportional change in mean annual rainfall between 1978-2007 and 2070-2099 for the B1 emissions scenario and A2 emissions scenario for each modelling simulation (smaller maps at right), and six-model-mean (the larger maps at left).



Seasonal Rainfall

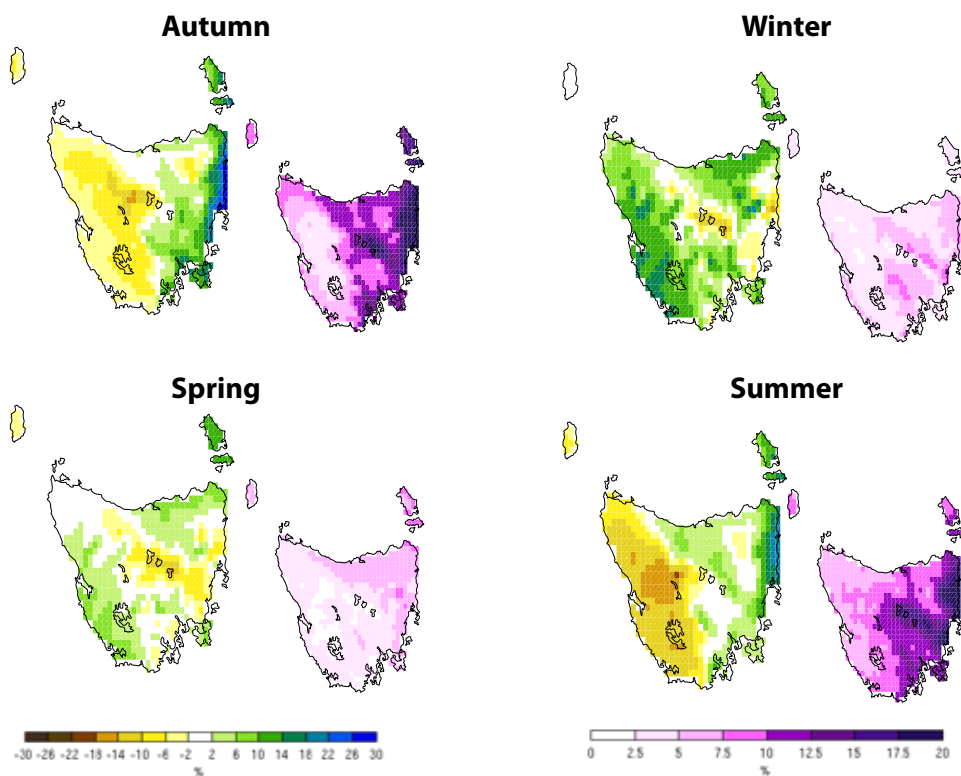
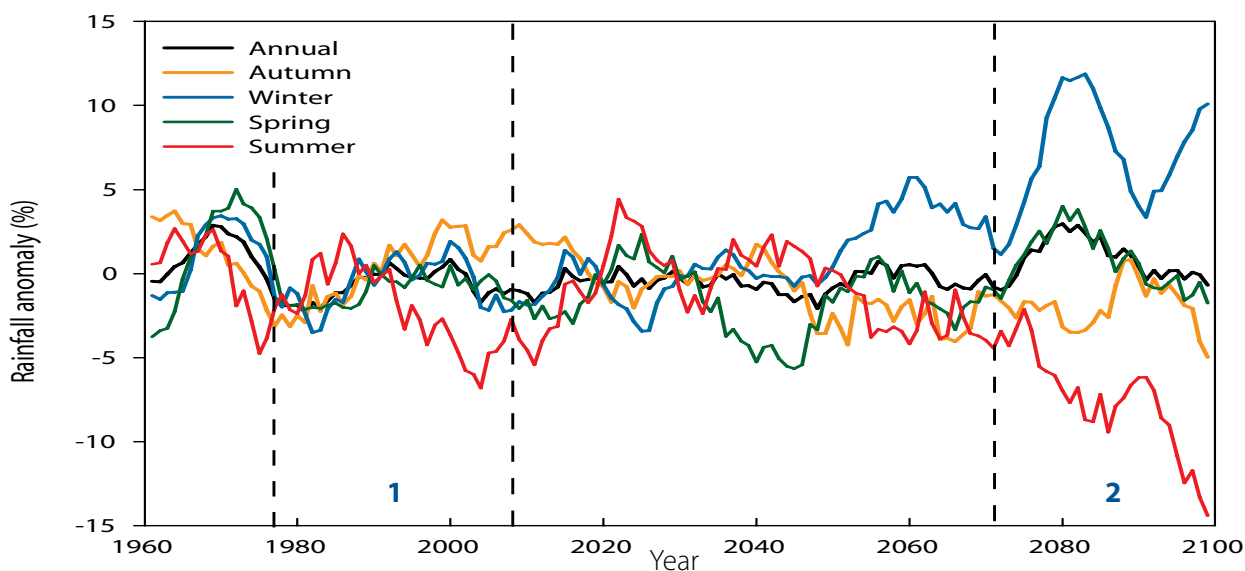
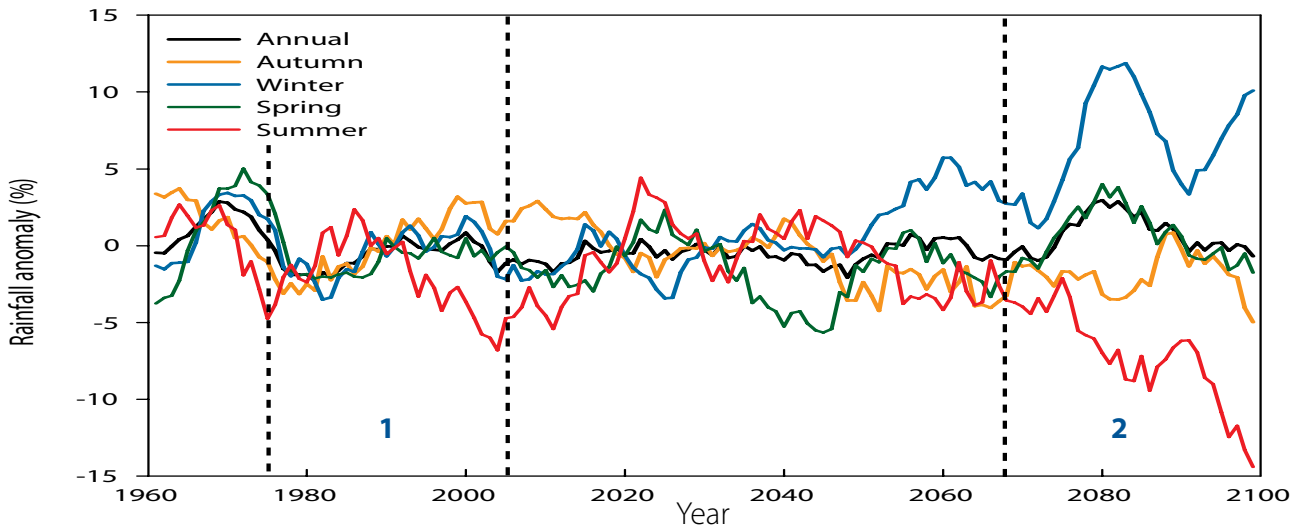


Figure 6.8 Six-model-mean Tasmanian rainfall under the A2 emissions scenario for each season. (a) Time series of the six-model-mean Tasmanian rainfall for each season, plotted as an 11-year moving average of the anomaly from the 1961-1990 mean. (b) Maps of the proportional change between Period 1 (1978-2007) and Period 2 (2070-2099). The small maps next to each plot show the standard deviation of the proportional change of the six modelling simulations.



Seasonal Rainfall



A2 Emissions Scenario

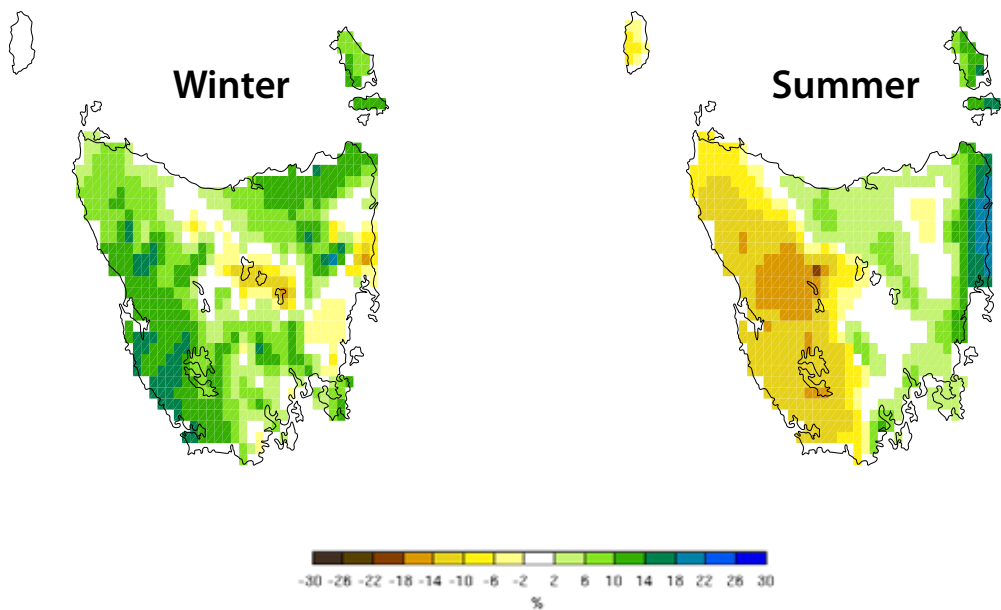
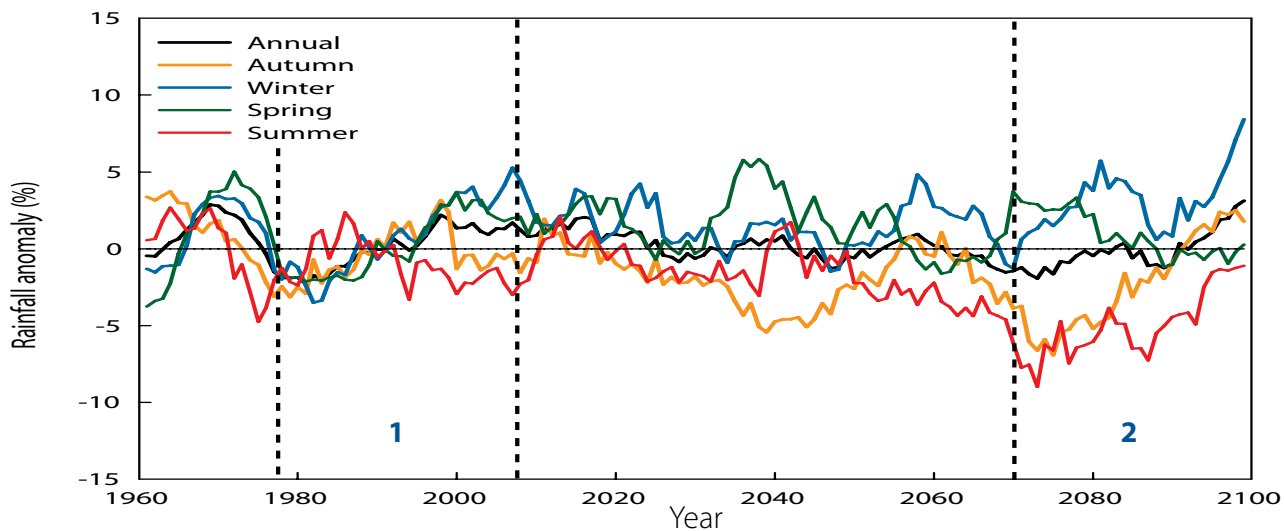


Figure 6.9 The time series of the six-model-mean Tasmanian rainfall anomaly under the A2 emissions scenario, plotted as an 11-year moving average of the anomaly from the 1961-1990 mean for annual rainfall (black lines) and for each calendar season (coloured lines). The maps show the spatial pattern of change between Period 1 (1978-2007) and Period 2 (2070-2099) for winter and summer.

Seasonal Rainfall



B1 Emissions Scenario

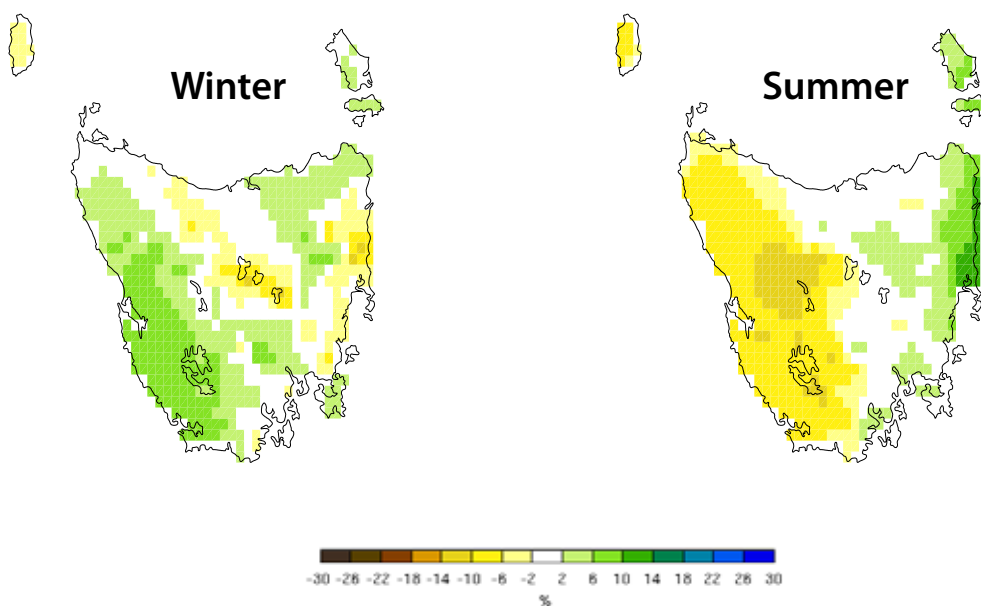


Figure 6.9 *cont.* The time series of the six-model-mean Tasmanian rainfall anomaly under the B1 emissions scenario, plotted as an 11-year moving average of the anomaly from the 1961-1990 mean for annual rainfall (black lines) and for each calendar season (coloured lines). The maps show the spatial pattern of change between Period 1 (1978-2007) and Period 2 (2070-2099) for winter and summer.

The plot for the Central Plateau and Upper Derwent Valley District shows a steady decrease in all seasons to 2100. The plot for the East Coast District shows a steady increase in rainfall in summer and autumn to 2100.

Some models show a different sign of change in rainfall compared to the six-model-mean for a particular location. However, the strongest changes are consistent across the range of all models, as shown by the mean and standard deviation values from the six models for individual districts (Figure 6.11).

There are not only changes to the mean rainfall, but also changes to the rainfall distributions. Changes to the periodicity of rainfall and the incidence of high intensity events are as important as the change to the mean for some areas. Further analysis of rainfall periodicity and distribution, including extremes and drought, is included in the extreme events report (White et al 2010).

6.3 Historic context of rainfall changes

Tasmanian annual rainfall from observations and the modelling projections under the A2 emissions scenario for the period 1900 to 2100 are shown in Figure 6.12. Observations are from 1900 to 2007 (high-quality rainfall data) and modelling simulations are from 1961 to 2100. The time series of simulated rainfall over the historical period is in the same range as in the observed rainfall, with no periods of extraordinarily high or low rainfall relative to observations. Each simulation generally shows a lower level of inter-annual variability than the observations (Fig 6.12a), although the range across the six models represents a range comparable to the natural variations in observed data (Fig 6.12c). There are few rainfall changes in the six modelling projections to 2100 that are as large or sustained as the decline from 1975 to the present seen in the observations. The modelling time series that most closely resembles the observations over the period of overlap, MIROC3.2(medres), by coincidence shows a

District Rainfall

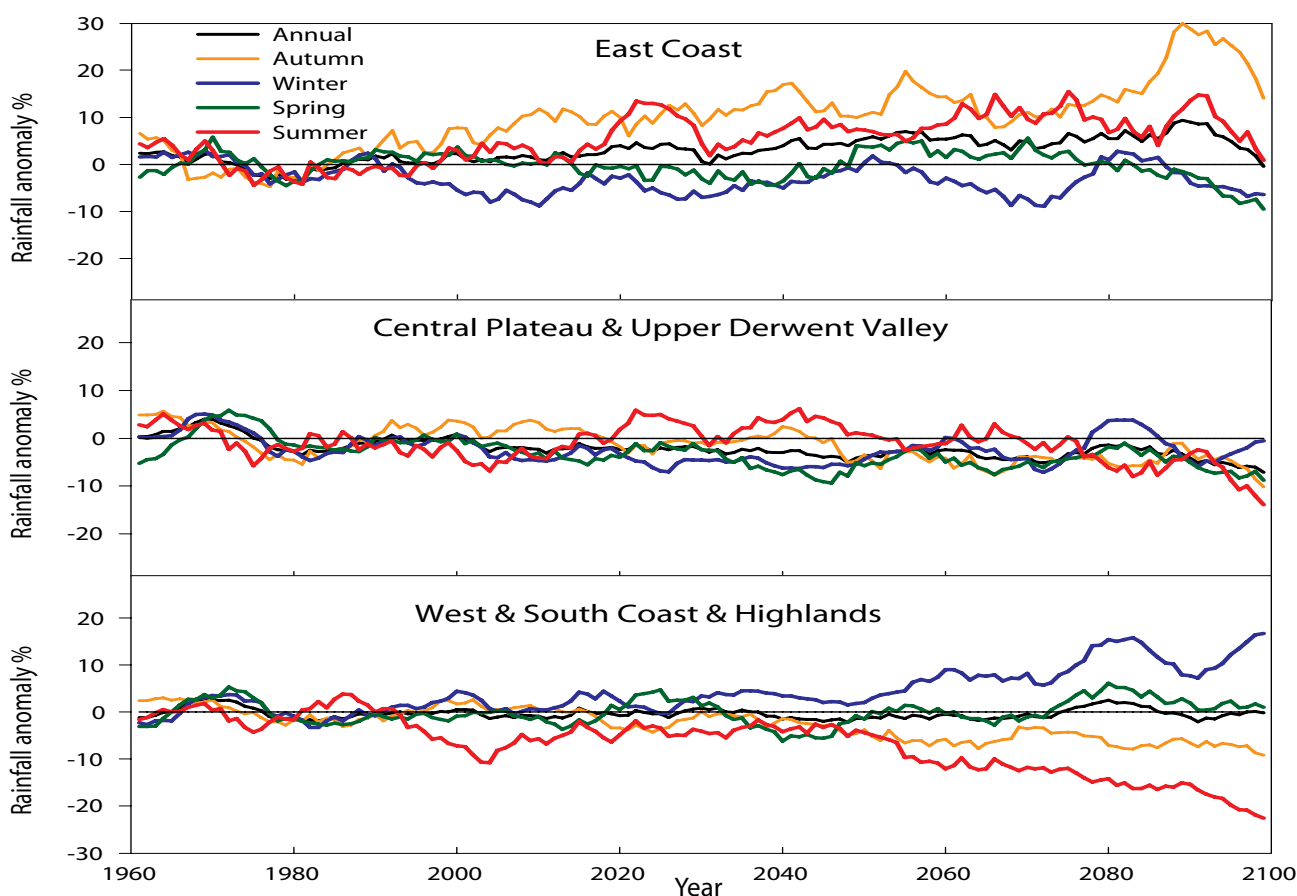


Figure 6.10 Time series of the six-model-mean 11-year moving average proportional rainfall anomaly from the 1961-1990 mean in three Bureau of Meteorology forecast districts under the A2 emissions scenario. The plots are for each calendar season (coloured lines) and annually (black lines).

similar decline in total annual rainfall between 1975 and 2007 (Figure 6.12b). Overall, the relatively small changes in the trend in rainfall over Tasmania, and the presence of long term trends (of varying sign) in the simulations, leads to the conclusion that within the uncertainty the long-term annual mean rainfall over Tasmania is likely to remain at current levels through to 2100. That is approximately 1390 mm plus or minus 200 mm per year.

While the projections show mean annual rainfall for Tasmania has only weak or negligible trends, there are strong trends in seasonal and regional rainfall. The time series of rainfall total for each season from the high-quality rainfall data and the modelling projections are shown in Figure 6.13. Autumn rainfall has shown the largest change of any season on a Tasmania-wide basis in the last 30 years. The modelling simulations do not show a rainfall decline between 1975 and 2007 that matches the observed record. However, the range of the projections is similar to the total range in the observed record, and

indicates that rainfall reductions of similar magnitude are possible throughout the modelling projections in autumn. This suggests that reduced autumn rainfall, similar to the recent observed period, is not an ongoing climate state to 2100 due to climate change. However, as outlined above, there are larger changes of rainfall in winter and summer than in autumn in the modelling projections (Figure 6.13). The changes in these seasons after 2050 are larger than any of the changes in the observed record.

It should be noted that these Tasmania-wide changes are almost entirely a function of the high rainfall region in the west and south-west, and do not directly reflect changes in the other six districts (Figure 2.1). Significant changes in other districts include steady decreases in all seasons in the central plateau, as well as an increase in summer and autumn rainfall in the east. The main changes in rainfall described here are related to remote climate drivers described in Section 7.

District Rainfall

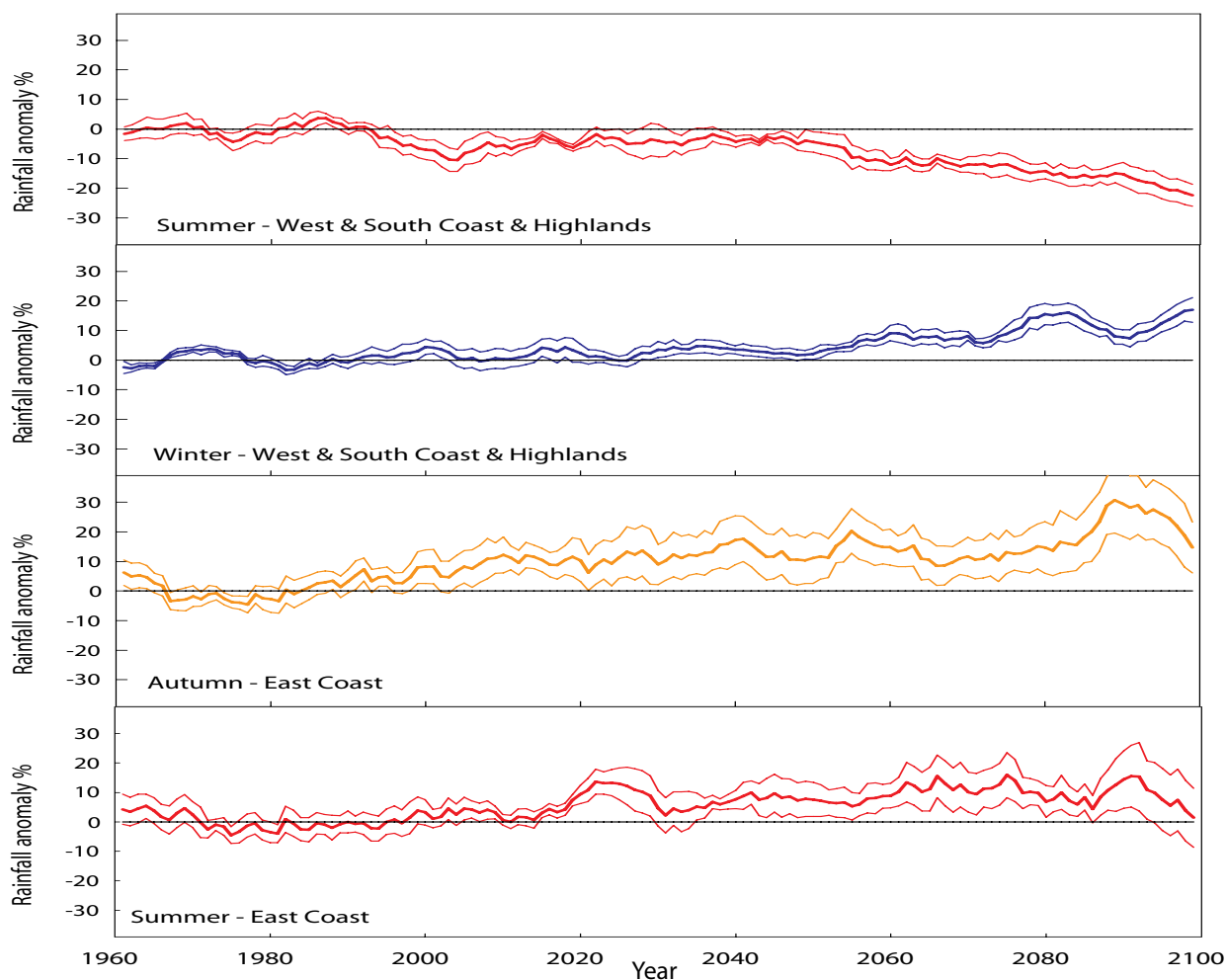


Figure 6.11 Rainfall anomaly (%) from the 1961-1990 mean value under the A2 emissions scenario for Bureau of Meteorology forecast districts for individual seasons (as marked). The bold lines show the six-model-mean, the faint lines show the mean, plus and minus the standard deviation of the six models.

Annual Rainfall

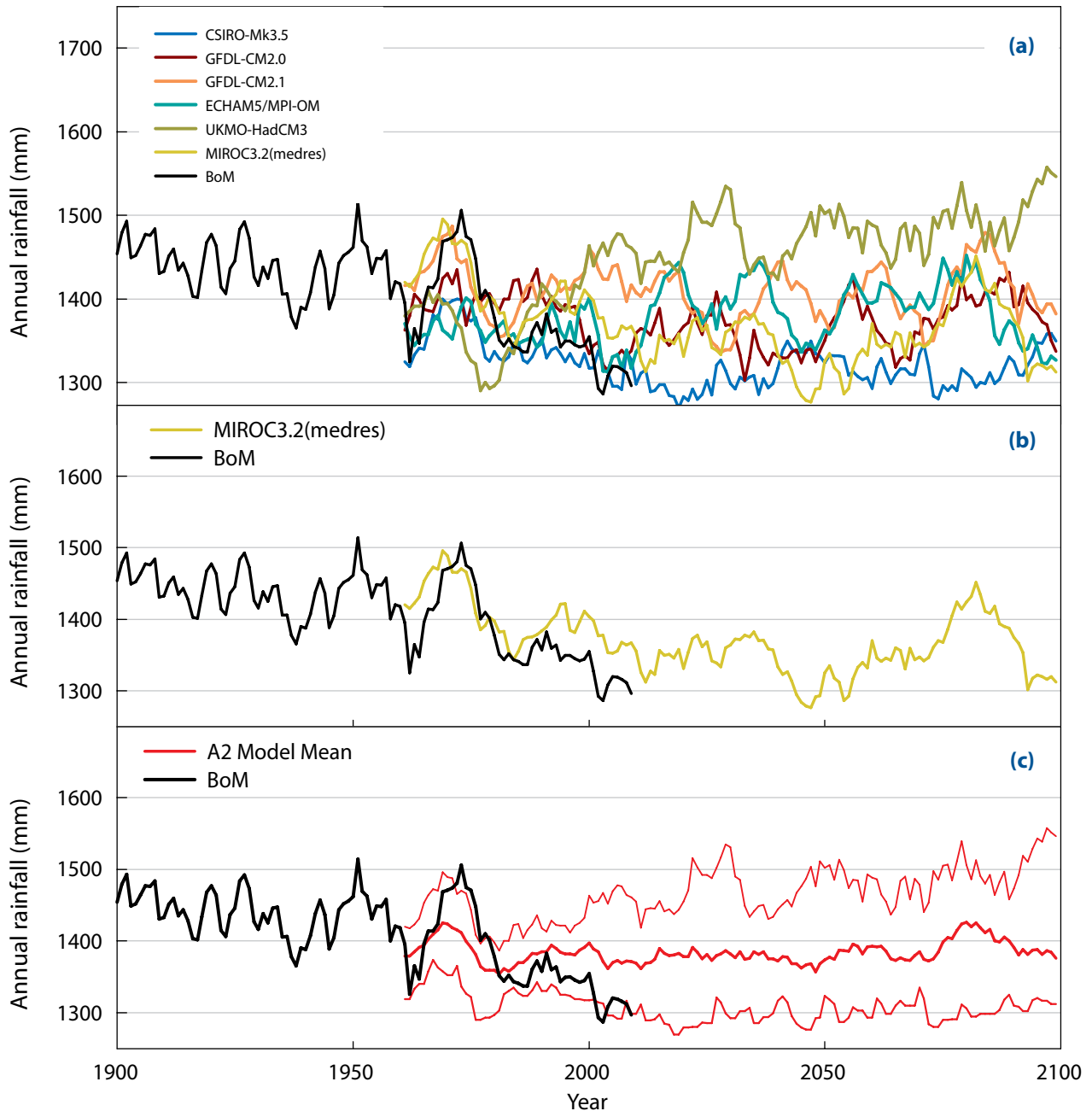


Figure 6.12 Time series of the 11-year moving average of annual total rainfall for Tasmania for the period 1900-2100 from Bureau of Meteorology high-quality rainfall data (black lines) and six downscaled modelling simulations under the A2 emissions scenario (coloured lines) for (a) each modelling simulation, (b) an example modelling simulation MIROC3.2(medres) and (c) the six-model-mean and modelling range (highest and lowest).



Seasonal Rainfall

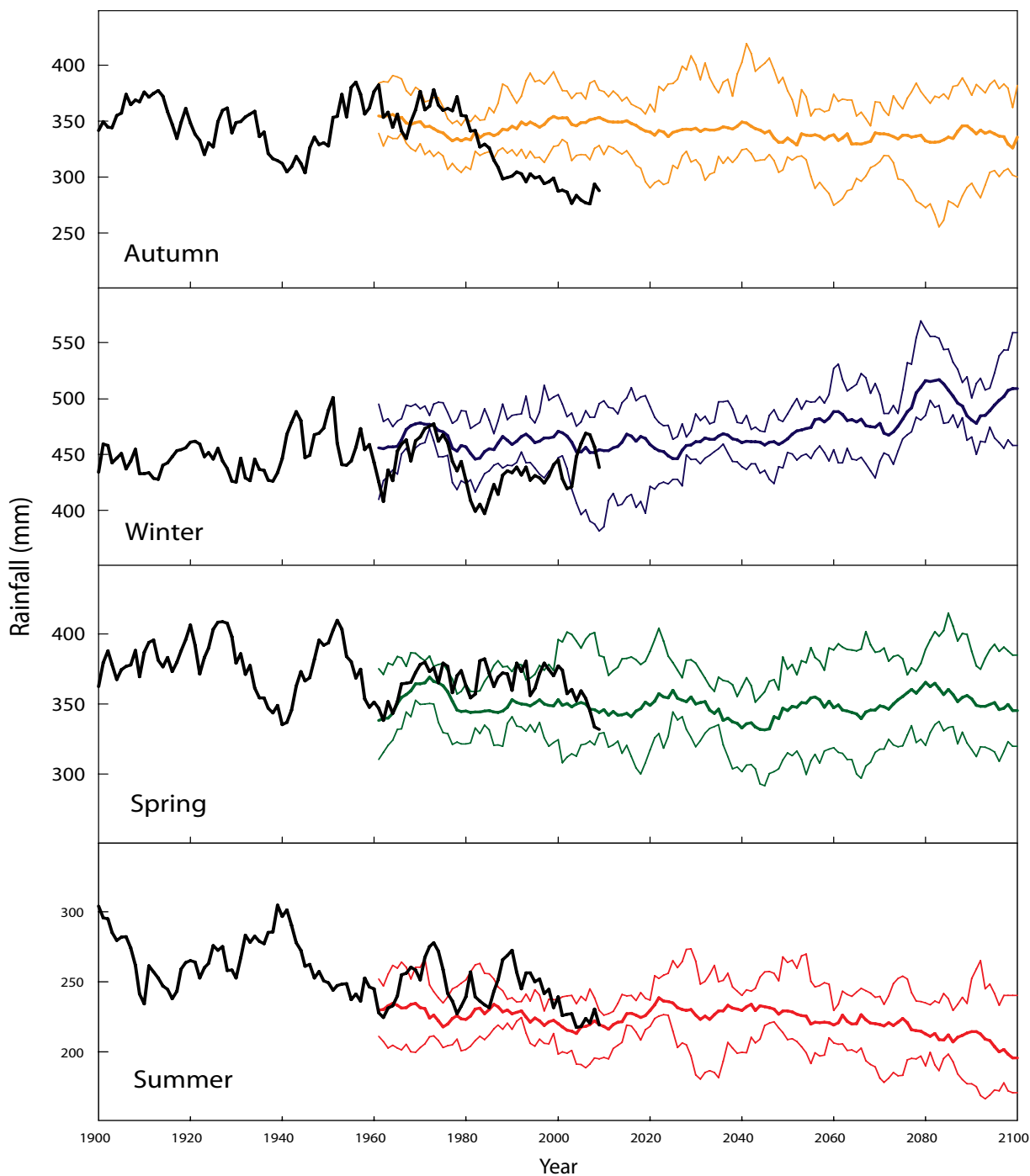


Figure 6.13 Time series of the 11-year moving average of total rainfall in each season for Tasmania for the period 1900-2100 from Bureau of Meteorology high-quality rainfall data (black lines), six-model-mean of the downscaled modelling simulations (bold coloured lines) and the modelling range (highest and lowest) under the A2 emissions scenario.

6.4 National and global context of temperature and rainfall changes

The changes to temperature and rainfall described in this report are consistent with the magnitude of mean changes projected for the region in global and regional modelling (Meehl et al 2007; Christensen et al 2007) and with the commonly used regional model report and online web tool *Climate Change in Australia* (CSIRO & Bureau of Meteorology 2007). However, the fine-scale modelling produced by Climate Futures for Tasmania has greater spatial resolution and thus provides more useful information at a local scale.

The projected change in mean temperature in Tasmania is less than both the national and global means. Figure 6.14 shows the projected change in mean temperature over the century for the A2 emissions scenario for the globe, the region and Tasmania. It shows the temperature rise is generally greater over land than over ocean, and is greater over inland continental Australia than over the coastal areas, Tasmania or New Zealand. The change in mean temperature under the A2 emissions scenario is 3.4 °C for the whole of the earth's surface (including oceans) and 2.9 °C for Tasmania. The equivalent mean difference for the B1 emissions scenario is 1.8 °C for the globe and 1.6 °C for Tasmania. This difference between the region and the global mean is consistent with global scale modelling from another emissions scenario included in IPCC AR4: for the A1B emissions scenario, projected temperature change was 2.8 °C for the whole earth's surface, 3.0 °C in northern Australasia and 2.6 °C in southern Australasia (Christensen et al 2007).

Annual and seasonal rainfall changes over Tasmania are more complex than changes in some other regions of Australasia and the globe both spatially and seasonally (Figure 6.15). While some areas such as south-west Western Australia show a projected reduction in rainfall over the entire district in all seasons, Tasmania shows a complex spatial pattern comprising both positive and negative changes that vary considerably in each season. The size of the projected Tasmanian rainfall changes is in the mid-range of changes over the nation measured as a proportional change (Figure 6.15). The possible drivers and mechanisms behind these patterns and magnitude of rainfall changes are explored further in Section 7.

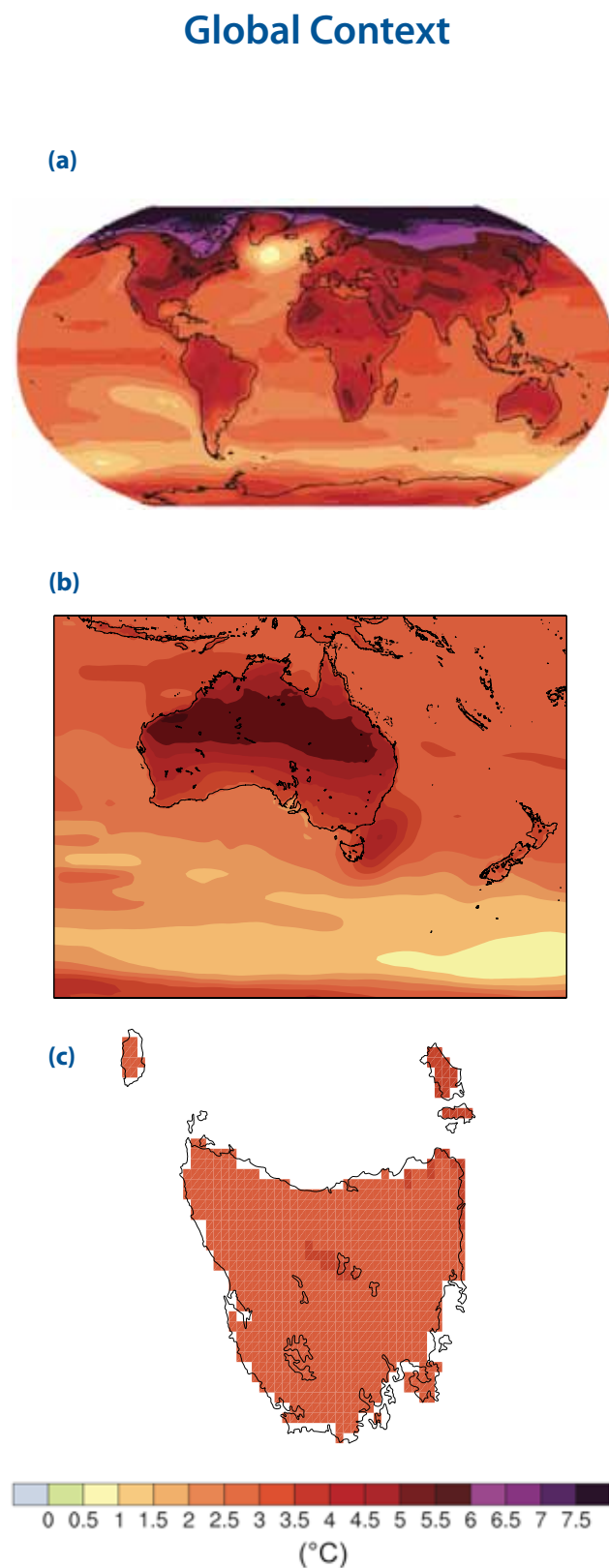


Figure 6.14 The projected difference in mean temperature between 1980-1999 and 2090-2099. (a) the mean of the 23 GCMs for the globe (adapted from IPCC 2007). (b) For the Australian region, the mean of the six 0.5-degree resolution models, (generated from this project). (c) For the Tasmanian land area, the mean of the six 0.1-degree models, (generated by project). NB. panels (b) and (c) are from unadjusted modelling outputs.

Regional Context

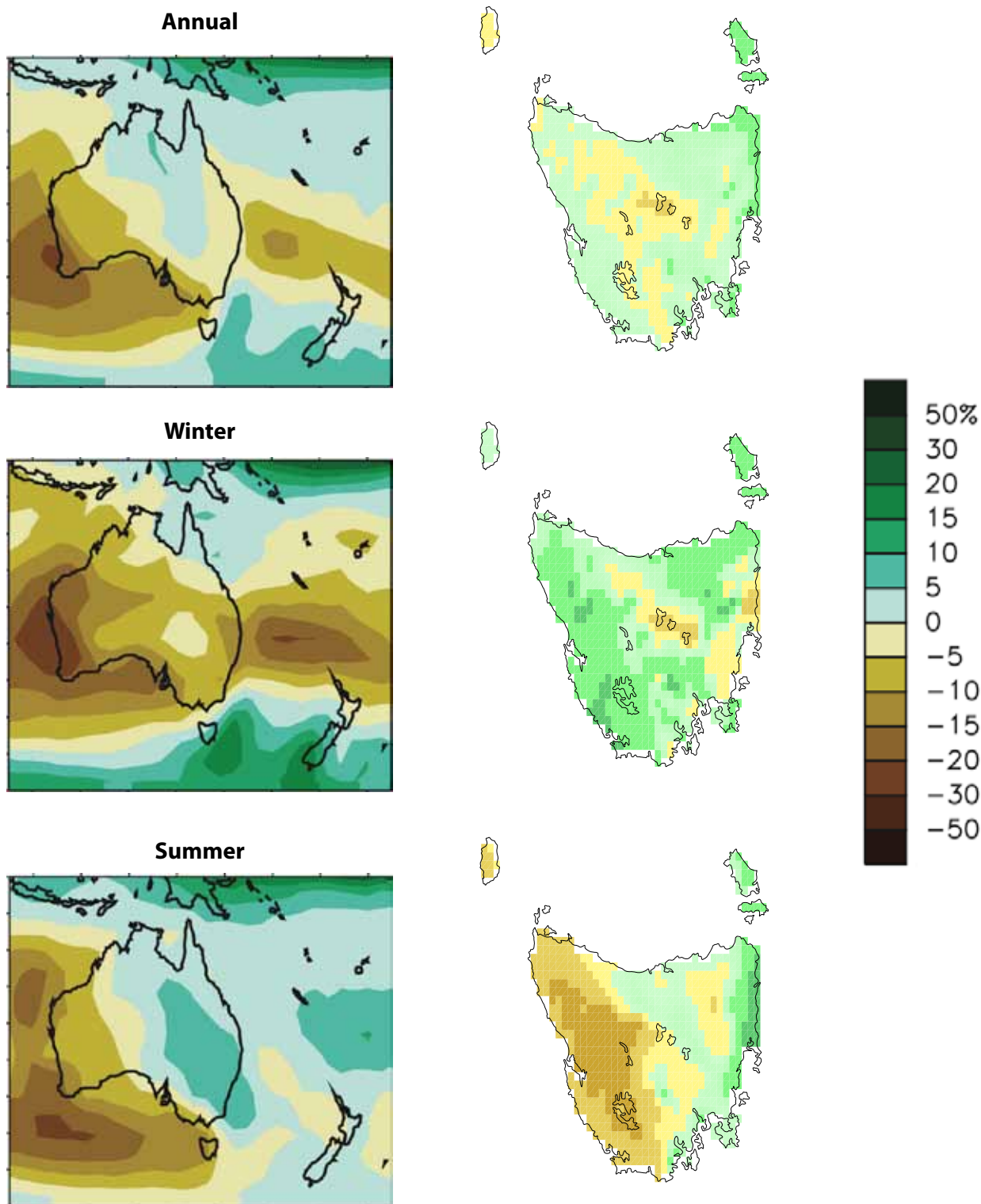


Figure 6.15 The proportional change in precipitation between 1980-1999 and 2080-2099. The left column is the six-model-mean of 21 GCM simulations annually, winter and summer, under the A2 emissions scenario (adapted from Christensen et al 2007). The right column maps are six-model-mean of the downscaled modelling simulations (generated by project).

6.5 Mean wind speed

Change to the average 10-metre wind speed over the land surface of Tasmania under the A2 emissions scenario shows a slight decline (<5%) by the end of the century (Figure 6.16a). The six-model-mean pattern of change is spatially varied (Figure 6.16b) and there are large differences between the spatial patterns of change in the six models (Figure 6.16d). A change in seasonality of mean wind speed is

apparent, with higher speeds in July to October and lower wind speeds in November through to May (Figure 6.16c). Wind speeds and the projected change to wind speeds are greater over the oceans surrounding Tasmania than over the land surface. Analysis of wind at the larger regional scale is found in Section 7.2. Further in-depth analysis of wind speed, wind gusts and wind hazards is included in the special wind report (Cechet et al 2010).

Wind Speed

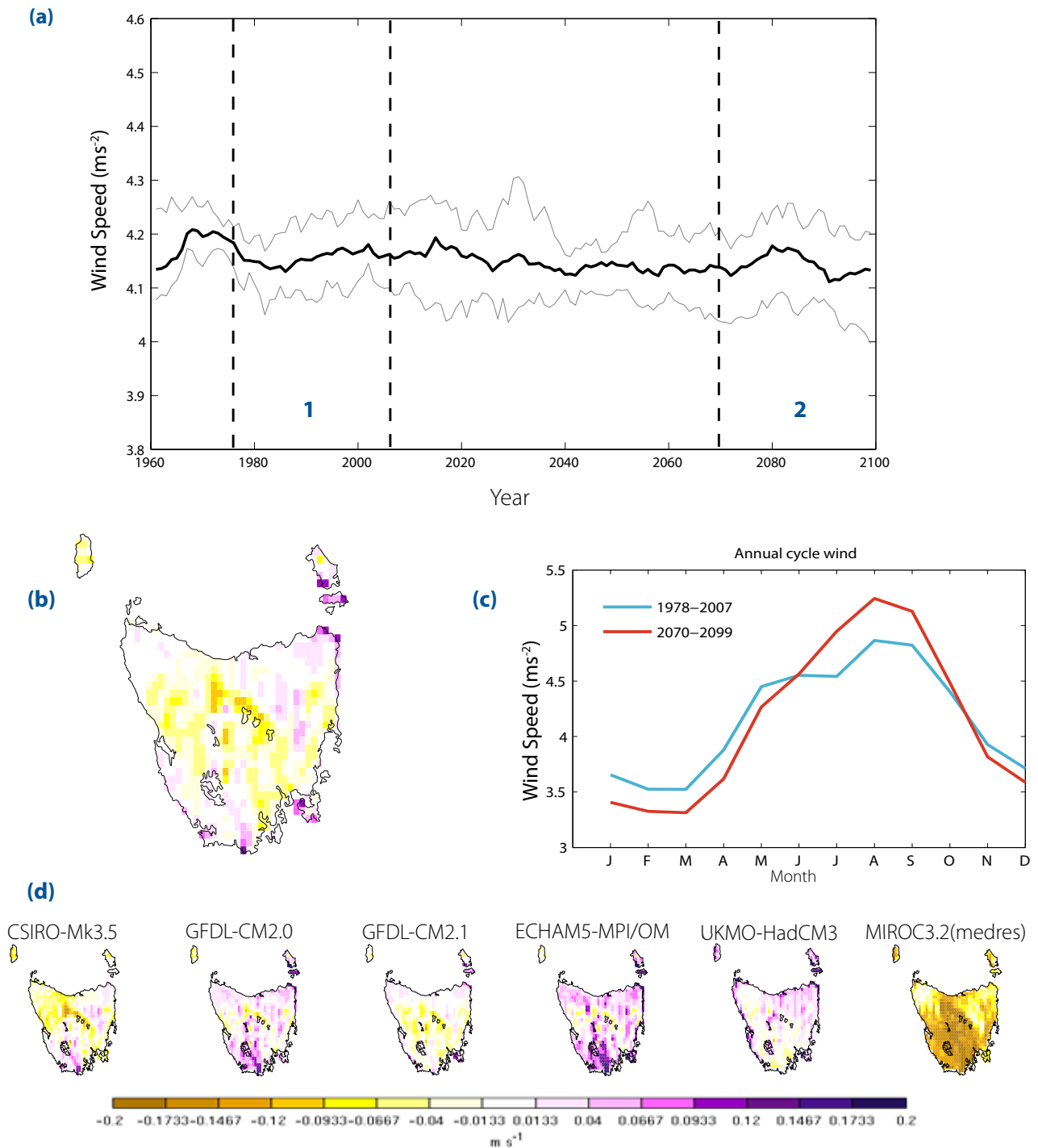


Figure 6.16 Mean 10 m wind speed. (a) The 11-year moving average time series of annual 10 m wind speed over the land surface of Tasmania in the six-model-mean (bold line) and the range of models (highest and lowest) faint lines. (b) The six-model-mean difference between Period 1 (1978-2007) and Period 2 (2070-2099). (c) The mean annual cycle for Tasmania in Periods 1 and 2. (d) The difference between Periods 1 and 2 for each downscaled model - same colour scale as for (b).

6.6 Cloud, radiation and relative humidity

Total cloud cover under the A2 emissions scenario decreases by the end of the century in the modelling projections with a spatially complex pattern of change (Figure 6.17a and Figure 6.17b). The response is also different in the different seasons, with the greatest reduction in cloud cover over the west coast in summer (Figure 6.17c and Figure 6.17d). The areas of greatest reduction in cloud cover are also the areas of greatest rainfall decline. The changes to cloud cover are less than 5%. The sign and magnitude of this change is consistent with the global-scale modelled trend for this region (Meehl et al 2007) and indicates that there are more reduced-cloud days or cloud-free days over Tasmania.

Average annual radiation over Tasmania shows a slight increase through the projections under the A2

emissions scenario (Figure 6.18a). The distinct east-west pattern in the change of solar radiation at the earth's surface is consistent with the change in annual mean cloud cover in the modelling projections in summer (Figure 6.18d). Summer changes to radiation have a greater influence on the annual pattern of change in radiation, than for cloud cover, since there is almost five times more radiation in summer. Changes to radiation are also quite small, generally less than 5%.

Annual average relative humidity under the A2 emissions scenario is seen to increase over much of Tasmania by 0.5% to 1.5%, except for the Central Highland region where a slight decrease is projected (Figure 6.19a and Figure 6.19b). There is a different spatial pattern of change in summer compared to winter (Figure 6.19d). These patterns are broadly similar to the changes in rainfall shown in Figure 6.8.

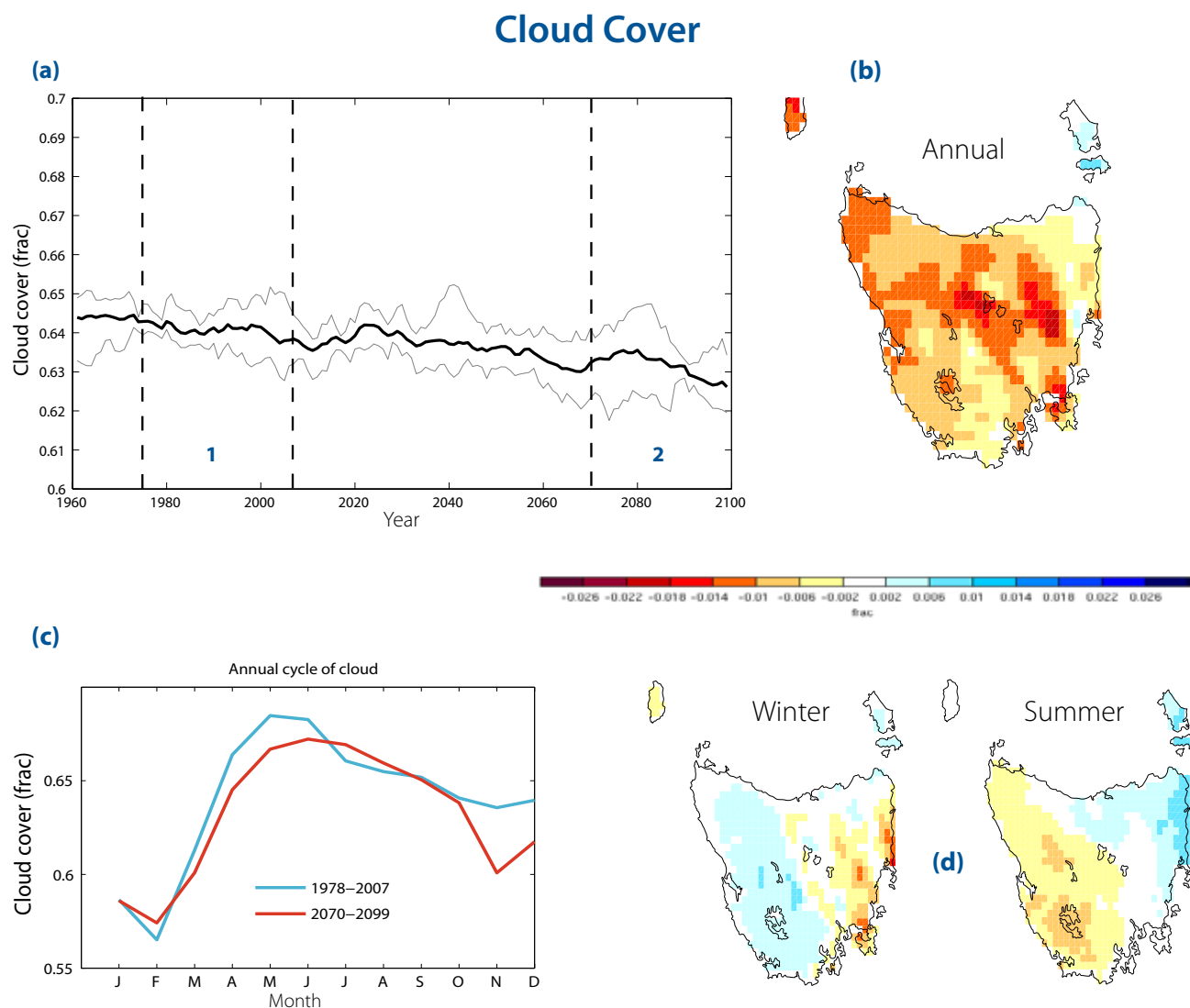


Figure 6.17 Mean cloud cover (a) Time series of the 11-year moving average total cloud cover over the land surface of Tasmania in the six-model-mean (bold line) and the range of models (highest and lowest) – faint lines. (b) The six-model-mean difference in cloud cover between Period 1 (1978-2007) and Period 2 (2070-2099). (c) The mean annual cycle of cloud cover in periods 1 and 2. (d) as for (b) but for summer and winter.

Solar Radiation

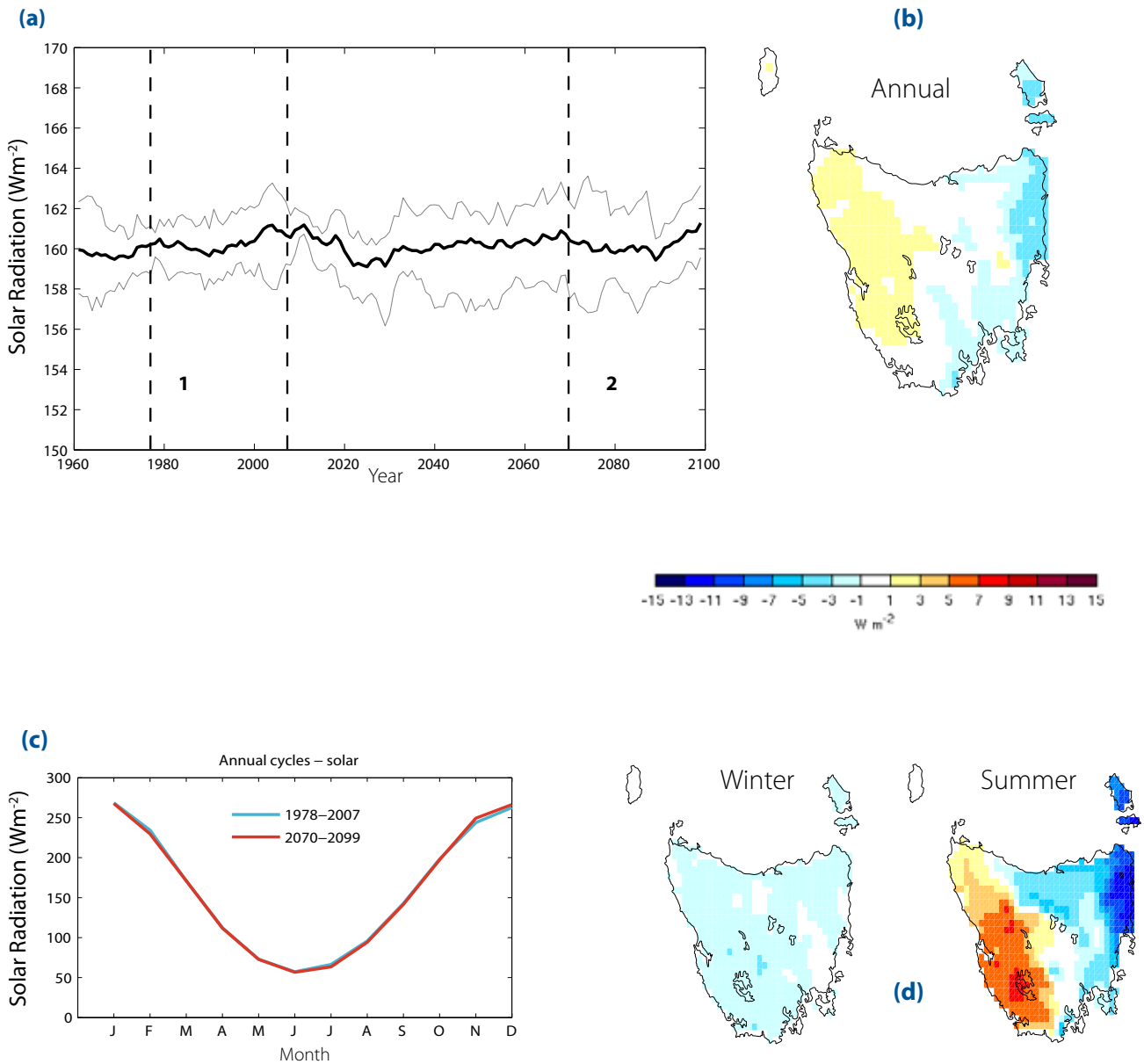


Figure 6.18 The downwelling solar radiation at the earth surface. (a) Time series of the 11-year moving average radiation over the land surface of Tasmania in the six-model-mean (bold line) and the range of models (highest and lowest) – faint lines. (b) The six-model-mean difference in radiation between Period 1 (1978-2007) and Period 2 (2070-2099). (c) The mean annual cycle of radiation in periods 1 and 2. (d) as for (b) but for summer and winter.



Relative Humidity

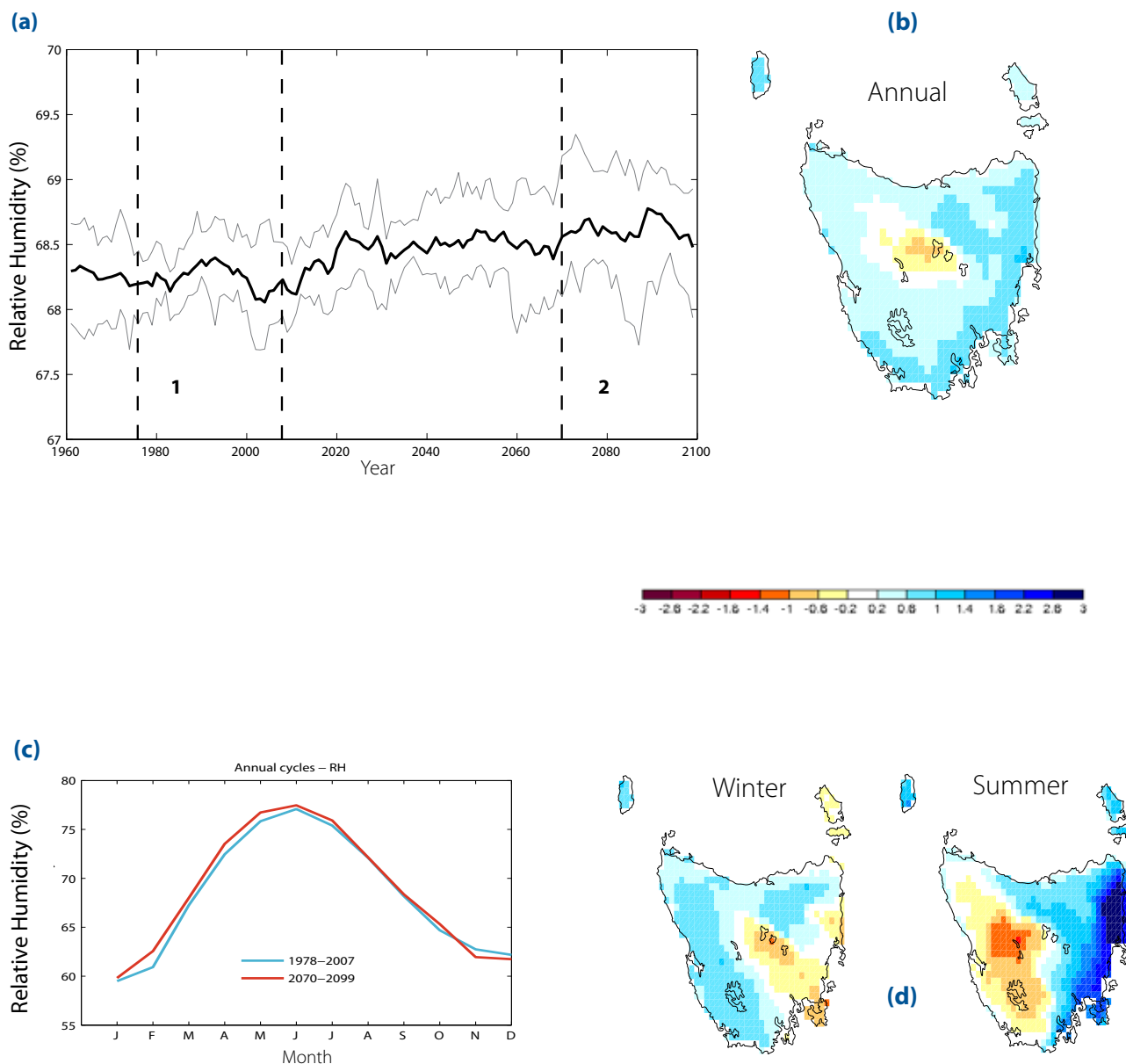


Figure 6.19 Mean relative humidity. (a) Time series of the 11-year moving average relative humidity over the land surface of Tasmania in the six-model-mean (bold line) and the range of models (highest and lowest) – faint lines. (b) The six-model-mean difference in the mean relative humidity between Period 1 (1978-2007) and Period 2 (2070-2099). (c) The mean annual cycle of relative humidity in periods 1 and 2. (d) as for (b) but for summer and winter.

6.7 Evaporation

There is a large and significant increase in simulated pan evaporation in the modelling projections under the A2 emissions scenario (Figure 6.20a). On an annual basis, the increase in evaporation has a fairly even distribution across Tasmania (Figure 6.20b). The increase in pan evaporation is greater in summer than in winter, and has a pattern of greater increase in the north and west and less in the east and south (Figure 6.20d). To quantify the change over the century, the same periods used for temperature were examined to account for the steep upward trend at the end of the century (1980-1999 to 2090-2099). The change between these two periods is 144 mm (modelling range is 128 mm to 163 mm), representing a 19% increase (modelling range is 17% to 21%). This

change represents a continuation of the general increase in pan evaporation in the observed record (Jovanovic et al 2006).

Pan evaporation in the modelling is calculated from first principles and accounts for influences from radiation, wind, humidity and temperature. The changes to radiation, wind and humidity are generally small and show periods or regions of positive and negative trends. Therefore, we can infer that the increase in pan evaporation is driven mostly by the increase in temperature. The east-west pattern of change in relative humidity and radiation appear to have some influence on the spatial pattern of increasing pan evaporation in summer.

Pan Evaporation

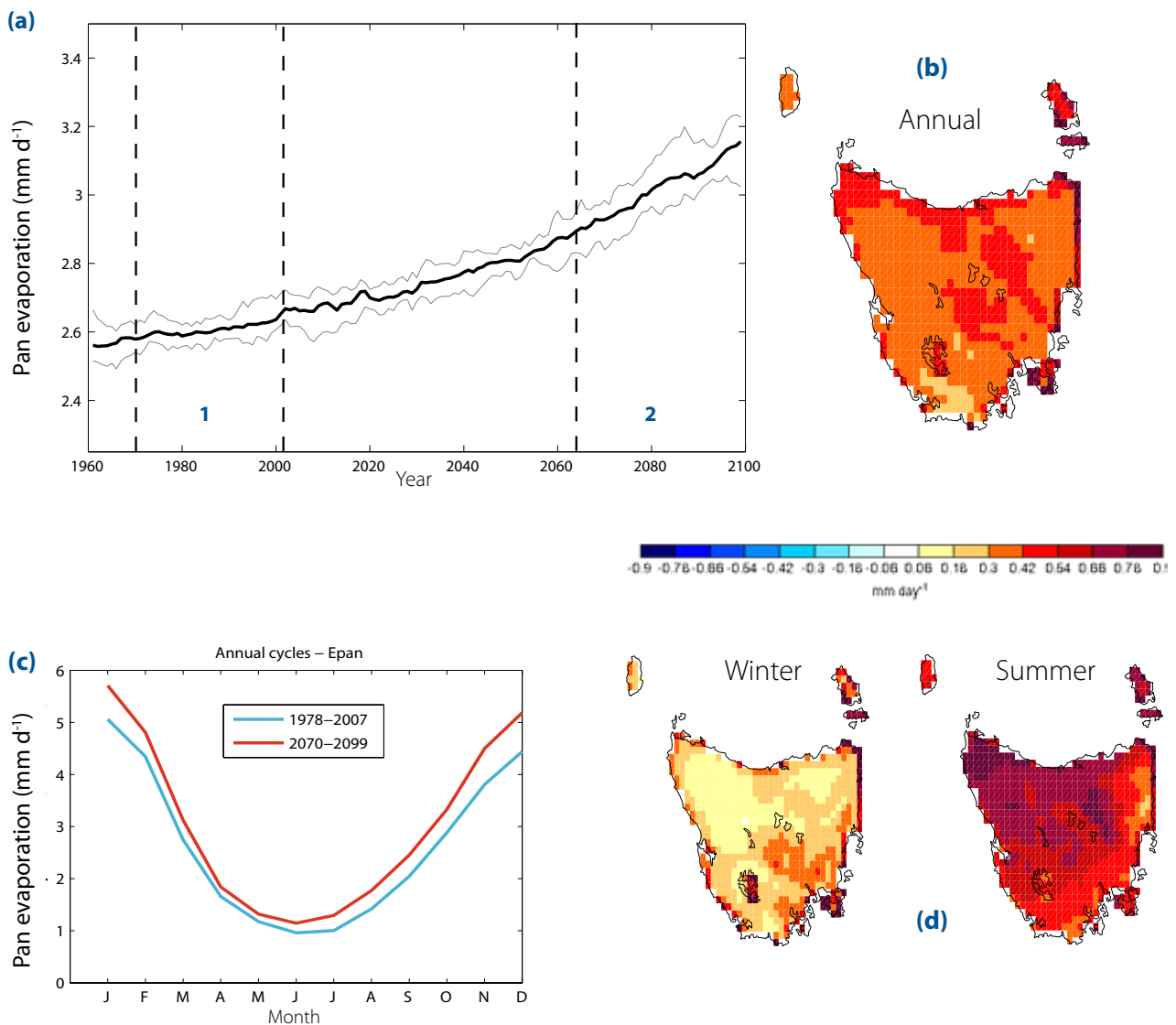


Figure 6.20 Simulated pan evaporation. (a) Time series of the 11-year moving average of daily pan evaporation for Tasmania in the six-model-mean (bold line) and the range of models (highest and lowest) – faint lines. (b) The six-model-mean difference in the daily pan evaporation between Period 1 (1978-2007) and Period 2 (2070-2099). (c) The mean annual cycle of pan evaporation in periods 1 and 2. (d) as for (b) but for the summer and winter. Pan evaporation from a simulated pan, calculated diagnostically at every time step from the modelling simulations.

The Conformal Cubic Atmospheric Model (CCAM) used for these climate simulations includes an internally consistent water balance scheme. This allows for a basic analysis of changes to actual evapotranspiration from the land surface given the modelled water availability. This includes the water loss through evaporation from soil and transpiration through plants. The total annual evapotranspiration shows an increase through the century (Figure 6.21a). The increase is greater over a strip along some coasts. This increase is proportionally greater in winter than in summer (Figure 6.21b and Figure 6.21c) when there is more water to evaporate. There is a slight decrease in evapotranspiration near the west coast in summer where evapotranspiration becomes more water limited.

The increase in evaporation suggests that for some locations, in some seasons, evaporation may be a significant contributing factor to water availability along with the change in precipitation. However, to get an accurate view of water availability, surface runoff and streamflow, the complex time-dependant processes must be accounted for. A thorough analysis and modelling of runoff and streamflow is presented in the water and catchments report (Bennett et al 2010).

Evaporation

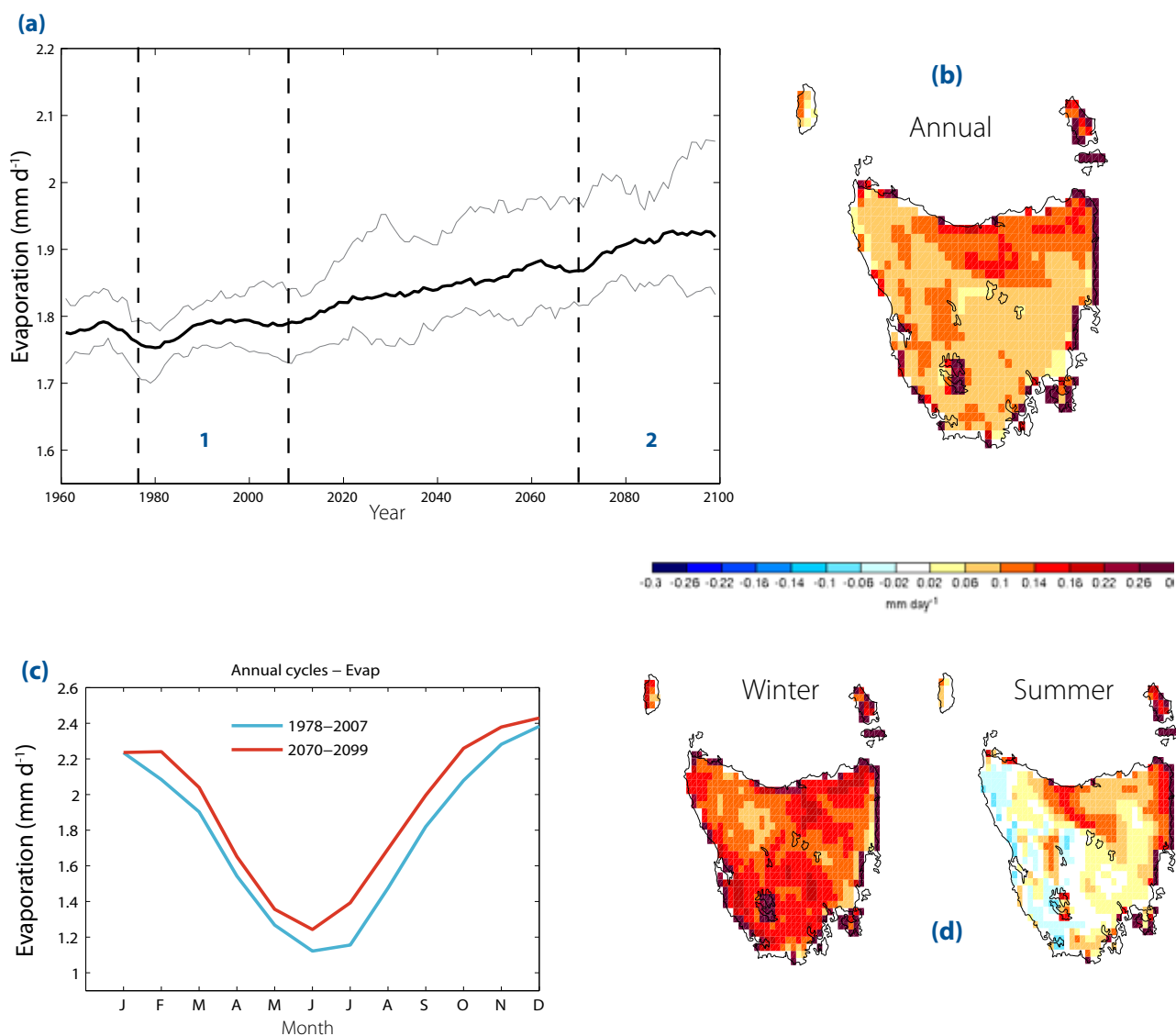


Figure 6.21 Evaporation from the earth surface. (a) Time series of the 11-year moving average of evaporation rate for Tasmania in the six-model-mean (bold line) and the modelling range (highest and lowest) – faint lines. (b) The six-model-mean difference in daily pan evaporation between Period 1 (1978-2007) and Period 2 (2070-2099). (c) The mean annual cycle of pan evaporation in periods 1 and 2. (d) as for (b) but for summer and winter.

7 Projections of climate drivers of rainfall variability

7. Projections of climate drivers of rainfall variability

This section examines the relationships of Tasmanian rainfall variability in the models and large-scale climate features and drivers. We compare and relate the modelled rainfall trends to some relevant climate indices. Firstly, the simulation of climate drivers by the models in the current climate is assessed and compared to observations. For models to project future climate conditions reliably, they must simulate the current climate state with some degree of fidelity. Furthermore, to be confident in the projected rainfall trends, we must be confident that rainfall patterns have the known relationship to climate drivers in the current climate. In other words, we must be sure we are simulating the current rainfall amounts delivered through the known mechanisms. Following this assessment, we examine the projected changes to the indices associated with these drivers.

To assess the simulation of the climate drivers for the present climate, we compared the modelling outputs to the 2.5-degree climate reanalysis dataset produced by the National Centers for Environmental Prediction (NCEP) and National Center for Atmospheric Research (NCAR), that is the NCEP/NCAR Reanalysis 1, (Kalnay et al 1996; Kistler et al 2001). This product is hereafter referred to as NCEP Reanalysis. A comparison to the NCEP Reanalysis is given as an indication of the performance of the models, but it should be noted that the NCEP Reanalysis modelling is not a perfect representation of the real pressure fields. Differences exist between this dataset and others such as the ERA40 Reanalysis produced by the European Centre for Medium-Range Weather Forecasts.

To examine pressure variables and climate drivers, we used the baseline climatology period of 1978 to 2007 rather than 1961 to 1990. This period covers the more recent climate, and the NCEP Reanalysis dataset contains significant biases in the southern hemisphere prior to 1970 (Hines et al 2000). The NCEP Reanalysis is compared to the intermediate downscaled modelling outputs at 0.5-degree resolution, as this contains the broad scale atmospheric features driving the rainfall response seen in the finer scale simulations. The large-scale features present in the modelling simulations are retained in the final stage (see Corney et al 2010). The NCEP Reanalysis and simulated climate are compared for the region between 5 degrees south and 65 degrees south and between 100 degrees east and 180 degrees east.

The general patterns of mean sea level pressure (MSLP) and wind give an indication of the processes driving atmospheric circulation, cloud and rainfall. The general patterns of pressure in the modelling simulations are compared with the NCEP Reanalysis for the current climate, and we then examined the projected changes into the future. In addition, some simple indices of pressure and wind that quantify certain important aspects of the circulation and flow are calculated. These analyses are designed to be an overview of the simulation of climate drivers in the downscaled modelling simulations and only the A2 emissions scenario is examined here. A complete and exhaustive analysis is beyond the scope of this report.

7.1 Patterns of mean sea level pressure (MSLP), Hadley Circulation

Global climate models (GCMs) have been found to simulate hemispheric climate regimes quite similar to those in observations (Robertson 2001; Achatz & Opsteegh 2003; Selten & Branstator 2004). This large-scale realism of the global and hemispheric scale is retained and more information is added at the medium and fine scale for the region through the downscaling process (see Corney et al 2010).

The pattern of mean sea level pressure (MSLP) in the mean of the six models for the region surrounding Tasmania is broadly similar to that of the NCEP Reanalysis in all seasons for the current climate (Figure 7.1). However, there are some differences in the spatial pattern between the simulations and the NCEP Reanalysis that are greater than the range between the six models. The pressure in the zone 60-65 degrees south is lower in the modelling simulations than in the NCEP Reanalysis for most seasons, and therefore the gradient of pressure between this latitude and Tasmania is larger. There also appears to be a difference in the shape of the Subtropical Ridge (STR) between the models and NCEP Reanalysis, discussed below. These small discrepancies may be from biases either in the NCEP Reanalysis, the models, or both. However, the general match between the two patterns indicates that the modelling projections can be used as a tool for examining climate changes in these key large scale climate drivers and their indices.

Also shown in Figure 7.1 are maps of six-model-mean change in MSLP between 1978-2007 and 2070-2099. In each plot, the pressure shows the greatest increase along the mid-latitudes to either side of Tasmania: over New Zealand and the south Indian Ocean. Pressure shows the greatest decrease at latitudes

south of 50 degrees south. The longitudinal pattern of the pressure change differs between seasons, visible as a different curvature of isobars. A time series of MSLP at Hobart shows that annual and autumn MSLP steadily increases, but spring MSLP has a less distinct pattern of increase with a higher level of variability (Figure 7.2).

The feature of the Hadley Circulation most relevant to the Tasmanian climate is the position and intensity of the STR. The mean annual position of the STR can be seen in Figure 7.1. The representation of the ridge in the model appears broadly similar to that found in the NCEP Reanalysis but with a difference in the mean shape of the STR across the Tasman Sea, between 130 degrees east and 180 degrees east. This difference is seen as a different degree of curvature of isobars in this region relative to the NCEP Reanalysis, in most seasons. This is a common deficiency in GCM simulations and is not improved in the downscaled simulations.

The latitude and intensity of the STR in the Australian region can be quantified using various indices of mean sea level pressure. We examined a monthly *L* Index of Drosowsky (2005) that extends earlier analysis by Pittock (1971) to quantify the latitude of the STR centred on 150 degrees east. We used the method of Larsen and Nicholls (2009) to quantify the intensity of the STR across the Australian continent (110 degrees east– 155 degrees east). The seasonal cycle of the *L* Index at 150 degrees east in the period 1978 to 2007 in the six-model-mean simulations is reasonably similar to the equivalent in NCEP

Reanalysis (Figure 7.3a). The maximum difference between NCEP Reanalysis and the modelling simulations is approximately 1.1 degrees, and occurs in September. The intensity of the STR in the baseline period in the simulations is higher than for NCEP Reanalysis in all months, and up to 4.3 hPa in May (Figure 7.3b). These plots indicate a seasonal cycle in the future period 2070 to 2099, showing the STR moving southward and intensifying into the future period.

The anomaly of the *L* Index and STR intensity from the mean 1978–2007 values in winter and summer are shown in Figure 7.3c and Figure 7.3d respectively. Assuming that any bias or offset between modelled and actual pressure remains constant throughout the projection to 2100, these projections show in summer the STR moves poleward by 1.05 degrees and intensifies by 1.05 hPa. In winter, the STR moves poleward by 0.44 degrees and intensifies by 0.55 hPa. The southerly movement of the STR over the 21st century is a continuation of an ongoing southerly shift over the late 20th century indicated in some studies (Murphy & Timbal 2008; Timbal 2009). However, one study showed there has been no significant trend in the position of the STR in recent decades (Drosowsky 2005). Yet, the size of this shift in the STR is approximately half that of the mean inter-annual variability (2 degrees), and at least a quarter of the northward shift from the last glacial period to the present (3–4 degrees) (Shulmeister et al 2004). The intensifying STR is consistent with the trend in the late 20th century (Larsen & Nicholls 2009).

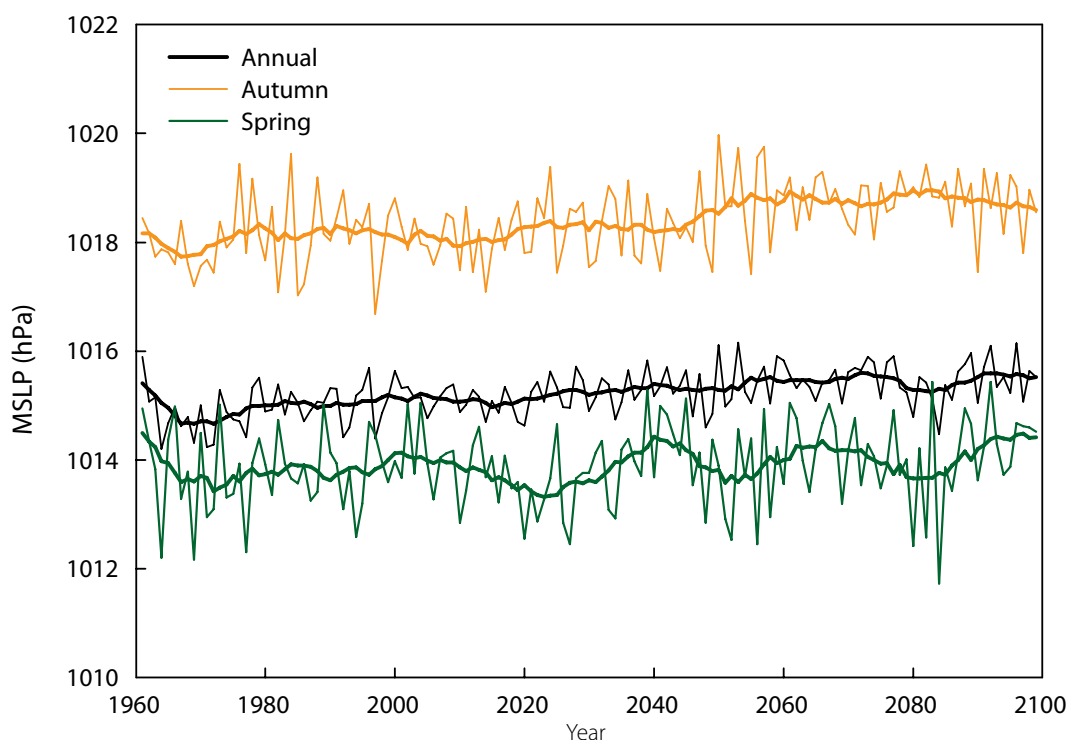


Figure 7.2 The six-model-mean value of mean sea level pressure (MSLP) at Hobart from 1961 to 2100 annually (black lines) and for autumn (orange lines) and spring (green lines) under the A2 emissions scenario.

Throughout the 20th century, there was consistently a negative correlation between the *L* Index and west coast Tasmanian rainfall (Drosowsky 2005). The steering of fronts is the primary mechanism causing this negative correlation. This means that when the STR is further south, more fronts are deflected southwards and less frontal rain falls on Tasmania. Assuming that this mechanism remains true in these projections of future climate, then the southerly shift of the STR in summer is consistent with the reduction in west coast summer rainfall in the simulations. Autumn and winter rainfall may have a closer relationship with STR intensity than STR position (Larsen & Nicholls 2009), and the reduction in west coast rainfall in autumn is consistent with the intensifying STR during this season.

West coast rainfall does not decline in winter, and in fact, it is seen to increase. The southerly movement and intensification of the STR in winter is not as marked as in other seasons, and does not correlate with the rainfall increase. However, changes to the regional scale pressure patterns in winter show changes that are subtler than the simple indices of STR can indicate (Figure 7.1). The increase in the meridional gradient of pressure south of Tasmania, as well as the pattern of increase in pressure to either side of Tasmania indicate an increase in westerlies to Tasmania. This is reflected in the change to the regional winds (discussed below).

Subtropical Ridge

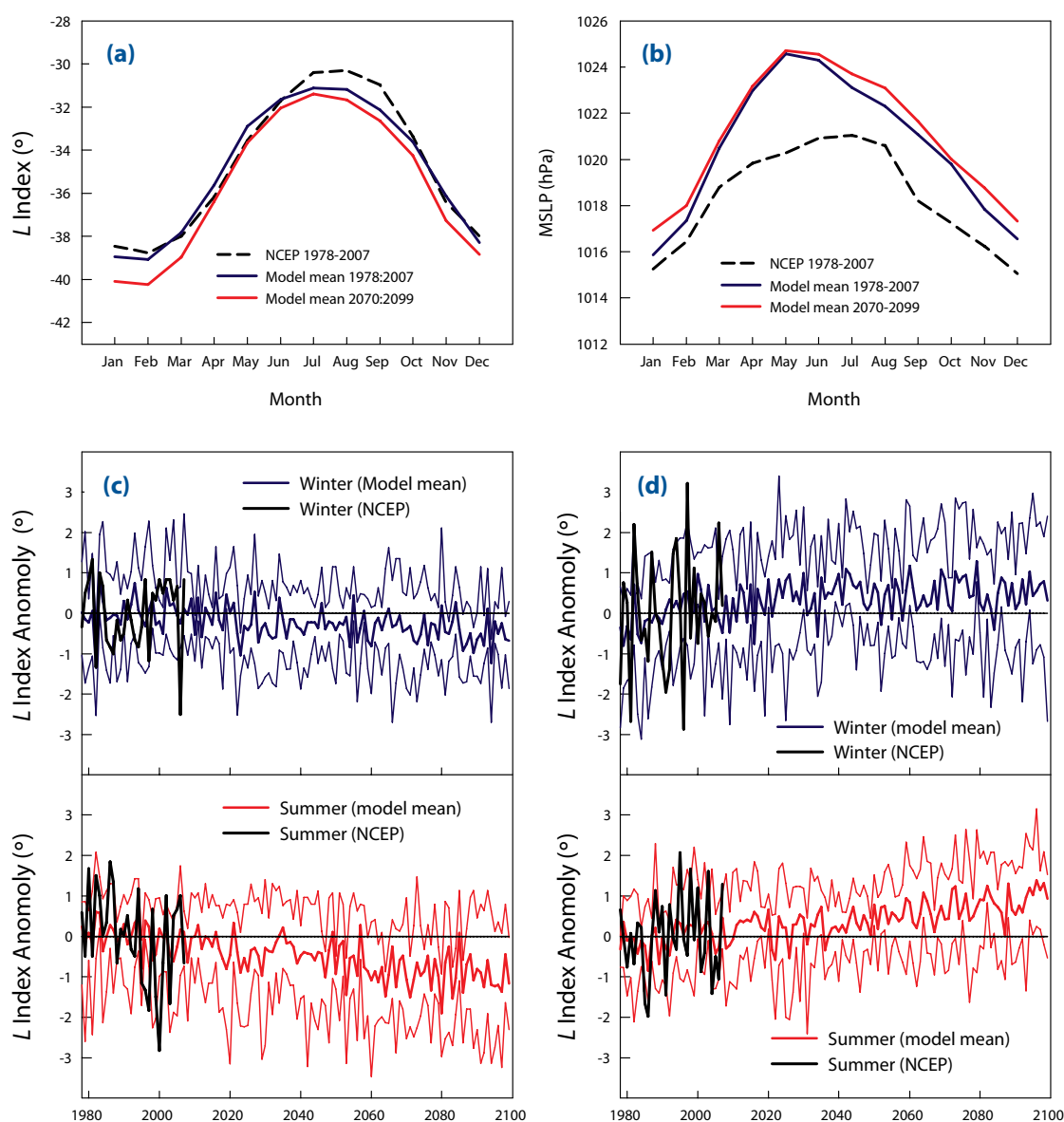


Figure 7.3 The position and intensity of the subtropical ridge (STR). (a) The annual cycle of *L* Index of STR latitude at 150° E in the NCEP Reanalysis, the six-model-mean for 1978-2007 and the six-model-mean for 2070-2099. (b) as for (a) but showing the intensity of the STR (central pressure) across Australia. (c) The *L* Index anomaly from 1978-2007 mean for six-model-mean, highest and lowest model and NCEP for summer and winter. (d) as for (c) but showing STR intensity (central pressure) anomaly.

7.2 Regional wind

The two components of the wind at the 850 hPa height were examined separately: the zonal or west-east component and the meridional or north-south component. The mean of these components during the baseline period 1978 to 2007 are shown in Figure 7.4, along with the change from this baseline to the end of the century (2070 to 2099). The annual change over Tasmania is a small increase in the zonal westerly flow and an increase in the northerly flow. The changes in surface wind can be related to the changes in pressure in Figure 7.1 through geostrophy. For example, the mean increase in

pressure over New Zealand leads to a decrease in the dominant westerlies immediately to the north of the anomaly, an increase in the northerly wind to the west of the anomaly and an increase in the westerlies to the south of the anomaly. As with other variables, the annual change represents the average of four larger and distinct seasonal changes, shown for zonal wind (west-east) in Figure 7.5. This figure shows an increase in the dominant westerlies over Tasmania during winter and spring, but a decrease in summer and autumn. These changes in seasonal wind are consistent with the changes to mean sea level pressure and the changes to rainfall described in Section 6.

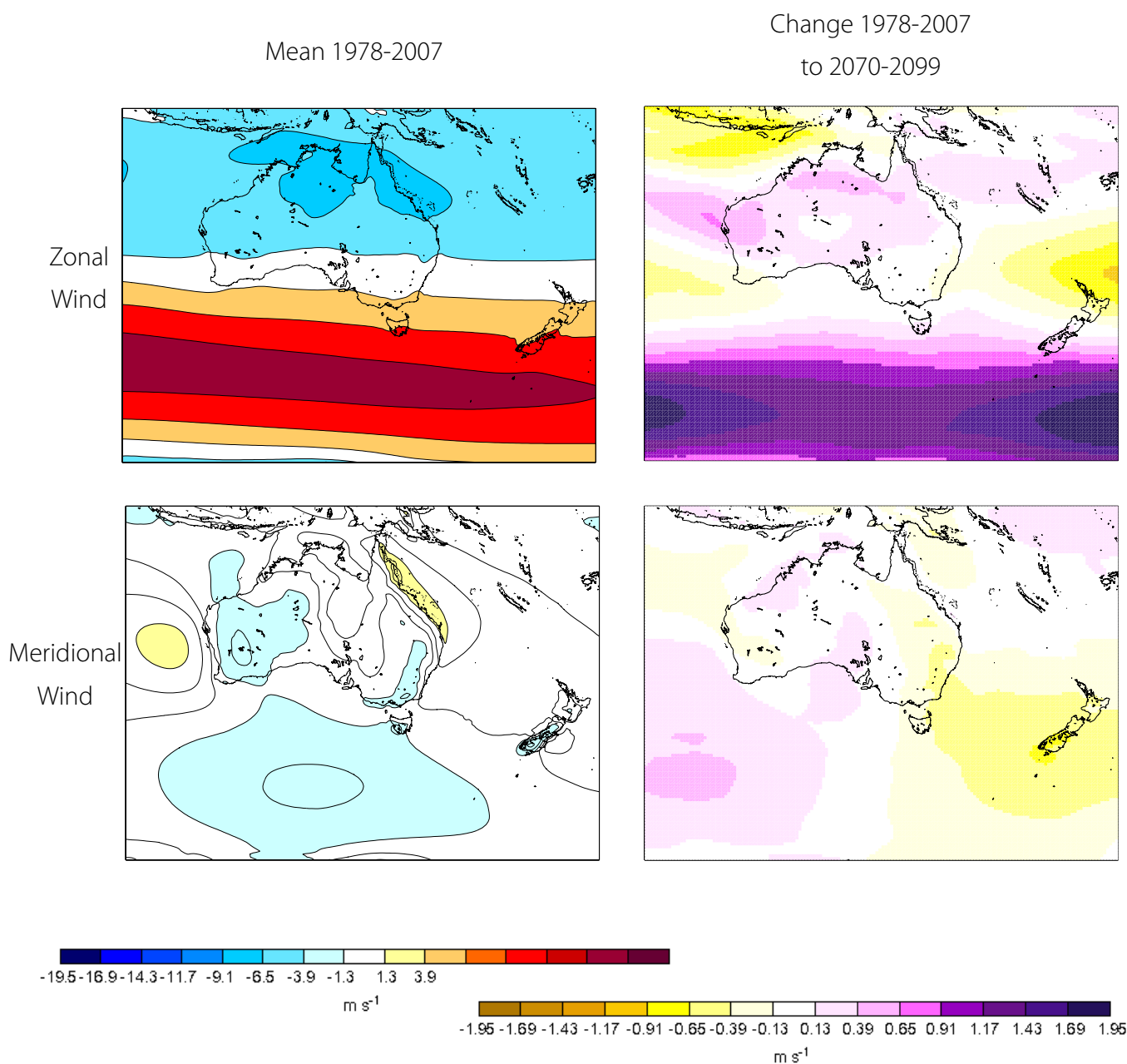


Figure 7.4 The six-model-mean value of simulated mean directional 850 hPa wind speed in the Australasian region. The top row is zonal wind speed (west-east) and the bottom row is meridional wind speed (north-south) in m s^{-1} . The left column is the mean over the recent period 1978-2007 and the right column shows change between 1978-2007 to 2070-2099. Note the different scale for mean and change.

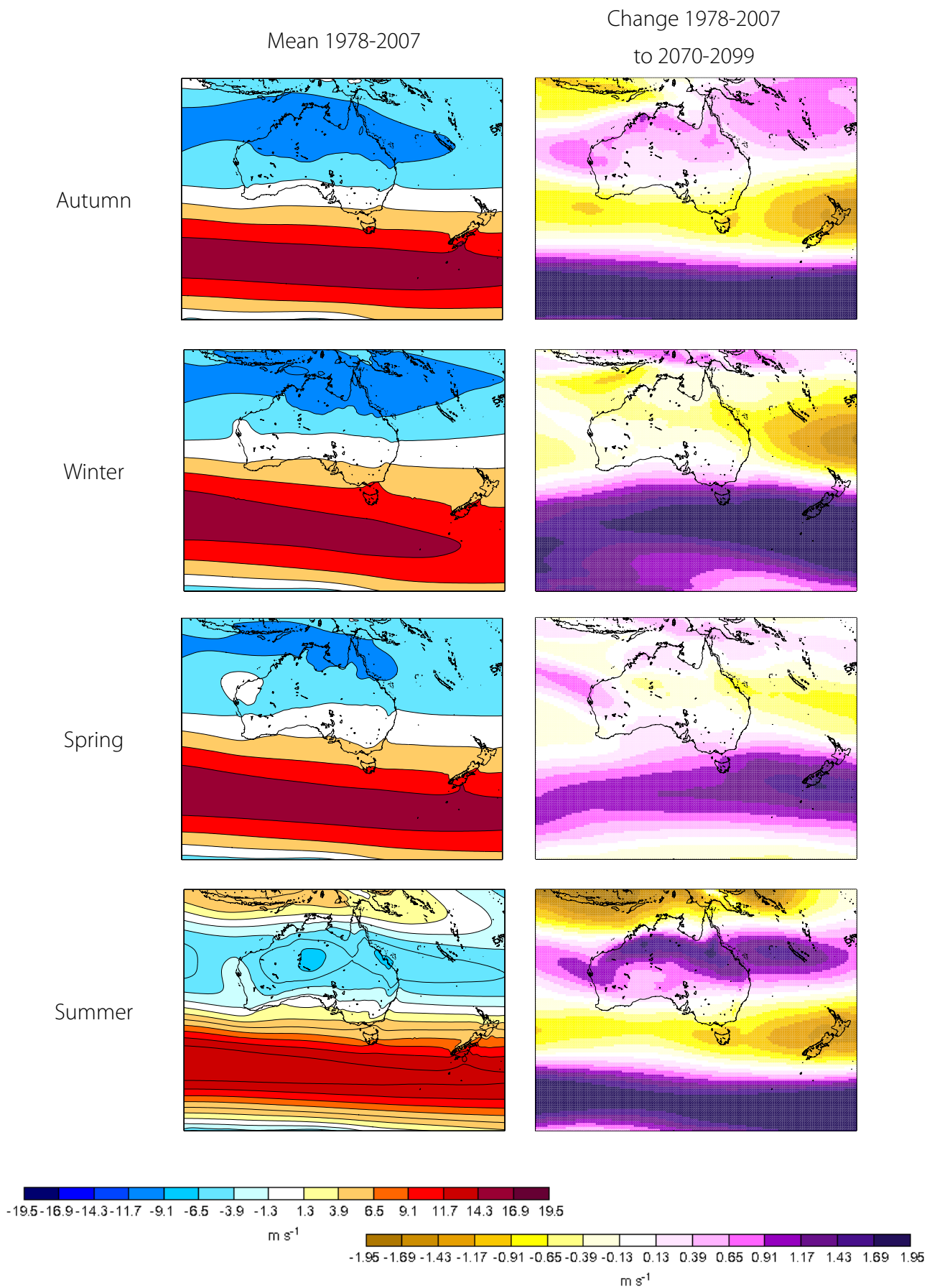


Figure 7.5 The six-model-mean value of simulated mean zonal 850 hPa wind speed in the Australasian region. The left column is the mean over the recent period 1978-2007 and the right column shows change between 1978-2007 to 2070-2099. Note different scale for mean and change



7.3 Atmospheric blocking

The changes to the mean sea level pressure (MSLP) and wind shown above are partly associated with changes in atmospheric blocking in this region. This in turn affects rainfall over Tasmania.

Results from the northern hemisphere show that coarse-scale global climate models (GCMs) tend to simulate the location of atmospheric blocking more accurately than the frequency and duration of atmospheric blocking, as simulated events are generally shorter and rarer than observed (Pelly & Hoskins 2003). However, there has been no systematic inter-comparison of observed and simulated atmospheric blocking in the southern hemisphere (Meehl et al 2007). A study of one GCM found that increased horizontal resolution combined with better physical parameterisations has led to improvements in simulations of atmospheric blocking and synoptic regimes over Europe (Meehl et al 2007), so improved resolution is likely to an improved representation of atmospheric blocking in these downscaled modelling simulations. There may also be a more accurate representation of the effect of atmospheric blocking on local rainfall in Tasmania.

In this project, the monthly Blocking Index appropriate to south-east Australia was examined (after Pook & Gibson 1999). This index is based on the zonal component of the 500 hPa wind along the 140 degrees east meridian from 25 degrees south to 60 degrees south. The Blocking Index in each downscaled modelling simulation was compared to that calculated from the NCEP Reanalysis (Figure 7.6a). The models have a similar seasonal cycle of the Blocking Index to the NCEP Reanalysis, but with a consistent low bias in the index across all seasons of approximately five index units.

The change in the annual cycle of the Blocking Index between the baseline and future periods (Figure 7.6b) shows a steady change in the seasonality of the index. The change in the seasonal cycle by the end of the century (Figure 7.6c) shows an increase in the first half of the year (January to May), and a reduction in the last half of the year (June to November). The summer Blocking Index displays a steady increase throughout the projection period (Figure 7.6d). The Blocking Index has shown a significant correlation with rainfall variability in some regions of Tasmania in observations (see Figure 3.2). Given that these correlations with atmospheric blocking hold through the century, the projected changes to atmospheric blocking are highly consistent with rainfall trends seen in Figure 6.8. The strongest trends in rainfall that are consistent with the change in Blocking Index are an increase in rainfall in the east during summer and autumn, and a decrease in west coast rainfall in autumn and winter.

Blocking Index

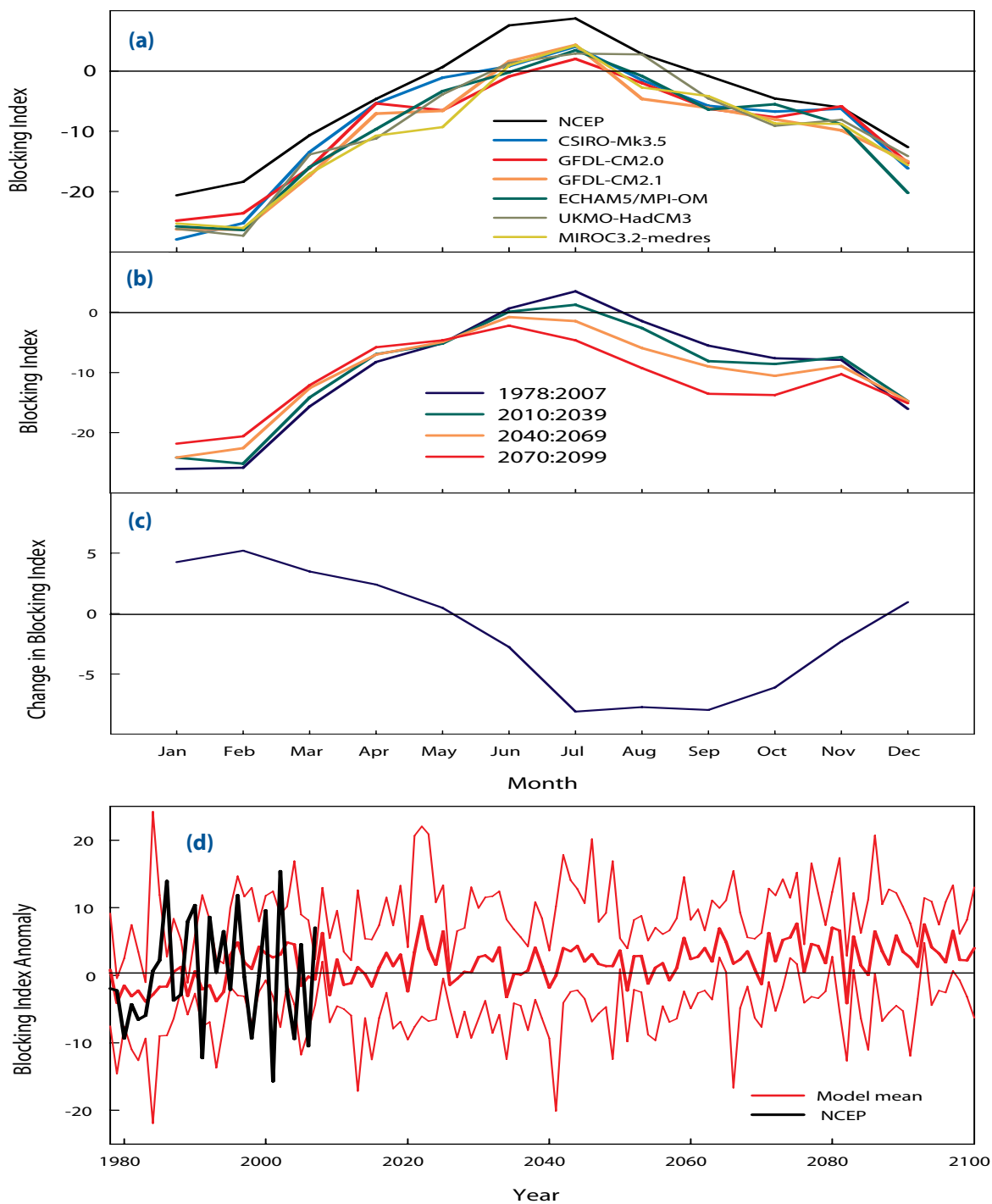


Figure 7.6 Monthly Blocking Index. (a) The mean annual cycle of the Blocking Index for 1978-2007 at 140° E for NCEP Reanalysis and for each modelling simulation under the A2 emissions scenario. (b) The mean annual cycle of the Blocking Index at 140° E for the six-model-mean in four climatology periods (1978-2007, 2010-2039, 2040-2069, 2070-2099). (c) The difference between the six-model-mean annual cycle at 1978-2007 to 2070-2099. (d) The time series of the six-model-mean summer Blocking Index.

7.4 Changes to sea surface temperature

Increased sea surface temperature (SST) can lead to a more energetic atmosphere, with increased moisture flux, changes to atmospheric stability and changes to MSLP. Changes in SST near Tasmania are likely to affect rainfall at a local scale. The downscaling process used SST from coupled ocean-atmosphere global climate models interpolated to the grid resolution of interest. This gives a better definition of SST around and up to the coastline. The interpolated SST is used as the boundary condition for the dynamic atmospheric model also run at a fine resolution. For these reasons, the downscaled model is expected to resolve the interface between land and ocean, and the atmospheric response to changes in SST at a scale fine enough to see regional differences.

There is a projected increase in mean SST around Tasmania in all seasons by the end of the century (Figure 7.7). There is a greater increase in SST in the

east and north-east than other regions, and a greater increase in autumn than other seasons (Figure 7.7c). The ocean models used to create the surface temperature fields all show an extension of the East Australian Current (EAC). This southward extension of the East Australian Current brings warmer water south and leads to an enhanced warming in the north-east region. Although each model shows a different pattern of SST for the Australian region (Figure 7.7b), all of the models are in agreement that the East Australian Current has extended southwards, probably in response to a strengthening of the south Pacific gyre, from the increased westerlies over the Southern Ocean. Increases in SST at the east coast caused by an extension of the East Australian Current are already seen in direct ocean measurements (Ridgway 2007), in line with our projections. These increase in mean SST by the end of the century leads to increased moisture in the atmosphere, and contributes to the increased relative humidity seen in Figure 6.15.

Sea Surface Temperature

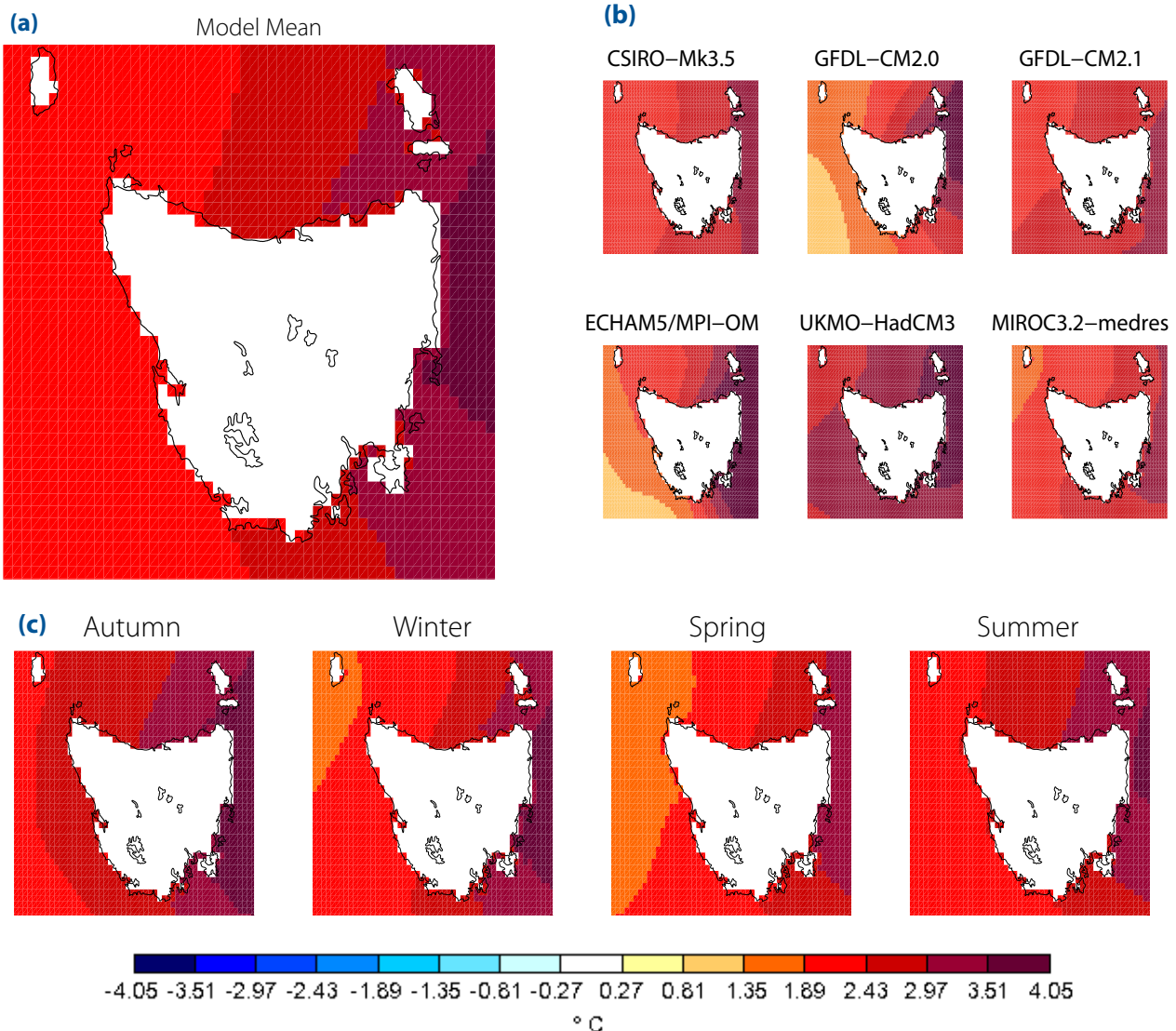


Figure 7.7 The change to sea surface temperature (SST) between 1978-2007 and 2070-2099. (a) six-model-mean annually, and (b) each model annually, and (c) the six-model-mean for each season.

7.5 Convection and atmospheric stability

Atmospheric stability and the potential for vertical movement of air in the air column are indicated by the convective available potential energy (CAPE) index. Positive values of CAPE indicate a region with potential for upward motion of air. A high CAPE value can indicate the presence of storminess. The mean CAPE in the modelling outputs of the current climate has a strong spatial pattern with highest values on the west coast and north-east (Figure 7.8a). CAPE increases by the end of the century, with the largest increase off the east coast of Tasmania (Figure 7.8b). This spatial pattern shows a strong correlation with the change in SST over the same period (Figure 7.7a), indicating the stability of the air column has decreased in response to the increase in input of heat and moisture from the underlying ocean. The increase in CAPE over Tasmania is gradual over time with no distinct jumps (Figure 7.8c).

Decreased stability in the atmosphere can indicate increased convection that in turn affects rainfall processes. In the simulation of the present climate, convective rainfall is approximately 35% of the total. This is not a significant component of the total rainfall in Tasmania, compared to other regions such as the tropics. There is an increase in the proportion of rain falling through convective mechanisms in the modelling projections to 2100 of up to 5% (Figure 7.9). The change in the proportion of convective rainfall shows an east-west gradient, similar to the change in CAPE and SST. These results taken together indicate that Tasmania, and especially the north-east, are likely to receive relatively more convective rainfall than in the recent past. This may include the incidence of high rainfall convective events such as thunderstorms.

7.6 Ocean-atmosphere phenomena

Global climate models (GCMs) realistically simulate the general aspects of the Southern Annular Mode (SAM) (Fyfe et al 1999; Cai et al 2003; Miller et al 2006). There is a spatial correlation of more than 0.95 between the pressure anomaly in the NCEP Reanalysis and in modelling simulations over the southern hemisphere in winter for all six GCMs used in the project (Meehl et al 2007). However, other features of the SAM in GCMs do not compare well to the NCEP Reanalysis, such as the amplitude, detailed zonal structure and temporal variations (Miller et al 2006; Raphael & Holland 2006). It is likely that further understanding of the SAM is needed before the SAM can be accurately simulated (Meehl et al 2007). The hemispheric scale features of the SAM simulated by the GCMs were retained through the process of downscaling, with some local scale detail of the atmospheric pressure patterns added.

The local influence of the SAM in the downscaled simulations is explored using a modified version of the Regional Antarctic Oscillation Index (AOIR) of Meneghini et al (2007). The index is based on the difference in mean sea level pressure (MSLP) at 40 degrees south and 65 degrees south in the Australian region. Here the index is calculated using the published method, but over the longitude range 100 degrees east to 180 degrees east instead of 90 degrees east to 180 degrees east. The value of this index in winter, spring and summer from both the NCEP Reanalysis and the modelling outputs is shown in Figure 7.10. While each individual model has less inter-annual variability than NCEP Reanalysis, there is a reasonable similarity between the range of the NCEP Reanalysis and the spread of the models. The AOIR increases in all modelling projections in all seasons. The trend in the AOIR has been positive for all seasons for the period 1955 to 2005 (Meneghini et al 2007), so our projections indicate a continuation of the current trend. This change means an increasing prevalence of the high phase of the SAM for the region, where mid-latitude westerlies tend to be weaker, leading to lower moisture transport to western Tasmania. This negative correlation between rainfall anomaly and the AOIR is strongest in summer, and the increase in the index is consistent with the reduction in rainfall in summer seen in our projections. In the observed data, there has been negative correlation of rainfall to AOIR in winter and spring, but the increase in the index is not consistent with the rainfall increase in the west, as seen in these seasons in the modelling projections. It should be noted that the SAM can only partially explain variability and trends in seasonal rainfall, and there are other influences on synoptic activity in the region (Meneghini et al 2007).

In the recent past, SAM has been driven not only by changes to the mean temperature, but also by stratospheric ozone depletion (Thompson & Solomon 2002). There will be some interplay between the different drivers into the future, as stratospheric ozone recovers and the influence of greenhouse warming becomes more prominent. Stratospheric ozone is prescribed in the modelling simulations to match observed ozone concentrations until the year 2000 and then follow an emissions scenario of ozone recovery described in the SRES (Nakićenović & Swart 2000). Although the drivers of stratospheric ozone concentration and greenhouse gas increases are present in the modelling simulations, we did not perform explicit analysis of the influence of these drivers on SAM.

Two other large-scale ocean-atmosphere phenomena that influence rainfall variability in Tasmania are the El Niño Southern Oscillation (ENSO) and the Indian Ocean Dipole (IOD). While there has been steady progress in GCM simulation of ENSO, leading to better representation of the spatial pattern of SST anomalies in the Pacific Ocean, serious systematic

CAPE Index

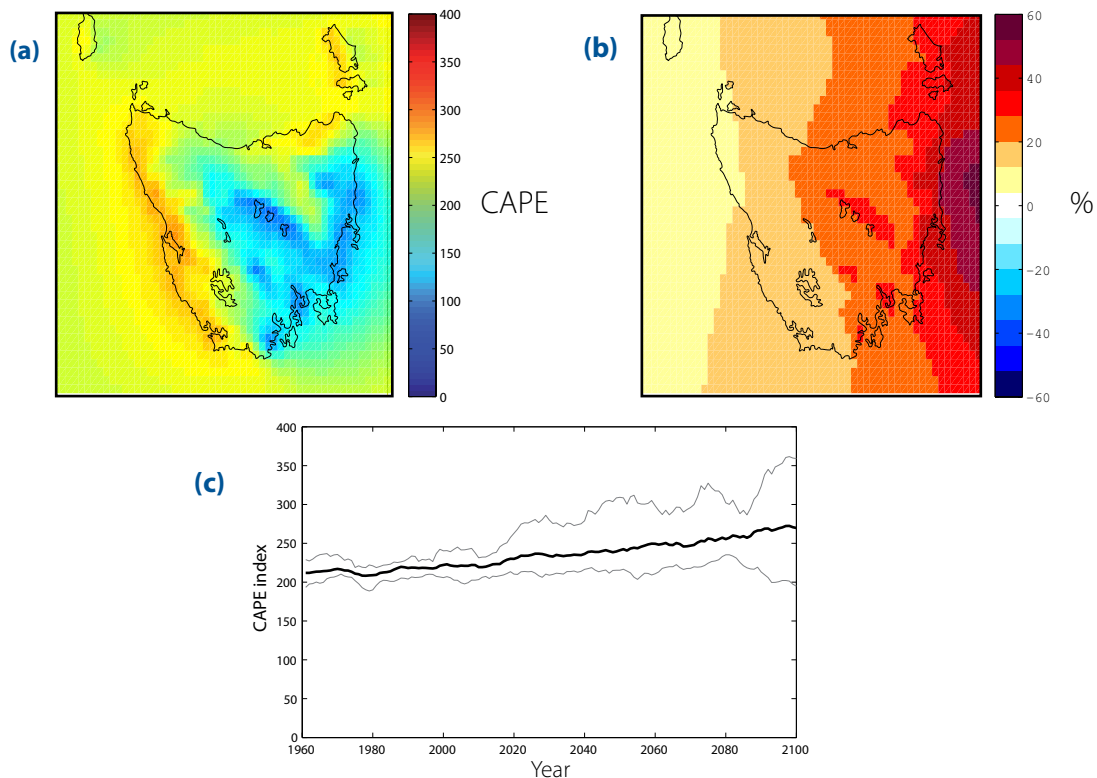


Figure 7.8 Mean CAPE Index. (a) The six-model-mean CAPE in 1978 to 2007. (b) The difference in CAPE between 1978-2007 and 2070-2099. (c) The time series of the 11-year smoothed annual mean CAPE over the land surface of Tasmania (shows six-model-mean and modelling range).

Convective Rainfall

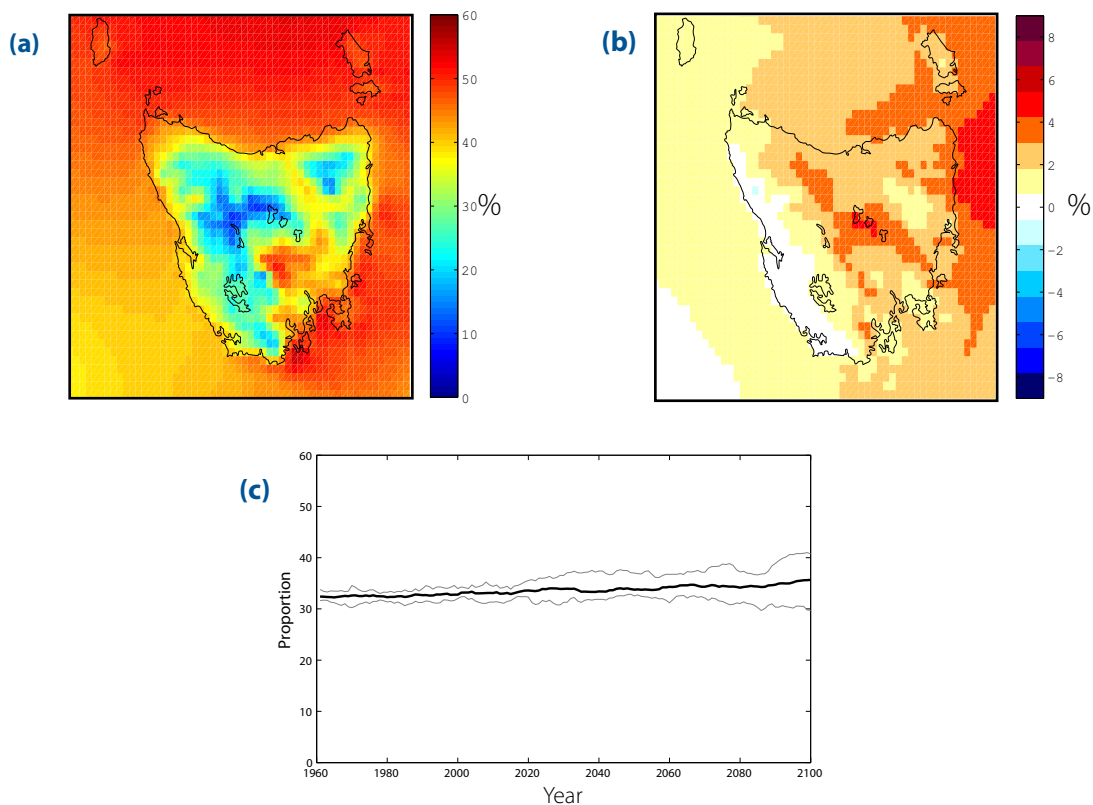


Figure 7.9 The proportion of convective rainfall in total rainfall. (a) The six-model-mean proportion in 1978-2007. (b) The difference between 1978-2007 and 2070-2099. (c) The time series of the 11-year smoothed annual mean proportion of convective rainfall for the land surface of Tasmania (shows six-model-mean and modelling range).

errors persist in both the simulated mean climate and the natural variability (Meehl et al 2007). Some models produce ENSO variability on time scales shorter than those observed (AchutaRao & Sperber 2002), have difficulty simulating the correct phase locking between the annual cycle and ENSO, or fail to represent the spatial and temporal structure of the El Niño-La Niña asymmetry (Monahan and Dai 2004). Also, it remains unclear how changes in the mean

climate will ultimately affect ENSO predictability (Collins et al 2002). In this project, no explicit analysis of ENSO or IOD has been made, so it is unknown how well the models simulate these phenomena and how the impact of these phenomena will change into the future. Further work is required in this regard and will be covered in subsequent publications.

Antarctic Oscillation Index

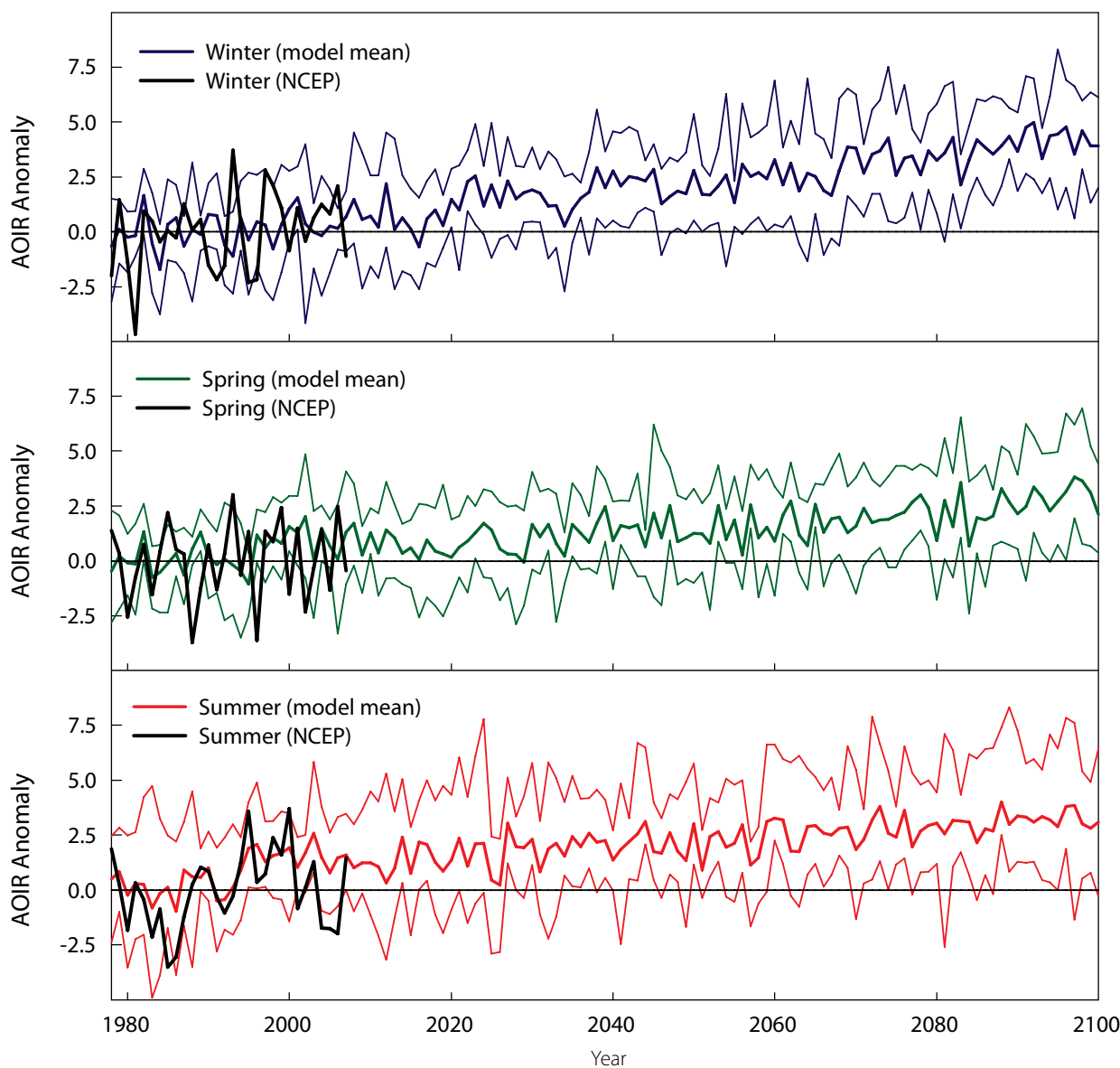


Figure 7.10 Time series of the regional Antarctic Oscillation Index (AOIR) anomaly from the 1961-1990 mean for NCEP Reanalysis and modelling simulations in winter, spring and summer (shown is the six-model-mean and the range of the six models).

8 Synthesis

8. Synthesis

The set of modelling simulations undertaken by the Climate Futures for Tasmania project represent a series of climate change experiments primarily driven by an increase in greenhouse gas composition in the atmosphere. Increased greenhouse gases in the atmosphere lead to an alteration of the radiative balance of the earth, which in turn leads to changes in the climate system. These changes include an alteration to the large-scale circulation of the atmosphere and oceans at the global scale, through various climate mechanisms at all scales, including the local expression of changes at an individual location.

To generate useful information about likely changes to the general climate under greenhouse warming, we examined modelling projections made for two emissions scenarios of possible emissions over the century. In this sense, the modelling simulations should not be treated as forecasts or predictions, but as projections under a certain emissions scenario. Presently the SRES emissions scenarios we used (A2 and B1) cover a plausible range of possible emissions. However, if the actual emissions over this century deviate greatly from these emissions scenarios, this would result in a different climate response than reported.

Under the high emissions scenario, the Climate Futures for Tasmania modelling projections indicate that the mean annual temperature of Tasmania would rise by an average of 2.9 °C over the 21st century (model range 2.6 °C to 3.3 °C). The equivalent change under the low emissions scenario is 1.6 °C (model range 1.3 °C to 2.0 °C). These changes are less than for the Australian and global average, due in part to the temperate Southern Ocean storing the excess heat and moderating the temperature of Tasmania. The pattern of the projected mean temperature change is fairly uniform over Tasmania. Daily minimum temperature is projected to increase more than daily maximum temperature, in agreement with the observed changes from the recent past.

The projection of total annual rainfall over Tasmania shows no significant change under the low and high emissions scenarios. However, there are significant changes projected in the spatial pattern of rainfall and in the timing of rainfall. Under the high emissions scenario, annual average rainfall shows a steadily emerging pattern of increased rainfall over most coastal regions and reduced rainfall over central Tasmania and in some areas of north-west



Tasmania. The changes in seasonal rainfall are more prominent than for annual total rainfall. After 2050, the projections show the west coast of Tasmania experiences a significant increase in winter rainfall and a significant decrease in summer rainfall. The central plateau district shows a steady decrease in rainfall in every season throughout the 21st century. A narrow strip down the east coast shows a steady increase in autumn and summer rainfall throughout the 21st century.

In the projections, there are some periods of reductions in autumn rainfall, that are similar to the recent observed period. This suggests that the recent reduction in autumn rainfall is not an ongoing climate state. Further research is needed to identify the causes of this observed reduction.

The rainfall trends in these projections are driven by an alteration to pressure, atmospheric circulation and wind over the Australian region, as well as an increase in sea surface temperatures (SST) off the coast of Tasmania. The general trend is for an increase in pressure in the mid-latitudes, with greater increases in pressure over New Zealand and to the south-west of Western Australia, than over Tasmania. There is also a reduction in pressure at the high latitudes, with some important seasonal differences. This is associated with changes in several climate indices, including a southward movement and intensification of the Subtropical Ridge (STR) especially in summer, shifts to the dominant geostrophic wind, and an increased frequency of the high phase of the Southern Annular Mode for this region. To the south of Tasmania, an increase in pressure associated with increased incidence of high-pressure systems is seen in summer and autumn, accompanied by an increase in atmospheric blocking.

Overall, the changes to Tasmanian rainfall projected over the 21st century are of a plausible magnitude and pattern, and are consistent with the plausible changes to large-scale mechanisms of climate examined. However, it should be noted that while the changes to climate drivers outlined in this report are generally consistent with the projected rainfall trends, they are not the only mechanisms involved.

The projected changes to the general climate in our modelling projections also affect a range of other environmental variables. Relative humidity is projected to increase around the coasts and decrease over the inland, high-altitude regions of Tasmania with a different pattern in each season. An increase in temperature over the 21st century is the dominant

driver for a significant increase in pan evaporation of up to 19%, which is likely to impact on water availability.

The magnitude of these changes is credible based on previous observations, and they are driven by plausible changes to known climate mechanisms. This increases the confidence that the modelling simulations are robust and provide useful indications of the response of the Tasmanian climate to anthropogenic greenhouse warming.

References

- Achatz U & Opsteegh JD 2003, 'Primitive-equation-based low-order models with seasonal cycle, Part II: Application to complexity and nonlinearity of large-scale atmospheric dynamics', *Journal of Atmospheric Science*, vol. 60, pp. 478-490.
- AchutaRao K & Sperber KR 2002, 'Simulation of the El Niño Southern Oscillation: results from the coupled model intercomparison project', *Climate Dynamics*, vol. 19, pp. 191-209.
- Alexander LV, Hope P, Collins D, Trewin B, Lynch A & Nicholls N 2007, 'Trends in Australia's climate means and extremes: a global context', *Australian Meteorological Magazine*, vol. 56, pp. 1-18.
- Ansell TJ, CJC Reason, IN Smith & K Keay 2000, 'Evidence for decadal variability in southern Australian rainfall and relationships with regional pressure and sea surface temperature', *International Journal of Climatology*, vol. 20, pp. 1113-1129.
- Arblaster JM & Meehl GA 2006, 'Contributions of External Forcings to Southern Annular Mode Trends', *Journal of Climate*, vol. 19, pp. 2896-2905.
- Ashok K, Nakamura H & Yamagata T 2007, 'Impacts of ENSO and Indian Ocean dipole events on the southern hemisphere storm-track activity during austral winter' *Journal of Climate*, vol. 20, pp. 3147-3163.
- Bennett JC, Ling FLN, Graham B, Grose MR, Corney SP, White CJ, Holz GK, Post DA, Gaynor SM & Bindoff NL 2010, *Climate Futures for Tasmania: water and catchments technical report*, Antarctic Climate and Ecosystems Cooperative Research Centre, Hobart, Tasmania.
- Bureau of Meteorology 1993, *Climate of Tasmania*, Canberra, ACT, Australian Government Publication Service.
- Cai WJ, Whetton PH & Karoly DJ 2003, 'The response of the Antarctic Oscillation to increasing and stabilized atmospheric CO₂' *Journal of Climate*, vol. 16, pp. 1525-1538.
- Cechet RP, Sanabria A, Divi CB, Thomas C, Yang T, Arthur C, Dunford M, Nadimpalli K, Power L, White CJ, Bennett JC, Corney SP, Holz GK, Grose MR, Gaynor SM & Bindoff NL 2010, *Climate Futures for Tasmania: severe wind hazard and risk technical report*, Antarctic Climate and Ecosystems Cooperative Research Centre, Hobart, Tasmania.
- Christensen JH, Hewitson B, Busuioc A, Chen A, Gao X, Held I, Jones R, Kolli RK, Kwon W-T, Laprise R, Magaña Rueda V, Mearns L, Menéndez CG, Räisänen J, Rinke A, Sarr A & Whetton P 2007, 'Regional climate projections', *Climate Change 2007: The Physical Science Basis. Contribution of Working Group I to the Fourth Assessment Report of the Intergovernmental Panel on Climate Change*, [Solomon S, Qin D, Manning M, Chen Z, Marquis M, Averyt KB, Tignor M & Miller HL (eds)], Cambridge University Press, Cambridge, United Kingdom and New York, NY, USA.
- Collins M, Frame D, Sinha B & Wilson C 2002, 'How far ahead could we predict El Niño?', *Geophysical Research Letters*, vol. 29, pp. 1492.
- Corney SP, Katzfey JJ, McGregor JL, Grose MR, Bennett JC, White CJ, Holz GK, Gaynor SM & Bindoff NL 2010, *Climate Futures for Tasmania: climate modelling technical report*, Antarctic Climate and Ecosystems Cooperative Research Centre, Hobart, Tasmania.
- CSIRO & Bureau of Meteorology 2007, *Climate change in Australia: impacts, adaptation and vulnerability, Technical Report*, CSIRO.
- CSIRO 2009, *Water Availability for Tasmania*, Report one of seven to the Australian Government from the CSIRO Tasmania Sustainable Yields Project. Australia, CSIRO Water for a Healthy Country Flagship.
- Della-Marta PM, Collins DA & Braganza K 2004, 'Updating Australia's high-quality annual temperature dataset', *Australian Meteorological Magazine*, vol. 53, pp. 75-93.
- Dong L, Vogelsang TJ & Colucci SJ 2008, 'Interdecadal Trend and ENSO-Related Interannual Variability in Southern Hemisphere Blocking', *Journal of Climate*, vol. 21, pp. 3068-3077.
- Drosowsky W 2005, 'The latitude of the subtropical ridge over eastern Australia: The L index revisited', *International Journal of Climatology*, Vol. 25, pp. 1291-1299.
- Fyfe JC, Boer GJ, & Flato GM 1999, 'The Arctic and Antarctic Oscillations and their projected changes under global warming', *Geophysical Research Letters*, vol. 11, pp. 1601-1604.

- Gallant AJE, Hennessy KJ, & Risbey J 2007, 'Trends in rainfall indices for six Australian regions: 1910-2005', *Australian Meteorological Magazine*, vol. 56, pp. 223-239.
- Godfred-Spenning CR & Gibson TT 1995, 'A synoptic climatology of rainfall in HEC catchments' *Antarctic CRC Research Report Number 5*, Antarctic Cooperative Research Centre, Hobart, Tasmania.
- Gong D & Wang S 1999, 'Definition of Antarctic oscillation index', *Geophysical Research Letters*, vol. 26, pp. 459-462.
- Haylock M & Nicholls N 2000, 'Trends in extreme rainfall indices for an updated high quality data set for Australia, 1910-1998' *International Journal of Climatology*, vol. 20, pp. 1533-1541.
- Hendon HH, Thompson DWJ, & Wheeler MC 2007, 'Australian rainfall and surface temperature variations associated with the Southern Hemisphere annular mode', *Journal of Climate*, vol. 20, pp. 2452-2467.
- Hennessy KJ, Suppiah R & Page CM 1999, 'Australian rainfall changes, 1910-1995', *Australian Meteorological Magazine*, vol. 48, pp. 1-13.
- Hill KJ, Santoso A & England MH 2009, 'Interannual Tasmanian Rainfall Variability Associated with Large-Scale Climate Modes', *Journal of Climate*, vol. 22, pp. 4383-4397.
- Hines KM, Bromwich DH, & Marshall GJ 2000, 'Artificial surface pressure trends in the NCEP-NCAR reanalysis over the Southern Ocean and Antarctica', *Journal of Climate*, vol. 13, pp. 3940-3952.
- Holz GK, Grose MR, Bennett JC, Corney SP, White CJ, Phelan D, Potter K, Kriticos D, Rawnsley R, Parsons D, Lisson S, Gaynor SM & Bindoff NL 2010, *Climate Futures for Tasmania: impacts on agricultural technical report*, Antarctic Climate and Ecosystems Cooperative Research Centre, Hobart, Tasmania.
- IPCC 2007, *Climate Change 2007: The Physical Science Basis. Contribution of Working Group I to the Fourth Assessment Report of the Intergovernmental Panel on Climate Change* [Solomon S, Qin D, Manning M, Chen Z, Marquis M, Averyt KB, Tignor M & Miller HL (eds)], Cambridge University Press, Cambridge, United Kingdom and New York, NY, USA.
- Jones DA & Simmonds I 1994, 'A climatology of Southern Hemisphere anticyclones' *Climate Dynamics*, vol. 10, pp. 333-348.
- Jones DA, Wang W, & Fawcett R 2009, 'High-quality spatial climate data-sets for Australia', *Australian Meteorological and Oceanographic Journal*, vol. 58, pp. 233-248.
- Jovanovic B, Jones DA, & Collins DA 2006, 'A high quality monthly pan evaporation dataset for Australia', *Climatic Change*, vol. 87, pp. 517-535.
- Kalnay E, Kanamitsu M, Kistler R, Collins W, Deaven D, Gandin L, Iredell M, Saha S, White G, Woollen J, Zhu Y, Leetmaa A, Reynolds R, Chelliah M, Ebisuzaki W, Higgins W, Janowiak J, Mo KC, Ropelewski C, Wang J, Jenne R & Joseph D 1996, 'The NCEP/NCAR 40-year reanalysis project', *Bulletin of the American Meteorological Society*, vol. 77, pp. 437-471.
- Keable MI, Simmonds I & Keay K 2002, 'Distribution and temporal variability of 500 hPa cyclones characteristics in the Southern Hemisphere', *International Journal of Climatology*, vol. 22, pp. 131-150.
- Kistler R, Kalnay E, Collins W, Saha S, White G, Woollen J, Chelliah M, Ebisuzaki W, Kanamitsu M, Kousky V, van den Dool H, Jenne R & Fiorino M 2001, 'The NCEP-NCAR 50-Year Reanalysis: Monthly Means CD-ROM and Documentation', *Bulletin of the American Meteorological Society*, vol. 82, pp. 247-267.
- Langford J 1965, 'Weather and Climate', *Atlas of Tasmania*, J. L. Davies, Hobart, Lands and Survey Department.
- Larsen SH & Nicholls N 2009, 'Southern Australian rainfall and the subtropical ridge: Variations, interrelationships, and trends' *Geophysical Research Letters*, vol. 36, pp. 5.
- Lavery B, Kariko A & Nicholls N 1992, 'A historical rainfall data set for Australia', *Australian Meteorological Magazine*, vol. 40, pp. 33-39.
- Le Quere C, Raupach MR, Canadell JG, Marland G, Bopp L, Ciais P, Conway TJ, Doney SC, Feely RA, Foster P, Friedlingstein P, Gurney K, Houghton RA, House JI, Huntingford C, Levy PE, Lomas MR, Majkut J, Metzl N, Ometto JP, Peters GP, Prentice IC, Randerson JT, Running SW, Sarmiento JL, Schuster U, Sitch S, Takahashi T, Viovy N, van der Werf GR &

- Woodward FI 2009, 'Trends in the sources and sinks of carbon dioxide', *Nature Geoscience*, vol. 2, pp. 831-836.
- Leighton RM & Deslandes R 1991, 'Monthly anticyclonicity and cyclonicity in the Australasian region: average for January, April, July and October', *Australian Meteorological Magazine*, vol. 39, pp. 149-154.
- Manton MJ, Della-Marta PM, Haylock MR, Hennessy KJ, Nicholls N, Chambers LE, Collins DA, Daw G, Finet A, Gunawan D, Inape K, Isobe H, Kestin TS, Lefale P, Leyu CH, Lwin T, Maitrepierre L, Ouprasitwong N, Page CM, Pahalad J, Plummer N, Salinger MJ, Suppiah R, Tran VL, Trewin B, Tibig I & Yee D 2001, 'Trends in extreme daily rainfall and temperature in Southeast Asia and the South Pacific: 1961-1998', *International Journal of Climatology*, vol. 21, pp. 269-284.
- Marshall GJ 2003, 'Trends in the southern annular mode from observations and reanalyses', *Journal of Climate*, vol. 16, pp. 4134-4143.
- McBride JL & Nicholls N 1983, 'Seasonal relationship between Australian rainfall and the Southern Oscillation', *Monthly Weather Review*, vol. 111, pp. 1998-2004.
- McIntosh PC, Pook MJ & McGregor J 2005, *Study of future and current climate: a scenario for the Tasmanian region (stages 2 & 3) (CSIRO) - a report for Hydro Tasmania*, CSIRO Marine and Atmospheric Research, Hobart, Tasmania.
- Meehl GA, Stocker TF, Collins WD, Friedlingstein P, Gaye AT, Gregory JM, Kitoh A, Knutti R, Murphy JM, Noda A, Raper SCB, Watterson IG, Weaver AJ & Zhao Z-C 2007, 'Global Climate Projections', *Climate Change 2007: The Physical Science Basis. Contribution of Working Group I to the Fourth Assessment Report of the Intergovernmental Panel on Climate Change*, [Solomon S, Qin D, Manning M, Chen Z, Marquis M, Averyt KB, Tignor M & Miller HL (eds)], Cambridge University Press, Cambridge, United Kingdom and New York, NY, USA.
- Meneghini B, Simmonds I & Smith IN 2007, 'Association between Australian rainfall and the Southern Annular Mode', *International Journal of Climatology*, vol. 27, pp. 109-121.
- Meyers G, McIntosh P, Pigot L & Pook MJ 2007, 'The Years of El Niño, La Niña, and Interactions with the Tropical Indian Ocean', *Journal of Climate*, vol. 20, pp. 2872-2880.
- Miller RL, Schmidt GA & Shindell DT 2006, 'Forced variations of annular modes in the 20th Century IPCC AR4 simulations', *Journal of Geophysical Research*, Vol. 111, D18101.
- Monahan AH & Dai A 2004, 'The spatial and temporal structure of ENSO nonlinearity', *Journal of Climate*, vol. 17, pp. 3026-3036.
- Murphy BF & Timbal B 2008, 'A review of recent climate variability and climate change in southeastern Australia', *International Journal of Climatology*, vol. 28, pp. 859-879.
- Nakićenović N & Swart R (eds) 2000, *Special Report on Emissions Scenarios. A Special Report of Working Group III of the Intergovernmental Panel on Climate Change*. Cambridge University Press, Cambridge, United Kingdom and New York, NY, USA.
- Nicholls N 1989, 'Sea surface temperatures and Australian winter rainfall', *Journal of Climate*, vol. 2, pp. 965-973.
- Nicholls N & Lavery B 1992, 'Australian rainfall trends during the twentieth century', *International Journal of Climatology*, vol. 12, pp. 153-163.
- Nicholls N, Lavery B, Frederiksen C, Drosowsky W & Torok S 1996, 'Recent apparent changes in relationships between the El Niño Southern Oscillation and Australian rainfall and temperature', *Geophysical Research Letters*, vol. 23, pp. 3357-3360.
- Pelly JL & Hoskins BJ 2003, 'How well does the ECMWF Ensemble Prediction System predict blocking?', *Quarterly Journal of the Royal Meteorological Society*, vol. 129, pp. 1683-1702.
- Pittock AB 1971, 'Rainfall and the general circulation', *Proceedings of the International Conference on Weather Modification*, Canberra, Australia, American Meteorological Society, pp. 330-338.
- Pittock AB 1983, 'Recent climatic change in Australia: implications of CO₂-warmed earth', *Climatic Change*, vol. 5, pp. 321-340.
- Pook MJ & Gibson TT 1999, 'Atmospheric blocking and storm tracks during SOP-1 of the FROST Project', *Australian Meteorological Magazine*, vol. 48, pp. 51-60.
- Pook MJ, McIntosh PC & Meyers GA 2006, 'The synoptic decomposition of cool-season rainfall in the Southeastern Australian cropping region', *Journal of Applied Meteorology and Climatology*, vol. 45, pp. 1156-1170.
- Power S, Haylock M, Colman R & Wang X 2006, 'The predictability of interdecadal

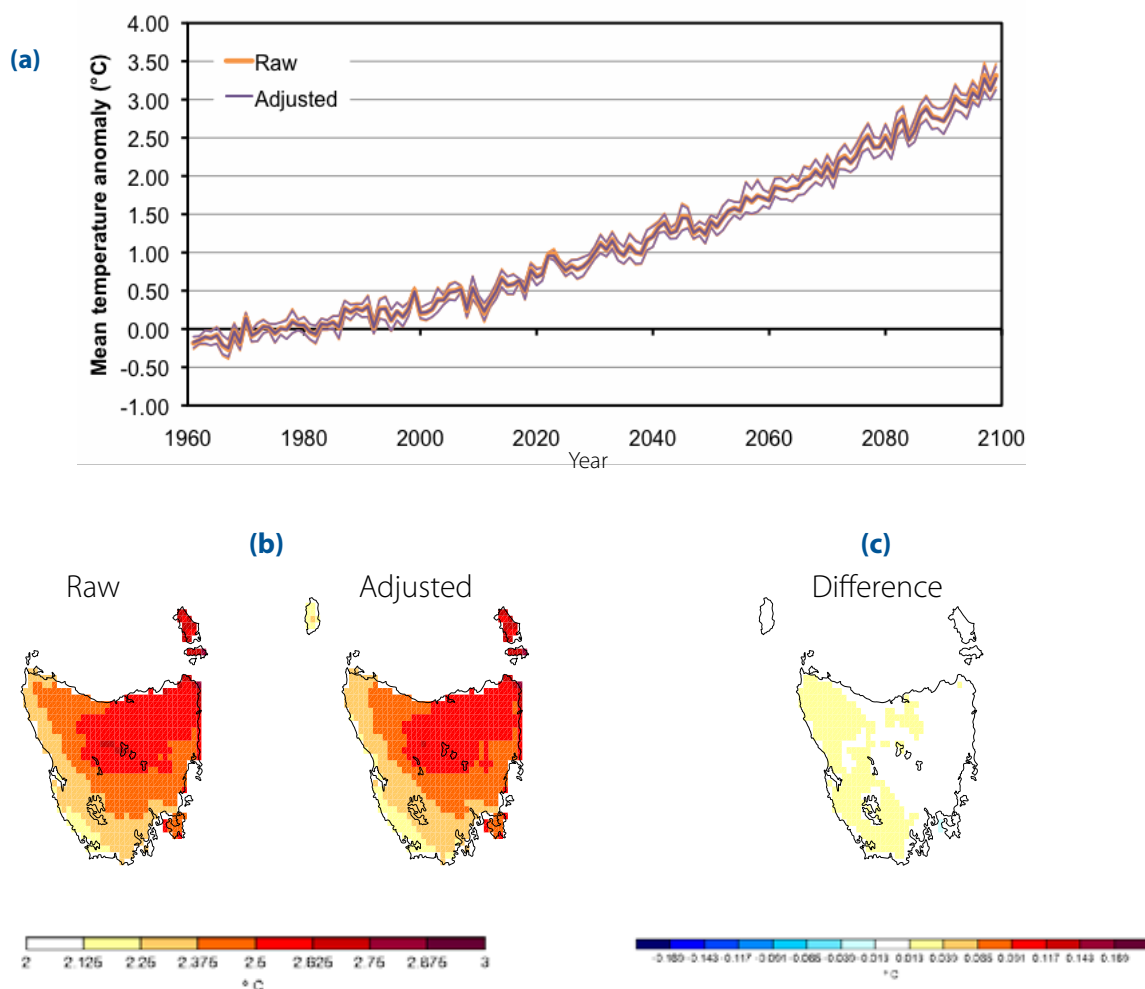
- changes in ENSO activity and ENSO teleconnections', *Journal of Climate*, vol. 19, pp. 4755-4771.
- Raphael MN & Holland MM 2006, 'Twentieth century simulation of the Southern Hemisphere climate in coupled models. Part 1: Large scale circulation variability', *Climate Dynamics*, vol. 26, pp. 217-228.
- Raupach MR, Briggs PR, Haverd V, King EA, Paget M & Trudinger CM 2008, Australian Water Availability Project (AWAP), final report for Phase 3', *CSIRO Marine and Atmospheric Research component*, . Canberra, Australia, CSIRO Marine and Atmospheric Research.
- Reynolds RW 1988, 'A real-time global sea surface temperature analysis', *Journal of Climate*, vol. 1, pp. 12.
- Ridgway KR 2007, 'Long-term trend and decadal variability of the southward penetration of the East Australian Current', *Geophysical Research Letters*, vol. 34, L13613.
- Risbey JS, Pook MJ, McIntosh PC, Wheeler MC & Hendon HH 2009, 'On the remote drivers of rainfall variability in Australia', *Monthly Weather Review*, vol. 137, pp. 3233-3253.
- Robertson AW 2001, 'Influence of ocean-atmosphere interaction on the Arctic Oscillation in two general circulation models', *Journal of Climate*, vol. 14, pp. 3240-3254.
- Saji NH, Goswami BN, Vinayachandran PN & Yamagata T 1999, 'A dipole mode in the tropical Indian Ocean', *Nature*, vol. 401, pp 360-363.
- Selten FM & Branstator G 2004, 'Preferred regime transition routes and evidence for an unstable periodic orbit in a baroclinic model', *Journal of Atmospheric Science*, vol. 61. pp. 2267-2268.
- Shepherd DJ 1995, 'Some characteristics of Tasmanian rainfall', *Australian Meteorological Magazine*, vol. 44, pp. 261-274.
- Shulmeister J, Goodwin I, Renwick J, Harle K, Armand L, McGlone MS, Cook E, Dodson J, Hesse PP, Mayewski P & Curran M 2004, 'The Southern Hemisphere westerlies in the Australasian sector over the last glacial cycle: a synthesis', *Quaternary International*, vol. 118-19, pp. 23-53.
- Simmonds I & Key K 2000, 'Variability of Southern Hemisphere extratropical cyclone behavior, 1958-97', *Journal of Climate*, vol. 13, pp. 550-561.
- Srikanthan R & Stewart BJ 1991, 'Analysis of Australian rainfall data with respect to climate variability and change', *Australian Meteorological Magazine*, vol. 39, pp. 11-20.
- Sturman A & Tapper N 1996, *The weather and climate of Australia and New Zealand*, Oxford University Press.
- Suppiah R & Hennessy KJ 1998, 'Trends in total rainfall, heavy rain events and number of dry days in Australia, 1910-1990', *International Journal of Climatology*, vol. 18, pp. 1141-1164.
- Taschetto AS & England MH 2008, 'An analysis of late twentieth century trends in Australian rainfall', *International Journal of Climatology*, vol. 29, pp. 791-807.
- Taschetto AS & England MH 2009, 'El Niño Modoki impacts on Australian rainfall', *Journal of Climate*, vol. 22, pp. 3167-3174.
- Thompson DWJ & Solomon S 2002, 'Interpretation of recent Southern Hemisphere climate change', *Science*, vol. 296. pp. 895-899.
- Timbal B 2009, 'The continuing decline in South-East Australian rainfall – Update to may 2009', *CAWCR Research Letters*, vol. 2, pp. 4-11.
- Timbal B & Murphy BF 2007, 'Observed climate change in the South-East of Australia and its relation to large-scale modes of variability', *BMRC Research Letters*, vol. 6, pp. 6-11.
- Torok SJ & Nicholls N 1996, 'A historical annual temperature dataset for Australia', *Australian Meteorological Magazine*, vol. 45, pp. 251-260.
- Trenberth, KE, Jones PD, Ambenje P, Bojariu R, Easterling D, Klein Tank A, Parker D, Rahimzadeh F, Renwick JA, Rusticucci M, Soden B & Zhai P 2007, 'Observations: Surface and Atmospheric Climate Change', *Climate Change 2007: The Physical Science Basis. Contribution of Working Group I to the Fourth Assessment Report of the Intergovernmental Panel on Climate Change*, [Solomon S, Qin D, Manning M, Chen Z, Marquis M, Averyt KB, Tignor M & Miller HL (eds)], Cambridge University Press, Cambridge, United Kingdom and New York, NY, USA.
- Wang G & Hendon HH 2007, 'Sensitivity of Australian Rainfall to Inter-El Niño Variations', *Journal of Climate*, vol. 20, pp. 4211-4226.
- White CJ, Sanabria LA, Grose MR, Corney SP, Bennett JC, Holz GK, McInnes KL, Cechet RP, Gaynor SM & Bindoff NL 2010, *Climate Futures for Tasmania: extreme events technical report*, Antarctic Climate and Ecosystems Cooperative Research Centre, Hobart, Tasmania.

Appendices

These plots show a comparison of the change to key climate variables in the raw and 'bias-adjusted' modelling outputs. Appendix 1 shows the change in mean temperature and Appendix 2 shows the change in annual total rainfall. Lines on the time series of both plots are difficult to distinguish as the raw and bias adjusted series' lay on top of each other.

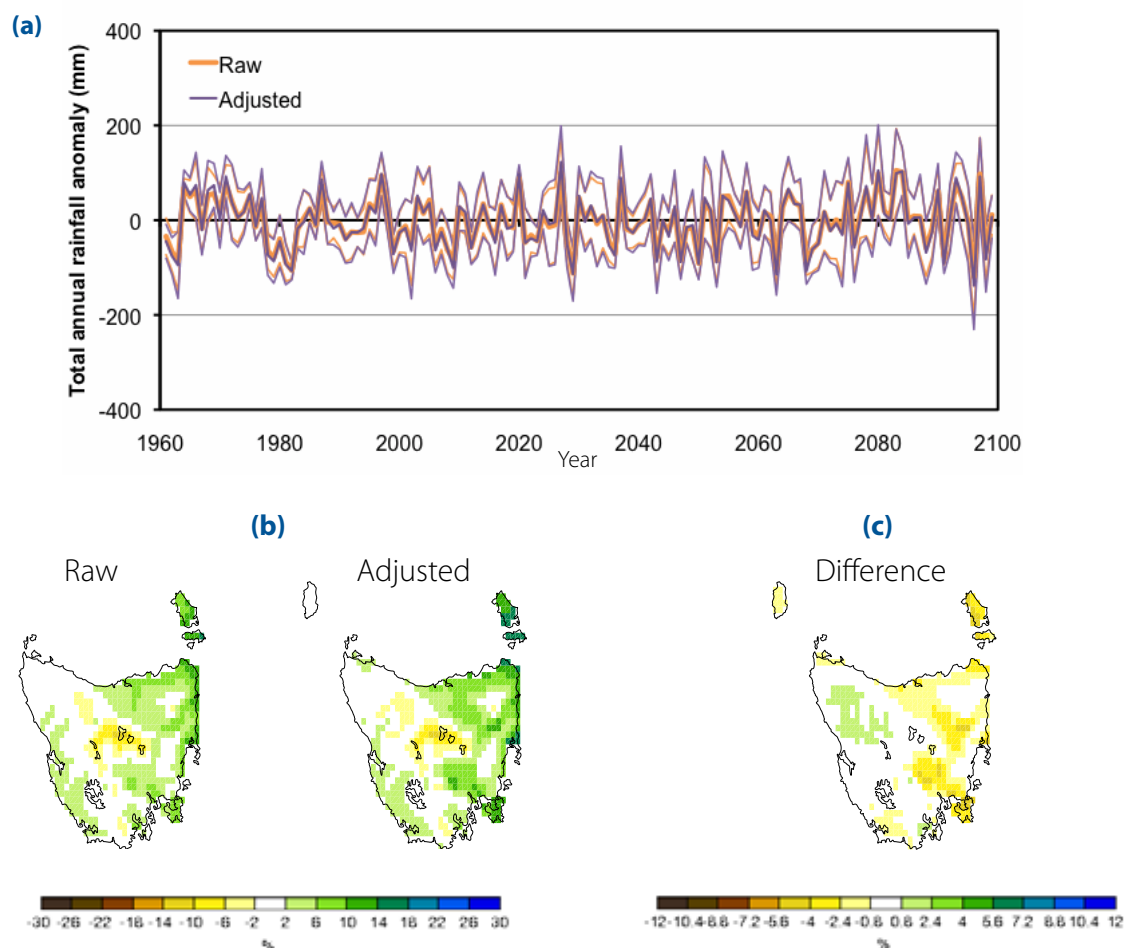
The maps of the spatial pattern of change between the recent period and the end of the century (Appendix 1b, Appendix 2b) appear very similar between the two outputs for both variables. Maps of the difference between the change maps of the two outputs (Appendix 1c and Appendix 2c) illustrate the difference more clearly. For mean temperature, the mean difference in change between the two outputs is 0.013 °C. The mean difference for rainfall is 1.13%. These differences, whilst not zero, are considerably smaller than any change examined in the report. Therefore, the raw and 'bias adjusted' outputs can be considered to have the same mean trends to within statistical uncertainty. Therefore, to examine changes to mean variables such as in this report, the raw modelling outputs can be used, and the 'bias adjusted' outputs can be used directly in applications such as agricultural, water runoff and extreme events analyses.

Appendix 1 - Temperature



Appendix 1 The six-model-mean Tasmanian mean temperature change (anomaly from 1978-2007 mean) for the raw modelling outputs and the bias-adjusted modelling outputs. (a) Time series of mean temperature anomaly and the standard deviation between the six models. (b) The spatial pattern of mean temperature change between 1978-2007 and 2070-2099 in each modelling output. (c) The difference between the two spatial patterns (Raw minus Adjusted).

Appendix 2 - Rainfall

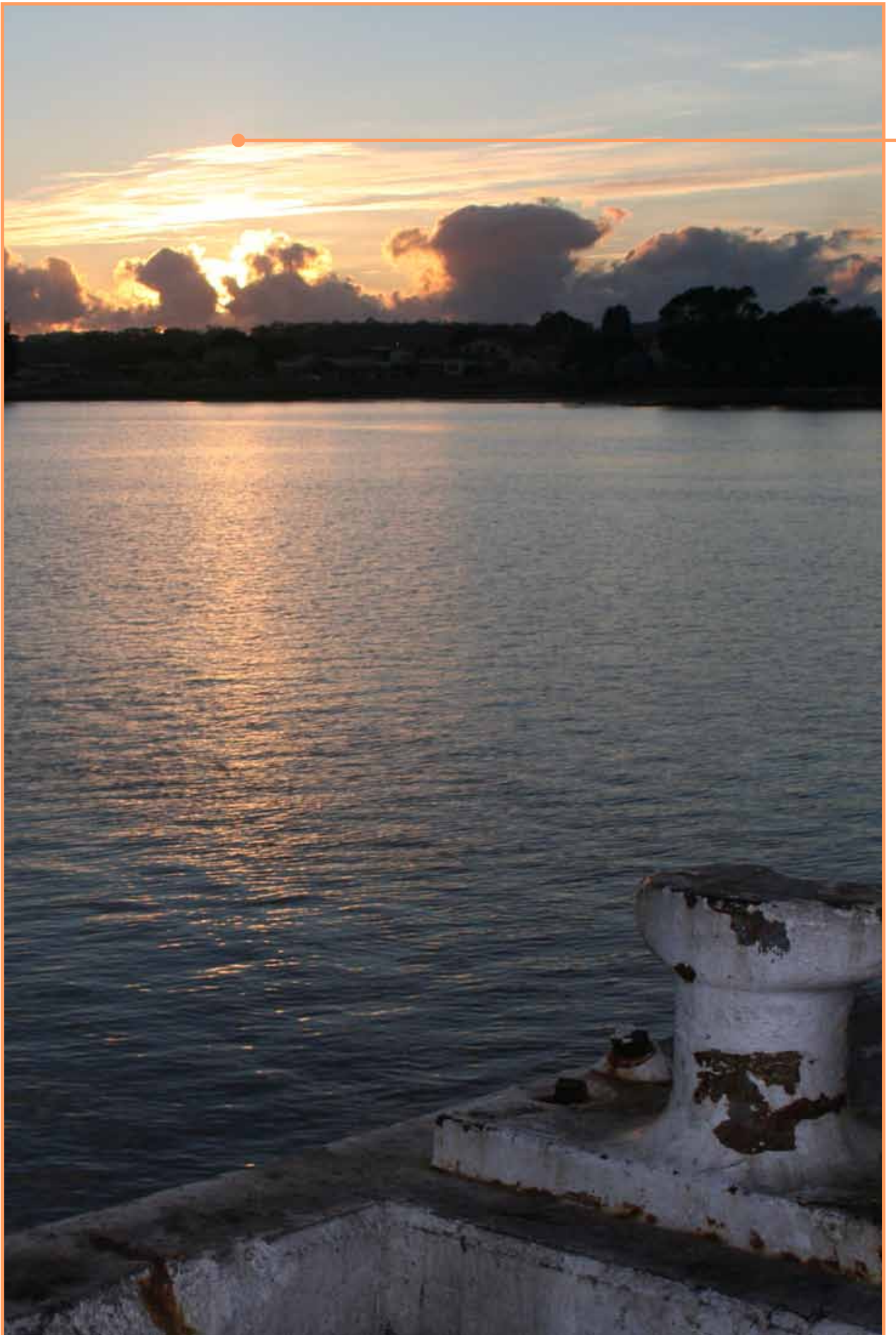


Appendix 2 The six-model-mean Tasmanian total annual rainfall change (anomaly from 1978-2007 mean) for the raw modelling outputs and the bias-adjusted modelling outputs. (a) Time series of annual total rainfall anomaly and standard deviation between the six models. (b) The spatial pattern of total annual rainfall change between 1978-2007 and 2070-2099 in each modelling output. (c) The difference between the two spatial patterns (Raw minus Adjusted).

Appendix 3 - Spatial Correlation

	B1-2025	A2-2025	B1-2055	A2-2055	B1-2085	A2-2085
B1-2025						
A2-2025	0.9688					
B1-2055	0.8270	0.8593				
A2-2055	0.5571	0.6133	0.8298			
B1-2085	0.8874	0.8874	0.9402	0.8055		
A2-2085	0.6616	0.6722	0.8809	0.8721	0.8985	

Appendix 3 Table of spatial correlation between model-mean patterns of change in different scenarios and to different periods in the simulations. Change is from the baseline period 1978-2007 to the periods 2025 (2010-2039), 2055 (2040-2069) and 2085 (2070-2099). Spatial correlations greater than 0.9 are bolded.



Project Acknowledgements

The Climate Futures for Tasmania project was funded primarily by the State Government of Tasmania, the Australian Government's Commonwealth Environment Research Facilities Program and Natural Disaster Mitigation Program. The project also received additional funding support from Hydro Tasmania.

Scientific leadership and contributions were made from a consortium of organisations including: Antarctic Climate & Ecosystems Cooperative Research Centre, Tasmania Department of Primary Industries and Water, Tasmanian State Emergency Service, Hydro Tasmania Consulting, Geoscience Australia, Bureau of Meteorology, CSIRO, Tasmanian Partnership for Advanced Computing, Tasmanian Institute of Agricultural Research and the University of Tasmania.

The generation of the Climate Futures for Tasmania climate simulations was commissioned by the Antarctic Climate & Ecosystems Cooperative Research Centre (ACE CRC), as part of its Climate Futures for Tasmania project. The climate simulations are freely available through the Tasmanian Partnership for Advanced Computing digital library at www.tpac.org.au.

The intellectual property rights in the climate simulations belong to the Antarctic Climate & Ecosystems Cooperative Research Centre. The Antarctic Climate & Ecosystems Cooperative Research Centre grants to every person a permanent, irrevocable, free, Australia wide, non-exclusive licence (including a right of sub-licence) to use, reproduce, adapt and exploit the Intellectual Property Rights of the simulations for any purpose, including a commercial purpose.

Climate Futures for Tasmania is possible with support through funding and research of a consortium of state and national partners.



Climate Futures for Tasmania is possible with support through funding and research of a consortium of state and national partners.



**ANTARCTIC CLIMATE
& ECOSYSTEMS**
COOPERATIVE RESEARCH CENTRE



Australian Government

**Department of Sustainability, Environment,
Water, Population and Communities**



Tasmania
Explore the possibilities



Australian Government

Attorney-General's Department



Australian Government

Bureau of Meteorology

The logo for Hydro Tasmania, consisting of three green circles of varying sizes arranged in a cluster.
**Hydro
Tasmania**
The power of natural thinking



Australian Government

Geoscience Australia

